Republic of Iraq
Ministry of Higher Education
and Scientific Research
University of Babylon
College of Engineering
Department of Civil Engineering

Finite Element Analysis of Tree-Like Steel Columns Under Combined Axial and Lateral Loads

A Thesis

Submitted to the College of Engineering at the University of Babylon in Partial Fulfillment of the Requirements for the Degree of Master in Engineering \civil Engineering \structures

By

Rabab Challoob Dekhn Naser

Supervised by

Assist. Prof. Dr. Khalid Kareem Shadhan

2022 A.D 1444 A.H

بسم الله الرحمن الرحيم

﴿ وَيَرْزُقْهُ مِنْ حَيْثُ لَا يَحْتَسِبُ ۚ وَمَن يَتَوَكَّلْ عَلَى اللَّهِ فَهُوَ حَسْبُهُ ۚ إِنَّ اللَّهَ بَالِغُ أَمْرِهِ ۚ قَدْ جَعَلَ اللَّهُ لِكُلِّ شَيْءٍ قَدْرًا﴾

صدق الله العلي العظيم

(سورة الطلاق الآية 3)

To the soul of my beloved father……

To my dear mother ……

To my husband and life partner……

Certificate

I certify that the preparation of this thesis titled **"Finite Element Analysis of Tree-Like Steel Columns Under Combined Axial and Lateral Loads**", is prepared by "**Rabab Challoob Dekhn**", under my supervision at the Department of Civil Engineering in the University of Babylon in partial fulfillment of the requirements for the degree of master in Civil Engineering (Structural Engineering).

Signature:

Name: Assist. Prof. Dr. Khalid K. Shadhan

Date: / / 2022

Acknowledgements

In the name of ALLAH, the most compassionate the most merciful. Praise be to ALLAH and pray and peace be on his prophet Mohammed his relatives and companions and on all those who follow him.

I want to express my sincere appreciation and deepest gratitude to ***Assist. Prof. Dr. Khalid K. Shadhan,*** whom I had the excellent luck and the honor of being under his supervision, for his continuous encouragement and invaluable guidance throughout this thesis.

All love and great thanks for ***University of Babylon,*** especially Department of Civil Engineering and all persons who work there from Deans, Heads, Lecturers and Staff that I knew during my period of study. Also,sincere thanks to all Universities in Iraq from its south to north that provided uscontinuously with different references of sciences.

I do not know how I can reach my immense respect and thank my family especially ***My Lovely Mother and my lovely husband*** for their care,patience and encouragement throughout the study period, "I am really indebted to them".

Also, I wish to thank ***My Sisters*** and ***Brothers,*** especially my sister ***Dr. Hadeel Dekhn and her husband Dr. Wissam Al-Taliby*** who participated in providing help during the period of the research. Finally, special thanks and gratitude for all people that love subsistence in peace.

Rabab Ch. Dekhn

2022

Abstract:

Few studies have been conducted on the structural behavior of steel columns with branches that are called tree-like columns. These kinds of columns have been used in many structures around the world especially those structures with large space. The purpose of this study was to investigate the failure load, vertical and lateral displacements, and failure mode of steel tree-like columns subjected to a combination of axial and lateral loading. The ratio of lateral load to axial load, the shape of cross-sectional area (A), the outer diameter to thickness ratio (D/t) and the number of branching levels (BL) have been selected as the design variables. A plane finite element model with one branching level and two branches within the level was first developed using ABAQUS/CAE 2017 software. The model has a trunk cross sectional area (A0) equals to 480 mm^2, the area of first branching level equal to half area of a cross section area of trunk (A1 = A0 / 2), total height and width for the specimen equals to 350 mm. The model was verified by using the experimental results obtained from another researcher in terms of load-displacement response. Then other five models are published to investigate the design variables. Each model was exposed to seven loading cases (axial loading only, axial loading plus (20%, 40%, 60%, 80% and 100%) lateral to axial load ratio, and lateral loading only). The results showed that increases the lateral to axial load ratio from 0% by (20, 40, 60, 80 and 100) % respectively, decreases the axial failure load between ((48-56), (69-74.4), (78-81.6), (82-85.4) and (85-87.8)) % respectively. While axial and lateral displacements are significantly increased. Also changing the cross-sectional area from rectangular to circular HSS with D/t ratio equals to 21, the failure load is decreased by 10% for the case of axial loading only and by 24.6% for the case of lateral loading only. Decreasing the D/t ratio from 21 to (14 and 8) respectively, increases the axial failure load by (11.1 and 24.4). The presence of axial load in combination with lateral load works to reduce the lateral displacement between (17 - 48.6) % for the tree-like column models. Furthermore, increasing the

number of branching levels from 1 to 2 increases the axial failure load by 10%.
the joint area is the critical part of tree-like column and stresses are higher at that part.

List of Content

Description	**Page**
Ayah from the Holy Quran	I
Dedication	II
Certificate	III
Acknowledgements	IV
Abstract	V
List of Contents	VII
Abbreviations	X
List of Figures	XI
List of Tables	XVI
1 Chapter one: Introduction	**1-7**
1.1 General Overview	1
1.2 Biomimicry in structural engineering	1
1.3 lateral loads	2
1.4 Examples of tree-like structures	4
1.5 Objectives and Scope	5
1.6 Research Significance	6
1.7 Thiess layout	7
2 Chapter two: Literature Review	**8-31**
2.1 General Overview	8
2.2 Historical overview about Tree-like structures	9
2.3 Agricultural Studies (Simulation of trees dimensions)	11
2.4 form finding studies	12
2.4.1 form-finding by Thread method	13
2.4.2 Form finding by Graphic statics method	15
2.5 previous studies about structural behavior of tree-like columns	18
2.6 previous studies about the joints of tree-like steel columns	23
2.7 previous studies on columns that are subjected to lateral loads	27

3 Chapter Three: Methodology and verification	**30-43**
3.1 General	30
3.2 Structures Modeling and Analysis	30
3.2.1 First stage: Pre-processing	30
3.2.1.1 Parts and Assembly	30
3.2.1.2 Material properties	35
3.2.1.3Interaction of Modeling	35
3.2.1.4 Loading and Boundary Conditions	37
3.2.1.5 Meshing	39
3.2.2 Second stage: simulation process	40
3.2.3 Third Stage: Post-Processing	41
3.3 verification	41
4 Chapter Four: Methodology and verification	**44-91**
4.1 General	44
4.2 tree-like columns groups	44
4.3 Non -Branched Column	46
4.3.1 Axial Failure Load and Displacement	48
4.3.2 Lateral Failure Load and Displacement	49
4.3.3 Failure mode	50
4.4 columns with one branching level.	53
4.4.1 Tree like Column with Rectangular Cross Section	54
4.4.1.1 Axial Failure Load and Displacement	55
4.4.1.2Lateral Failure Load and Displacement	56
4.4.1.3 Failure mode	57
4.4.2 Tree like Column with circular HSS Cross Section	60
4.4.2.1 Tree -like Column with circular Cross Section and D/t ratio equals to 21.	61
4.4.2.1.1 Axial Failure Load and Displacement	62
4.4.2.1.2 Lateral Failure Load and Displacement	63
4.4.2.1.3 Failure mode	64
4.4.2.2 Tree like Column with circular Cross Section and D/t ratio equals to 14.	67

4.4.2.2.1 Axial Failure Load and Displacement	69
4.4.2.2.2 Lateral Failure Load and Displacement	70
4.4.2.2.3 Failure mode	71
4.4.2.3 Tree like Column with circular Cross Section and D/t Ratio equals to 8.	74
4.4.2.3.1 Axial Failure Load and Displacement	75
4.4.2.3.2 Lateral Failure Load and Displacement	76
4.4.2.3.3 Failure mode	78
4.5 column with two branching level.	80
4.5.1 Axial Failure Load and Displacement	81
4.5.2 Lateral Failure Load and Displacement	82
4.5.3 Failure mode	84
4.6 effect of the shape of the cross-sectional area on the behavior of the tree-like columns	86
4.7 effect of the ratio of the outer diameter to thickness (D/t) on the behavior of tree-like columns	88
4.8 effect of the number of branching levels on the behavior of the tree-like columns	90
5 Chapter Five: Conclusions and further work recommendation.	**92-93**
5.1 conclusions	92
5.2 Recommendations for Future Work	93
References	**94-97**

Abbreviations:

Abbreviation	**Description**
AISC	American Institute of Steel Construction
ANSYS	ANalysis SYStem
BL	Branches level
BN	Branches numbers
CCALR	Critical Constant Axial Load Ratio
D/t	Diameter to thickness ratio
HB	Branch's height
HSS	Hollow Steel Sections
HT	total height of branch
FEM	Finite Element Model
Fig.	Figure
GA	Generation Algorithm
i.e.	With other meaning
Kg	Kilogram
m	meter
mm	Millimeter
Max.	Maximum
MPa	Mega Pascal (MN/m^2) (equal to N/mm^2 (MPa))
No.	Number (issue)
Pp.	Pages
Ref.	Reference
Sec.	Section
SAP 2000	Structural Analysis Program
USA	United States of America
W	Specimens' width
3D	Three Dimensions
2D	Two Dimensions
1st	First
3rd	Third
17th	Seventeenth

List of Figures

Fig. No.	Title	Page
1-1	Steps of Biomimicry Structural Design.	2
1-2	Tree-like column structures: (a) Germany Stuttgart Airport, (b) ION Orchard Center, (c) Stanste Airport, (d) Detroit Airport and (e) Shenzhen Cultural Center.	4
2-1	(a) Corinthian columns from roman period, (b) Chinese Dougong Brackets, (c) Gothic style fan vault in Sainte Chapelle, (d) Interior view of the Sagrada Familia.	9
2-2	(a) The Steel Frame and Columns of Palazzo DelLavoro, (b) Completed Columns croup.	10
2-3	The Interface of the program that Guess the Tree Shape.	12
2-4	Gaudi's famous hanging model of the Sagrada Familia.	14
2-5	Frei Otto's hanging model.	14
2-6	Physical thread model made by Kolodziejczyk.	15
2-7	Branching structure with constant length by Matthias Neureither.	16
2-8	Hunt et al. Form-Finding method geometry definitions.	17
2-9	Model proposed by Jonas Henri Houston.	18
2-10	Treehouse design Founded by Buelow. (a) Front view, (b) Rear view.	19
2-11	Specimens with different branches and conducted by A. A. Khamees.	22
2-12	Specimens with different branching height conducted by A. A. Khamees.	23
2-13	Classification of Tree-like column joints.	23
2-14	Branching Joint Finite Element Model, (b) Joint Manufactured by J. Oliveira et al.	24
2-15	Failure mode of joints by FE analysis, (a) Trunk yield mode, (b) Local buckling mode, (c) Branches tearing yield mode.	25
2-16	The loading unit and the joint specimen, (b) The joint's geometrical characteristics, (c) Failure mode for the joint	26

2-17	Main modes of HSS columns failure with combined loading; (a) global mode and (b) local mode.	29
3-1	The Assembled parts of tree-like steel column model.	31
3-2	details and dimensions of tree like column specimens.	34
3-3	Stress versus strain curves used in the FE models	35
3-4	Interaction between lower fixing plate and tree-like column specimen.	36
3-5	Interaction between tree-like column specimen and the upper fixing plates.	36
3-6	Interaction between the upper fixing plates and the loading plate.	37
3-7	Applied load and boundary conditions when axial load only is applied.	38
3-8	Applied load and boundary conditions when axial and lateral loads are applied.	38
3-9	Applied load and boundary conditions when lateral load only is applied.	39
3-10	Models mesh density, (a) Rectangular model, (b) HSS circular model.	40
3-11	Load deflection curve of TR-1-2-0:100 for experimental specimen versus calibrated finite element model.	42
3-12	Correlation between experimental load and finite element load for TR-1-2-0:100.	43
3-13	Mode of failure for experimental specimen Versus calibrated FE mode.	43
4-1	Group No.1 (Influence of the shape of cross-sectional area).	44
4-2	group No.2 (effect of the D/t ratio).	45
4-3	group No. 3 (effect of number of branching level).	45

4-4	Axial load-displacement response for TC14-0-0 model at different loading ratios.	47
4-5	Lateral load-displacement response for TC14-0-0 model at different loading ratios	47
4-6	Axial failure load versus load ratio for TC14-0-0 model.	48
4-7	Axial displacement at failure versus Load ratio for TC14-0-0 model.	49
4-8	Lateral failure load versus load ratio for TC14-0-0 Model.	50
4-9	Lateral Displacement at Failure versus Load Ratio for TC14-0-0 Model.	50
4-10	Failure modes for single column TC14-0-0.	51
4-11	Axial load-displacement response for TR-1-2 models at different loading ratios.	55
4-12	Lateral load-displacement response for TR-1-2 models at different loading ratios.	55
4-13	Axial failure load versus load ratio for TR-1-2 model.	56
4-14	Axial Failure Displacement versus Load Ratio for TR-1-2 Model.	56
4-15	Lateral Failure Load versus Load Ratio for TR-1-2 Model.	57
4-16	Lateral Failure Displacement versus Load Ratio for TR-1-2 Model.	57
4-17	Failure modes for TR-1-2 column.	58
4-18	Axial load-displacement response for TC21-1-2 model at different loading ratios.	62
4-19	Lateral load-displacement response for TC21-1-2 model at different loading ratios.	62

4-20	Axial failure load versus load ratio for TC21-1-2 model.	63
4-21	Axial failure displacement versus load ratio for TC21-1-2 model.	63
4-22	Lateral failure load versus load ratio for TC21-1-2 model.	64
4-23	Lateral failure displacement versus load ratio for TC21-1-2 model.	64
4-24	Failure modes for TC21-1-2 column.	65
4-25	Axial load-displacement response for TC14-1-2 model at different loading ratios.	68
4-26	Lateral load-displacement response for TC14-1-2 model at different loading ratios.	69
4-27	Axial failure load versus load ratio for TC14-1-2 model.	70
4-28	Axial failure displacement versus load ratio for TC14-1-2 model.	70
4-29	Lateral failure load versus load ratio for TC14-1-2 model.	71
4-30	Lateral failure displacement versus load ratio for TC14-1-2 model.	71
4-31	Failure modes for TC14-1-2 column.	72
4-32	Axial failure load versus load ratio for TC8-1-2 model.	75
4-33	Lateral failure load versus load ratio for TC8-1-2 model.	76
4-34	Axial failure load versus load ratio for TC8-1-2 model.	76
4-35	Axial failure displacement versus load ratio for TC8-1-2 model.	77
4-36	Lateral failure load versus load ratio for TC8-1-2 model.	77
4-37	Lateral failure displacement versus load ratio for TC8-1-2 model.	78
4-38	failure modes for TC8-1-2 column.	78
4-39	Axial load-displacement response for TC14-2-4 model at different loading ratios.	81

4-40	Lateral load-displacement response for TC14-2-4 model at different loading ratios.	82
4-41	Axial failure load versus load ratio for TC14-2-4 model.	82
4-42	Axial failure displacement versus load ratio for TC14-2-4 model.	83
4-43	Lateral failure load versus load ratio for TC14-2-4 model.	84
4-44	Lateral failure displacement versus load ratio for TC14-1-2 model.	84
4-45	Failure modes for T14-2-4 column.	85
4-46	Axial load deflection curves for TR-1-2-0:100 and TC21-1-2-0:100 columns.	88
4-47	Lateral load deflection curves for TR-1-2-100:0 and TC21-1-2-100:0 columns.	88
4-48	Axial failure load versus the D/t ratio.	89
4-49	Axial displacement at failure versus D/t ratio.	90
4-50	Lateral failure load (KN) versus the D/t ratio.	90
4-51	Lateral displacement at failure versus D/t ratio.	90
4-52	Axial failure load versus number of branching levels.	91
4-53	Axial displacement at failure versus number of branching levels.	91
4-54	Lateral failure load versus number of branching levels.	92
4-55	lateral displacement at failure versus number of branching levels.	92

List of Tables

Table No.	Title	Page
1-1	Minimum design wind pressure allowed for buildings and other structures.	3
3-1	Dimensions and Details of Specimens.	33
3-2	Experimental results versus FE results for TR-1-2 model.	42
4-1	Results of a Circular Single Column (TC14-0-0) with Different Loading Conditions.	47
4-2	Results of Rectangular Tree like Column (TR-1-2) with Different Loading Conditions.	53
4-3	Results of circular Tree like Column (TC21-1-2) with Different Loading Conditions.	59
4-4	Results of circular Tree like Column (TC14-1-2) with Different Loading Conditions.	64
4-5	Results of circular Tree like Column (TC8-1-2) with Different Loading Conditions.	69
4-6	Results of circular Tree like Column (TC14-2-4) with Different Loading Conditions.	74

CHAPTER ONE

Introduction

1.1 General Overview

Engineers use nature as an inspiring source when designing construction projects. Learning from nature is not a new concept, but it is an updated method that is found in many fields. Nature's inspiration is usually related to mathematics to avoid apparent inspiration and create logical structural designs. To understand the complexities of natural forms, architects and engineers can use mathematical rules as a reference. To describe the geometry of real trees that is non-Euclidean in mathematics, many concepts like non-linear, complex, and fractal geometries have recently been used [1]. The relationship between trees and architecture dates from prehistoric times until the present day. Trees and plants are frequently used for decoration in architecture. The attraction of tree shapes is not limited to aesthetic purposes. Architectural and construction engineers have also tried to imitate the structural and mechanical characteristics, which are the most important aspects of tree-like forms, using developed mathematical concepts. The advancement of "graphic statics," which is a theoretical method for understanding the relationship between structural shapes and the equilibrium of forces, has made architects able to create a lot of dendriform structures with a unique style. Through the use of developed reinforced concrete technology and cantilever techniques, architects constructed more complicated dendriform structures such as mushrooms or umbrella shapes in the early to mid-twentieth century.

1.2 Biomimicry in Structural Engineering

Biomimicry terms were used in researches for the first time in 1962 [2]. It refers to the science of learning from nature. Janine Benyus reintroduced biomimicry in her book as she mentioned that this science examines nature's

best and most adaptable ideas for human benefit. She proposed that natural inspiration can be observed on three levels (organizational, behavioral, and system). On each level, five dimensions could be applied (form, material, construction, process, and function) [3]. These levels and dimensions are very important in structural design. Nature has 3.8 billion years of evolution and is considered the first source of inspiration for architects and engineers in their designs. Architects have used nature as a base for designing more adaptive structures as they use shapes from nature to solve complicated design needs. The most well-known type of biomimicry involves embodying the shape and form of nature. Many of the structural designs inspired by the natural environment are considered great achievements, such as the Sydney Opera House. Suspension bridges are built on the same principles as spider webs. The Pantheon of Rome can be regarded as a biomimicry example in terms of structural behavior because its roof mimics a seashell. The Pantheon's roof's strength comes from its multidimensional curvature, which mimics a seashell due to its lighter weight than traditional reinforced concrete. The structural design and biomimicry procedures can be summarized as shown in Fig (1.1).

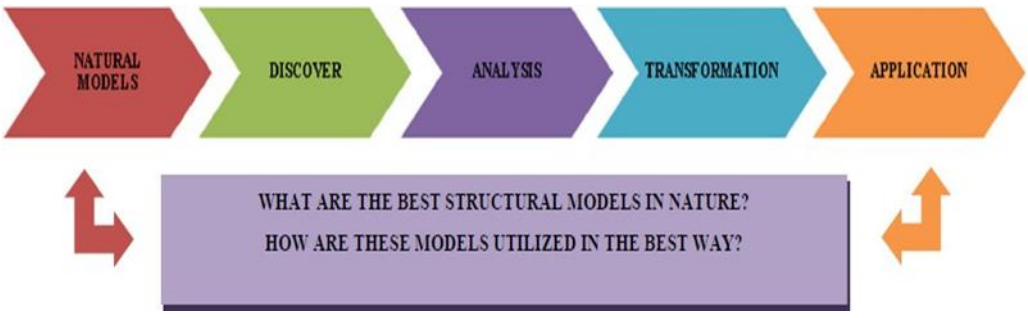

Fig(1.1):Steps of Biomimicry Structural Design [4].

1.3 Lateral Loads

Lateral loads are live loads applied to a structure horizontally and parallel to the ground. Gravity loads, on the other hand, are imposed vertically as downward forces. Wind, earthquakes, water pressure, as well as earth pressure,

are all examples of lateral loads to which structures may be subjected. When building slender structures, the wind is one of the most critical aspects to consider [5]. The wind is physically expressed in a structural design by a speed profile reaching a building. The speed profile properties and impacts are determined by the wind velocity, the geometry of the building, and the protection provided by the terrain and surrounding obstacles. The environment has a significant impact on wind loads in a specific building, and careful consideration of them is only possible if empirical data from wind tunnel studies are available [6]. According to A58 [7].the minimum design pressures allowed for wind from any direction are shown in table (1-1);where the height should be measured above the ground level adjacent to the building or structure. Except for farm buildings or similar structures, the minimum earthquake lateral load for any building or other structure is equal to 5% of the dead load [7].

Table (1.1): Minimum Design Wind Pressure Allowed for Buildings and Other Structures.

Height zone	Wind pressure
m	**kN/m^2**
Less than 15.24 ----------	0.957
15.24 to 30.175 ----------	1.149
30.48 to 60.655 ----------	1.340
60.96 to 91.135 ----------	1.436
91.44 to 121.62 ----------	1.532
121.92 to 152.1 ----------	1.580
152.4 to 182.58 ----------	1.627
182.88 to 243.54 ----------	1.675
243.84 to 304.5 ----------	1.723
304.8 to 365.46----------	1.771
365.76 to 426.42----------	1.819
426.72 to 487.38----------	1.867
487.68 and over ----------	1.915

1.4 Examples of Tree-Like Structures

Because of its attractive design and excellent mechanical performance, the tree-like column structure has been widely adopted in engineering practice. The first use of the tree-like column construction was at Germany's Stuttgart Airport in 1991. Several famous structures, like the ION Orchard shopping center in Singapore, Stansted Airport in London, Detroit Airport in the United States, and the Shenzhen Cultural Center in China have quickly spread its use [8]. All structures are shown in Fig (1.1).

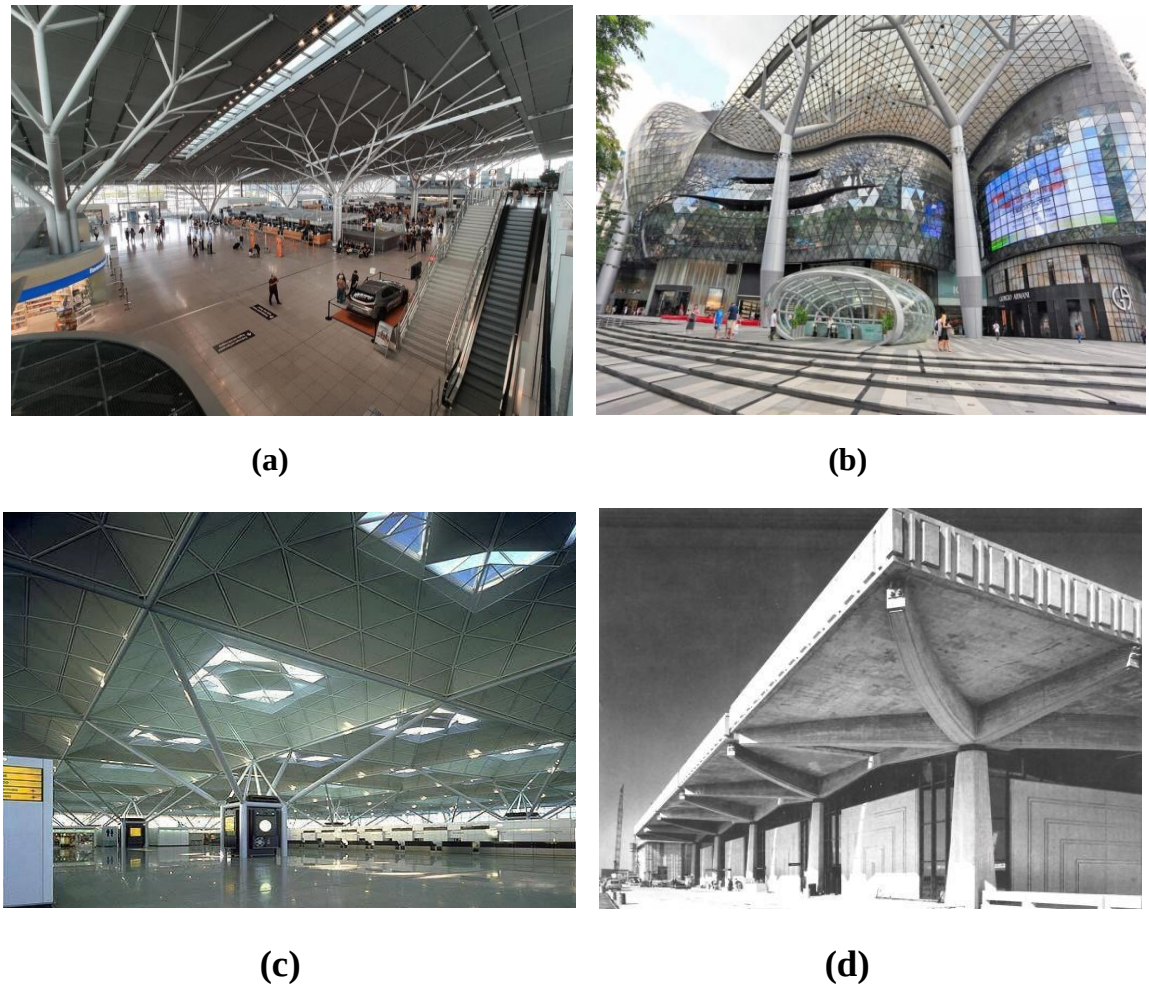

(a) **(b)**

(c) **(d)**

Fig (1.2): Tree-like column structures: (a) Germany Stuttgart Airport, (b) ION Orchard Center in Singapore, (c) Stansted Airport in London, and (d) Detroit Airport in united states.

(e)

Continue Fig (1.2): Tree-like Column Structures: (e) Shenzhen Cultural Center in China [9]

There are some other buildings with tree-like columns as listed below:

1. The Shanghai South Railway Station in China.

2. The Beijing national stadium in China.

3. Chongqing Olympic Stadium in China.

4. The Changsha South Railway Station in China.

5. Tianjin Cube Water Park in China.

6. Tote Restaurant in Mumbai in India.

7. Qatar National Convention Centre in Al-Doha in Qatar.

8. Palace De Justice in Melon in France.

9. University of Guelph in Ontario in Canada.

10. Berlin's Olympic Stadium in Germany

1.5 Objectives and Scope

The main target of this research is to numerically determine the structural behavior of branching steel columns subjected to axial and lateral loads. The objectives of this study can be summarized as follows:

1. Devolvement a 3D finite element model on ABAQUS 2017 program.
2. Comparison of FE results with laboratory results obtained from another researcher.
3. Finding numerically the effect of lateral to axial load ratio on the axial failure loads and displacements of the tree-like column.
4. Finding numerically the effect of the shape of cross-sectional area on the behavior of tree-like column under axial and lateral loads.
5. Finding Numerically the effect of the outer dimeter to thickness (D/t) ratio on the behavior of the tree-like column under axial and lateral loads.
6. Finding numerically the behavior of tree-like column under different number of branching levels under axial and lateral loads.

1.6 Research Significance

The tree-like steel column was investigated in this study as a result of the tremendous urban expansion experienced by the world and our beloved country, Iraq, as a result of the building industry revolution and bold and intricate facility designs. The following is a summary of the current work significance:

1. Provide a specific information about tree-like steel column form-finding methods.
2. Apparently, the tree-like columns are not being numerically studied under the action of lateral loading. In this research, the structural behavior of the tree-like steel column was investigated under the action of axial and combined loading.
3. Find the effect of lateral to axial load ratios, shape of cross-sectional area, number of branching levels on the ultimate failure load and displacement as well as the mode of failure of a tree-like steel column. So, the results help the engineering to understand the tree-like column when designing it.

1.7 Thesis Layout

This study is divided into five chapters the **Chapter one** is an introduction and explanation of the tree-like structures and includes the purpose of the study. **Chapter two** is a literature review of experimental and numerical studies on tree-like structures. **Chapter three** includes the modeling steps, where the FE models are created by using the (ABAQUS CAE/2017) program. And it also contains the model's dimensions and properties of the materials as well as the verification step. **Chapter four** shows the results of the finite element analysis (axial and lateral failure loads and displacements, load deflection curves, and failure modes). While **Chapter five** is the conclusion of the study and suggestions for further research.

CHAPTER TWO

Literature Review

2.1 General Overview

This chapter aims to get a better understanding of the structural behavior of tree-like steel columns (branching steel columns or dendriform columns). A review of the existing literature would be conducted. This chapter is divided into four parts. The first is a historical summary of the development of tree-like structures, while the second is an agricultural study, followed by studies about form-finding, and finally, structural studies are reviewed.

2.2 Historical Overview about Tree-Like Structures

Tree-like structures are structures that imitate the shape and structure of trees or plants in nature. These structures are also called dendritic structures, where the term "Dendri" comes from the Latin word "Dendron", which means "tree". Since the prehistoric ages, humans have been fascinated with tree-like forms, and many cave paintings and art showing the figures of trees and plants have been discovered. As shown in Fig (2.1) (a), Corinthian columns from the Roman period are a well-known example of tree-like structures with flower designs on top. The Chinese Dougong Brackets were the first examples of a real wooden dendriform that appeared a few centuries later in eastern Asia. As shown in Fig 2.1 (b), these wooden brackets were layered, so that each bracket cantilevers over the lower bracket. In this way, the loads on a large surface could be transferred to one point or column. This technique was called Dougong, and it was found before the birth of Christ but became a prominent decorative element in palace constructions and religious temples throughout the medieval period, particularly during the Song dynasty (960 AD to 1279 AD). [8]

Cathedrals being constructed in Europe are excellent examples of the dendriform structures that appeared in fan vault architecture. The vault is an abstract representation of a tree form. A structure branching out from a column or wall creates arches that form the ceiling of vaults. Fig 2.1 (c) shows the Gothic style fan vault in Sainte-Chapelle in Paris.

Antonio Gaudi produced a unique style of branching structures between 1880 and 1920 AD. By using the forms of trees and plants in his design, he was able to combine architectural form and structural efficiency. He often said, "There is no better structure than the trunk of a tree or a human skeleton" [9]. These natural preferences may be found in the Sagrada Familia Cathedral in Barcelona, where the structure was based on a hanging model using cables and branches, as shown in Fig (2.1) (d).

(a) **(b)**

Fig (2.1): (a) Corinthian Columns from Roman Period, (b) Chinese Dougong Brackets [9]

(c) **(d)**

Continue Fig (2.1): (c) Gothic style Fan Vault in Sainte Chapelle [9], (d) Interior View of the Sagrada Familia [10]

The principles of complex tree structure have been separated into Euclidean geometry and simple hyperbolic geometry. Engineers in the early and mid-twentieth centuries-built tree-like columns that looked like mushrooms or forms, as shown in Fig (2.2).

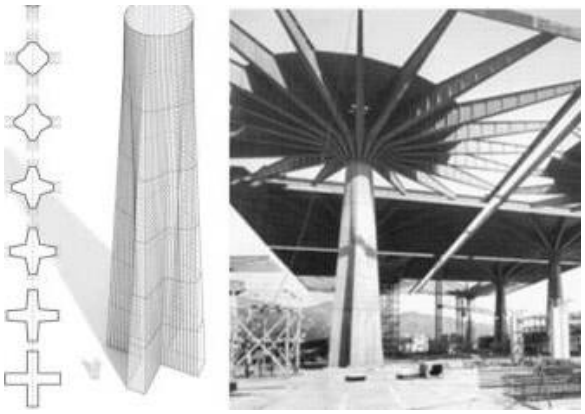

(a) **(b)**

Fig (2.2) :(a) The Steel Frame and Columns of Palazzo DelLavoro, (b) Completed Columns Croup [11]

In many fields of innovation, from technology and industrial design to architecture and interior design, ambiguity has lately been a subject for design. Designers inspired by the shape and structure of trees began to create column-

like trees with a complicated fractal structure around this time. Apart from the development of concrete technologies and high-quality timbers and splints in the late twentieth century, the advent of lightweight yet stable steel gave architects and designers plenty of opportunities to develop intricate designs in tree-like columns. Frei Otto who is a German architect was one of the first designers to build tree-like columns using steel.

2.3 Agricultural Studies (Simulation of Trees Dimensions)

To understand the engineering concept of simulating trees naturally, agricultural studies should be obtained to determine the proportionality of trees dimensions like the relation between trees diameter and its height and height of the tree to crown diameter or guessing the shape of trees. The dimensions of trees are different from one tree to another also it is different for the same tree.

In 2001, Zhi et al. [12] investigated tree branching patterns and methods for predicting their patterns. They also investigated the angles between branches and the length of the branch in relation to the trunk's length. This research can be used to determine tree forms and branch patterns.

In 2003, Hart et al. [13] the Researchers developed a program that estimates the geometry of trees based on variables entered the program. Also, they studied tree shape and the factors that affect it by dividing these factors into two categories: external and internal .at the end of this study. They conclude that the major factors were external factors.

Linsen et al**.** (2005) [14] studied the branches and trunks of trees and the relationship between their overall dimensions. They developed a program that simulates the exterior of trees realistically, as shown in Fig (2.3). By entering information that relates to the behavior of trees in terms of growth and level, one gets a system that predicts how the trees will look over a given time. The results

were extremely accurate in terms of designing the trees and their branches, as well as eliminating errors throughout the planting.

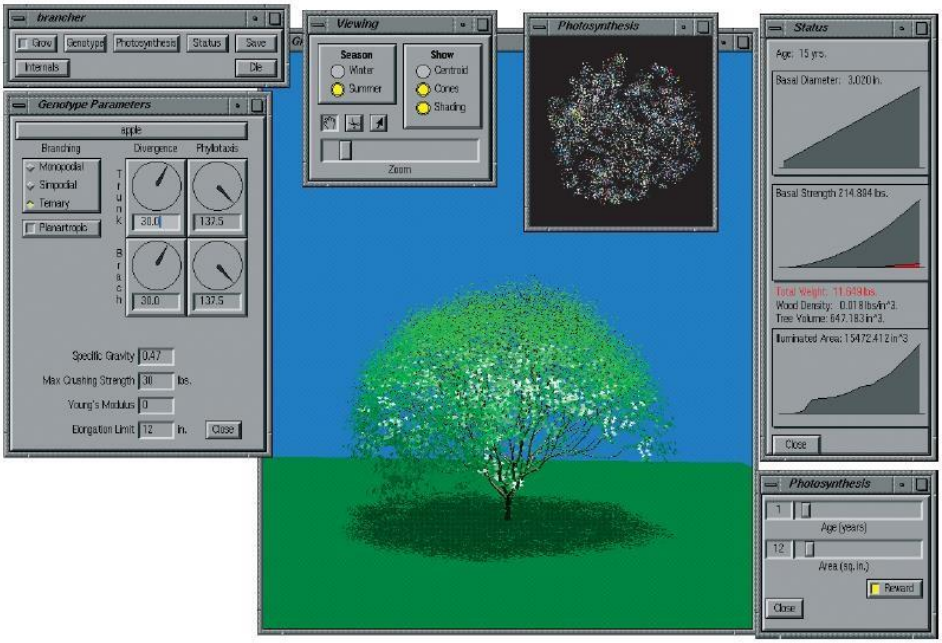

Fig (2.3): The Interface of the Program that Guess the Tree Shape. [14]

2.4 Form Finding Studies

In recent years, the relationship between architecture and construction has changed greatly. This change might be due to the hurried race for originality, surprise, or media impact that private and political goals demand while pursuing famous monuments for the purpose of gaining fame or attention. The demand for such unique structures has resulted in many problems with structural design. The first problem is technological advancements designed to meet the high demand for creative forms. Existing technologies have reduced the requirement for user intelligence to a minimum. Many people, regardless of their experience, can bring the form to reality without knowledge of structural behavior. The Rhinoceros program is an example of this technology. A computerized editorial application with a form-find button. All that a person needs to construct a structure is the ability to open the software, draw some

preliminary geometry, and then click "form find." The guiding principles that should be the driving force behind the form are replaced by the ability to traverse a programming interface and the desire to design something visually attractive. Martinez-Calzon says, "The computer has fostered an unconstrained birth of novel canonical forms that are far from structurally sound." [15]. Previous researchers' techniques for determining the optimal shape for tree-like columns varied, owing to differences in researcher time and style. Architects and interior designers are only concerned with simulating the outside shape, regardless of the tree-like column total bearing capability. The load-carrying capacity of tree-like columns and their failure mode are the most important to structural engineers.

2.4.1 Form-Finding by Thread Method

The thread form-finding method is an effective method for determining the best structure for a specific load condition. Tension-based hanging models are used for estimating a structural approximation for a load situation. The model is hung by little bags filled with sand, like the hanging model of the Sagrada Familia in Barcelona that was made by Antonio Gaudi. As shown in Fig (2.4), the model is hung by little bags filled with sand. This sand represents the vertical loading on the structure and creates the string network. Since only suspended models suffer from tension, they have great structural efficiency. All forces are reversed when the model is reversed, and the most efficient structure for the compression load situation is formed. This principle of reversing tension into compression has served as a basis for many other form-finding model studies.

Fig (2.4): Gaudi's Famous Hanging Model of the Sagrada Familia [10]

In 1972, Otto [16] worked on the design of tree-like columns and branching structures. Using the thread approach, which is a physical form-finding method, he created several different branching systems. An analytical investigation into a lightweight and efficient structure was carried out, taking into consideration essential features of the architecture-nature connection. In addition to his great work, which includes suspended construction, grid shells, and coats, Otto was the pioneer of light tree-like columns of steel in the 20th century, and he worked intensively on the tree-like column model that is shown in Fig (2.5). In this model, he used small weights to represent a uniformly distributed load.

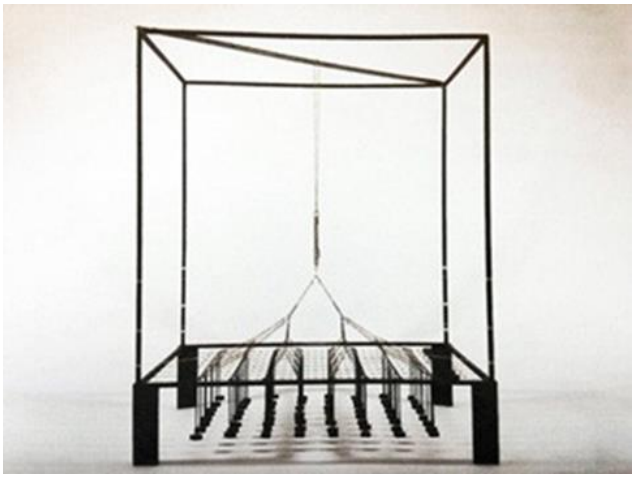

Fig (2.5): Frei Otto's Hanging Model.

In 1992**,** Kolodziejczyk [17] used string patterns submerged in water to obtain pseudo-minimum path shapes formed by water surface tension at the strings. The slackness of the strings influences the original shape (usually between 5% and 10%). This method can be used to study both 2D and 3D forms. A 3D model of a tree-like column founded by Marek Kolodziejczyk is shown in Fig (2.6).

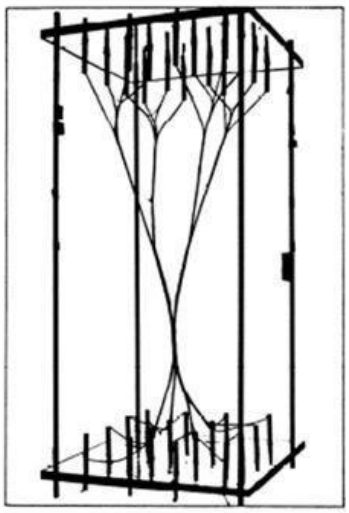

. **Fig (2.6): Physical Thread Model Made by Kolodziejczyk [17]**

2.4.2 Form Finding by Graphic Statics Method

In this method, equilibrium forces are found using computer-aided mathematical operations. To design tree-like columns, the user specifies input parameters, and the algorithm determines the equilibrium shape and member sizes. It's possible to try a variety of shapes and loading patterns.

In 1992**,** Neureuther [17] demonstrated software that generates branch formations based on angle, level, pattern, and other factors. In his work, he used many combinations of status parameters to highlight the breadth of geometric possibilities. Fig (2.7) is an example of a pattern mentioned in the program. The program can effectively view a variety of branching structure configurations, but it has no relation to structural behavior.

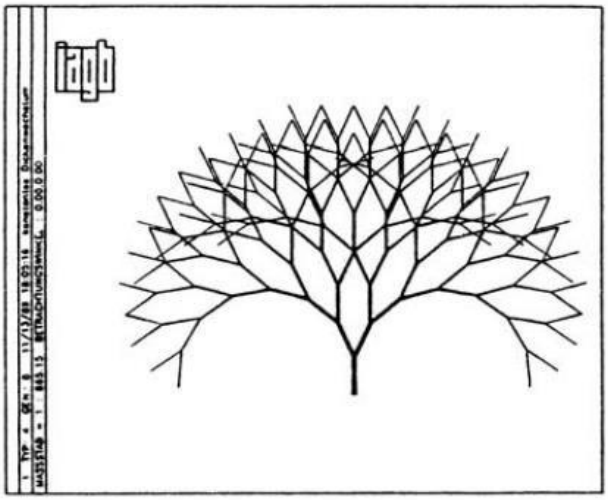

Fig (2.7): **Branching Structure with Constant Length by Matthias Neureither [17]**

In 2009, Hunt et al. [18] developed the graphic statics approach for determining the shape of a tree-like column. The research outlines are basic computer software that assisted in the creation of spatial tree-like columns. The user enters various input parameters, and the software determines the form of the equilibrium and the sizes of the members. A parametric analysis is used to look at a variety of geometries and loading patterns in this study. This study used the traditional method, in which hanging models were chosen to estimate the equilibrium form of tree-like columns. The hanging model is made from flexible threads or chains. The thread or chain is suspended and locked together at multiple points (branching nodes) so that it can rotate freely on the nodes. Normally, two-dimensional trees are addressed; however, the computer procedure is also correct for three-dimensional geometries.

The following are the laws that govern geometry in this study:

1. The self-weight and additional point loads are added at the nodes.

2. An element is divided into two elements in each internal node.

3. The top node number should be equal to the power of two, like 2^1, 2^2, 2^3, etc. As a result, n+2 equals the number of vertical rows of nodes as shown in Fig (2.8).

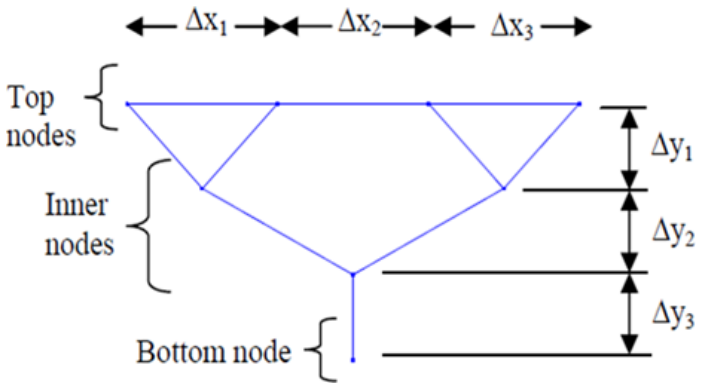

Fig (2.8): Hunt et al. Form-Finding Method Geometry Definitions [18]

In 2011**,** Houston [19] highlighted a shaping approach that avoids the need for high-end equipment and complicated mathematical models, structural concepts of load flow were the root of that approach. The researcher presents a method for determining the shape of solid masses that relates the flow of stresses to prospective load-bearing façades. The dendriform, which is the tree-like column shape, is the focus of this research. This research looks at how dendriform may be proven to be qualitatively exemplifying load flow while maintaining architectural aesthetics by studying typical load flow trends and removing the minimally stressed material from the solid body. The researcher devised a method for determining the geometry of the branching column as shown in Fig (2.9). The method combines two techniques: classical statics and graphical statics.

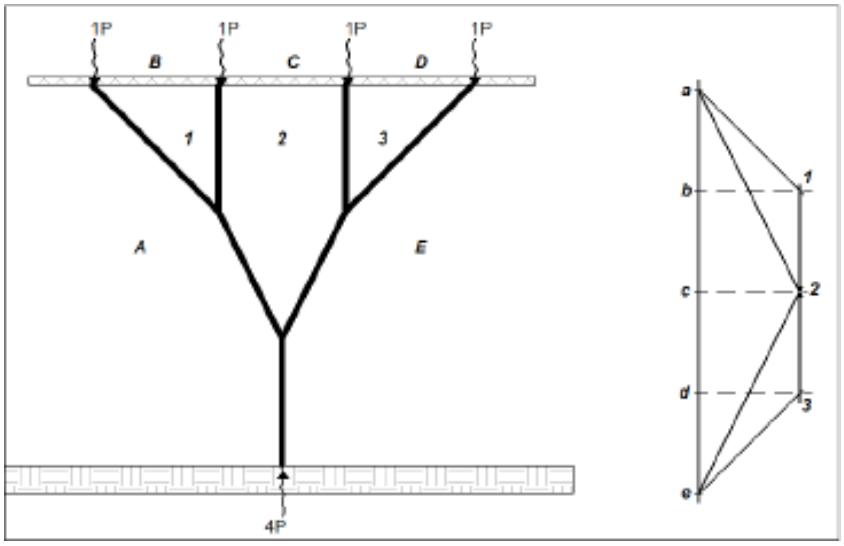

Fig (2.9): Model Proposed by Jonas Henri Houston [19]

2.5 Previous Studies about Structural Behavior of Tree-Like Columns

Tree-like columns are increasingly used in civil engineering as a result of their innovative and fantastic configurations and suitable strength-bearing properties. The path of a form-finding process is an important step in the design stage of the tree-like columns since they are a very complicated space frame structure. A lot of researchers have studied the structural behavior of tree-like columns. These studies can be listed as below:

In 2006**,** Minggui and Feng [20] explained how to design, manufacture, and install tree-like columns made of steel pipes. The goal of the study was to share the experience of employing tree-like columns with steel tubes in large-scale projects and in creative steel structure architecture, in order to improve tree-like column with steel tube design processes. They used the SAP 2000 program to examine a park pavilion construction with a long corridor made up of single rows of trees. The tree height, length, and width are 10 meters, 20 meters, and 10 meters, respectively. The wind load was added to the self-weight load by the tree-like column. These studies concentrated on the foundations of tree-like structures exposed to a constant wind load and did not investigate the arrangement of

branches or form in general. According to the study findings, failure in this kind of column, which is exposed to wind load, occurs first in the foundation. The research conclusion can be summarized as follows:

1. To prevent collapse, the foundation for single-row or single-root tree-like columns must be stable and "deep-rooted."
2. Because a tree-like column has a large column distance, it is best to employ a pile foundation.
3. To prevent over-rising, a separate column base should be used, which should be enlarged in the direction of bending moments.

In 2006, Buelow [21] described approaches for locating tree-like columns and reviewed some of the earlier work on these structures. He also used a specific design example of a treehouse made for disabled children; Fig (2.10) shows the results of the form-finding approaches with thread models. To make this model, the researcher employed hollow round steel parts of one size. The researcher found that this design is effective for usage in wide regions subjected to strong winds, as well as for quick construction and a limited number of features.

(a) **(b)**

Fig (2.10): Treehouse Design Founded by Buelow. (a) Front view, (b) Rear view [21]

In 2010, Chen Jun et al. [22] investigated the ultimate strength, shape, durability, and materials used to construct tree-like steel columns. The results of an actual project (Golden Tree of Shenzhen Cultural Center) study were compared to the design details using ANSYS software. The researchers also planned a series of trials to determine the effect of the joint. They concluded that the tree-like steel column is ideal for usage in many places because of its attractive appearance, lightweight, and high bearing strength. In addition, the branching junction is critical because it serves as a turning point in the failure stage.

In 2013, Hui-jun et al. [23] investigated the reliability, sensitivity, and correlation of the tree-like column. As variables, they consider steel young modulus, member wall thickness, external radius, and vertical load. According to their layouts, the tree-like columns were divided into four categories. Maximum nodal deflection, maximum strain, natural frequency, and model buckling value are among the four types of performance functions that are considered. This study is one of the few that investigated the facts of branching columns. The following points can be used to describe their findings:

1. The external vertical load was strongly related to the maximum sensitive nodal deflection.
2. In the column bottom and second level branches, the buckling eigenvalue and natural frequency of the first value are more sensitive to material and geometrical parameters.

In 2014, Jose et al. [24] introduced an analytical study for the Melilla project's Natural Interpretation Centre. The proposed designs were examined on computer programs, and the best design for implementation was selected. The researchers also investigated the best approach for branch distribution as well as the best surface nature. Because the project is being conducted in a place with a variable

and very windy climate, they created an indication of the materials used in the implementation and their suitability for the structural design of the project.

In 2018, Zhao et al. [25] employed a systematic method for analyzing and designing tree-like steel columns. This method includes all stages of designing the tree-like columns, starting from establishing the topology to defining the cross-sectional area. First, a topological technique based on existing finite element codes was introduced, and then it was used to do a form-finding study. After optimizing the shape, GA was used to create the cross-section area. The GA may be used to determine optimized area ratios at various levels. The conclusion was that even when the maximum permitted change happened, the optimal area proportions of the components of different levels remained consistent, and the square of a cross-section area was computed to be the buckling load factor ratio of a distinct case. According to the requirement for buckling capacity, the maximum area of the components can be established.

In 2020, Khamees and Shadhan [26] studied experimentally the effects of the horizontal spacing between branches, the numbers of branches and branching levels on seventeen steel tree-like column specimens with rectangular cross-sectional area under static axial load, each specimen have total height (HT) equal to 350 mm and total width (WT) equal to 350 mm. the branches height to total height (HB/HT) were varied from (25% to 75%) while the specimen width to total width (W/WT) were varied from (25 % to 100 %). they found that by increasing the horizontal spacing between branches, the failure and buckling loads decreased with an increase in vertical displacement. Increased branches number resulted in a slight increase in failure load when vertical displacement was also increased, while increasing the number of branching levels leads to a decrease in failure load and an increase in vertical displacement.

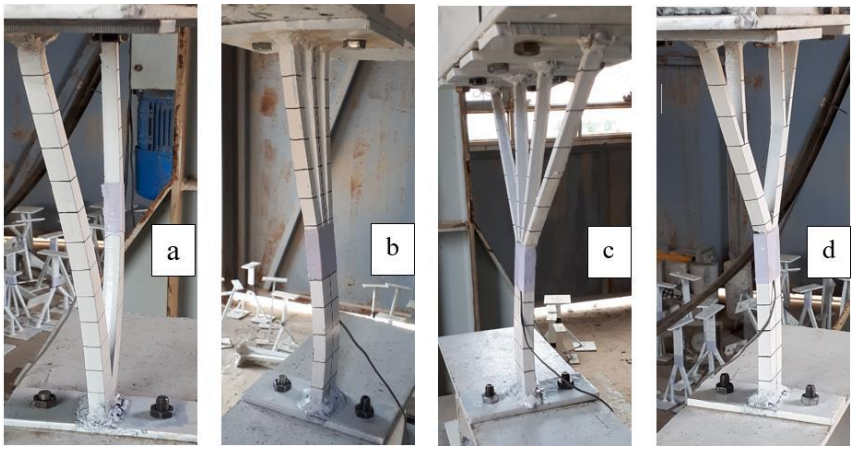

Fig (2.11): Specimens with different branches conducted by A. A. Khamees [26]

In 2021, Khamees and Shadhan [27] Conducted an experimental study on seventeen plane steel specimens with a rectangular cross-sectional, the area of trunks (A0) equals to 480 mm^2, the area of first branched level equal to half area of a cross section area of trunk (A1 = A0 / 2). While the area of second branching level equal to quarter area of a cross section area of trunk (A2 = A0 / 4) or (A2 = A1 / 2). each specimen has a total height equals to 350 mm and total width equals to 350 mm. they studied effect of the height of the branch and the width of the sample on the behavior of the Tree-like columns. They found that increasing the ratio of the specimen width to the column's total width under static loading resulted in lower failure and buckling loads and higher maximum vertical displacement. They also discovered that as the branch height to total height ratio is increased, the failure load and buckling load increase until the ratio hits 100%, at which point the failure load and buckling load drop.

Fig (2.12): Specimens with Different Branching Height Conducted by A. A. Khamees [27]

2.6 Previous Studies about the Joints of Tree-Like Steel Columns

The tree-like column joint is the starting point for the tree-like column branches. As shown in Figure (2.13), each column has several branches that are classified based on their location on the column. The branching joint is an important part of the tree-like columns, and some researchers believe it is the key to failure.

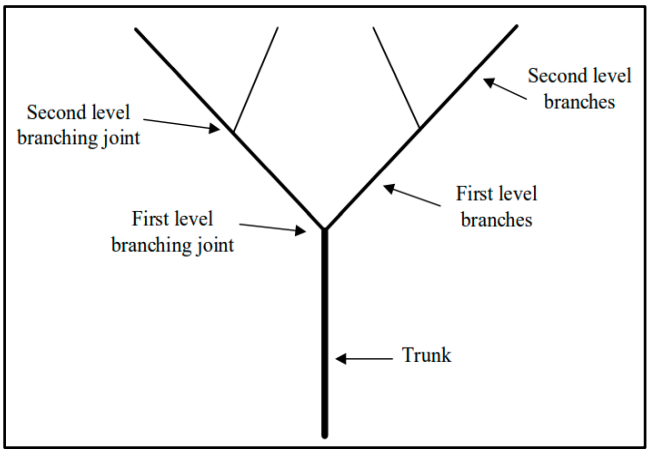

Fig (2.13): Classification of Tree-like column joints. [26]

In 2013, Oliveira et al. [28] looked at how the branching joint affected the final capacity of the tree-like column and how it was implemented. They used the finite element method to analyze the University of Guelph's tree-like column as a study topic (CA-TIA ME2 software package). The boundary conditions for the finite element model were fixing support at the end of the lower trunk and evenly

distributing applied loads from each higher branch to the end of the respective branch, each branch of the joint model was subjected to concentrated loads. They concluded that the generated strains in the branching joint are significant and could be the cause of the columns' failure. They also suggested that the branching column be built from hollow circular steel sections. They've developed a few techniques for incorporating this type of construction and using it to support large-space structures. The finite element model and experimental specimen for the joint are shown in Fig (2.14).

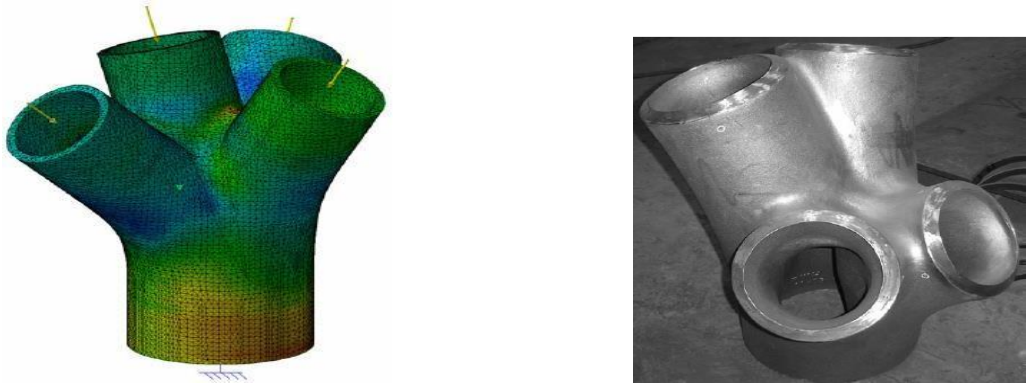

(a) **(b)**

Fig (2.14): (a) Branching Joint Finite Element Model, (b) Joint Manufactured by J. Oliveira et al [28]

In 2014, Weihua and Wenfeng. [29] studied the stress distribution numerically by using the ANSYS program. They analyze stress distribution and the location of maximum stress on the joint under three loading cases: axial loading, bending moment, and axial loading. The effects of the Radis horn and the different chord lengths have been carefully studied. The joint maximum stress under three load cases is dramatically lower than its yield strength, indicating that the joint has adequate safety storage. When the load is successfully applied to the different branches and under the same load condition, the maximum stress and stress distribution of the joint are varied, as the degree of influence. When the proper

inner and outer chamfering radiuses are chosen, the maximum joint stress is considerably lowered. The length of the branches has a negligible impact on the maximum join stress.

In 2014**,** Zhu et al. [30] examined the mechanical properties, estimating approaches, and structural topology optimization for three branching joints. A parametric analysis was performed to completely understand the impact of the diameter, wall thickness, and fillet of the branch radius, the angle between the trunk and branches, and other factors on the stress of the joint. The ANSYS program was used to study the branching junction with steel properties: steel, JB/T6402, cast-steel. It has a tensile capacity of 235 N/mm2 and an elastic modulus of $2.0x10^5$ N/mm2. They also used the SOLIDWORK program to model and mesh branch joints with the tetrahedral element type. They concluded that the maximum joint stress was significantly affected by bending moment. Fig (2.15) shows the three simulated modes of failure of a three-branch joint including: the trunk yield mode, the local buckling mode, and the branches tearing mode.

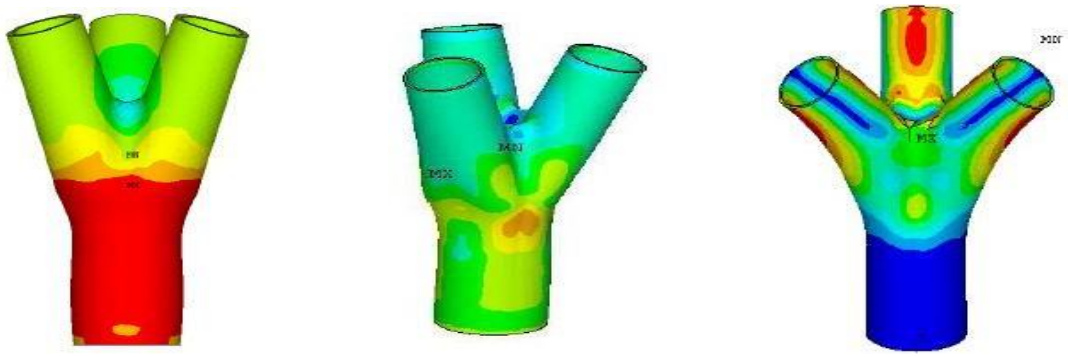

a **b** **c**

Fig (2.15): Failure mode of joints by FE analysis, (a) Trunk yield mode, (b) Local buckling mode, (c) Branches tearing yield mode. [23]

In 2017, Wenfeng Dua [31] studied the performance of a ZG20SiMn steel full-scale three-branch joints of a tree-like column structure subjected to eccentric load. The investigation was conducted in a numerical simulation and experimental verification framework using SOLID WORK numerical code followed by ANSYS code analysis. The analyzed joint had a modulus of elasticity, a yield strength, and a Poisson's ratio of 2.0 x10^5 N/mm^2, 235 MPa, and 0.3, respectively. The joint main pipe length was 806 mm, the diameter was 495 mm, and wall thickness was 39.5 mm. The branching pipe of the studied steel joint had a length of 1200 mm, a diameter of 345 mm, and a wall thickness of 34.6 mm. Also, the chamfer R1 was 994mm and the chamfer R2 was 20.46mm. The authors concluded that failure of joints under eccentric load causes them to experience buckling at the compression side of the main pipe. Fig (2.16) shows the details of the specimen and the failure mode.

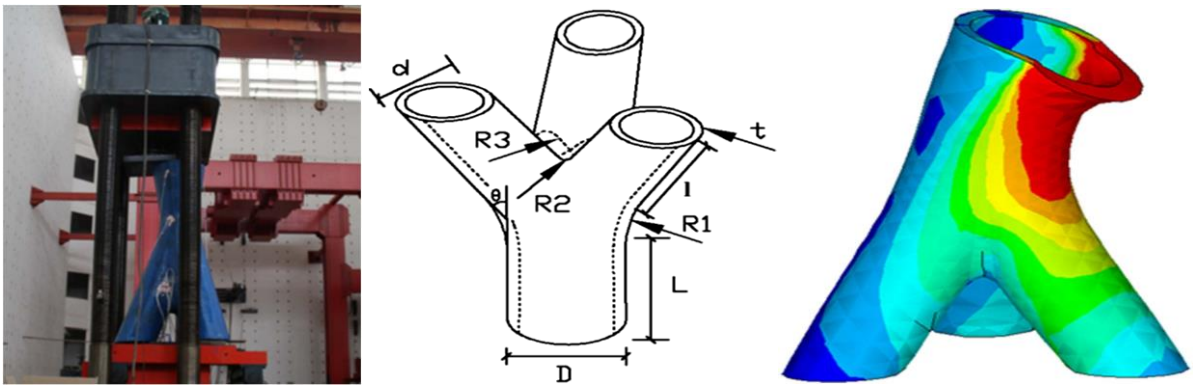

Fig (2.16): (a) The loading unit and the joint specimen, (b) The joint's geometrical characteristics, (c) Failure mode for the joint model [31]

2.7 Previous Studies on Columns that are subjected to Lateral Loads

The studies about tree-like columns were conducted to investigate the structural behavior of these columns under the action of axial loading only. So, this section will review the research on non-branched that are subjected to combined axial and lateral loads.

Nassr et al., 2013 [32] studied the dynamic performance of thirteen wide flange steel columns subjected to intense, quick, and out of plane blast loading in addition to a static axial load equivalent to 25% of the column's static axial capacity. The static axial load was applied to the columns by prestressing. The study concluded the following:

1. The maximum lateral displacement due to blast pressure may decrease due to the P-δ effect, or increased due to the elongation of the column.
2. Applying 25% of the column static axial capacity, the lateral displacement was lowered by the axial more clearly compared to a similar case when no axial force existed providing that the column didn’t experience plastic deformation.
3. While P-effect governed the response of the columns that had plastic deformation, axial load seemed to increase the column's maximum lateral deformation by up to 158%.

Hosseini et al., 2013[33] tested the structural behavior of laced columns with a ¾ scale subjected to cyclic lateral loading. Lacing was accomplished by two main chords and plates.

The researchers concluded the following:

1. The laced columns ductility was found to be mainly influenced by axial compressive loading. The columns ductility was also noticed to be greatly decreased at large axial loads.

2. A decline in the strength and stiffness of the analyzed structure was noticed to occur due to the axial load. However, this decline did not seem to be related to the distance between the chords by any means. The decline of the stiffness was more noticeable than the decline of strength.
3. The built-up laced columns demonstrated rather good seismic properties in the tests, suggesting that they might be used in moderately earthquake-prone areas.

Sediek et al., 2020 [34] studied the response of HSS columns subjected to both axial and lateral loads. In their study, an earthquake was simulated using the symmetric cyclic loading protocol. The studied columns were selected such that several factors were covered including ratios of local and global slenderness. The response of HSS columns was assessed based on the critical constant axial load ratio and the post drift strength ratio. After expressing the two above-mentioned performance rations based finite element data, and with the aid of regression analysis, the following four main conclusions could be reached:

i. HSS columns could fail in two modes including global and local modes. Global mode failure occurs when no local buckling in the hinge region exists. Local failure mode occurred in the presence of high local buckling at the column supports. The performance of HSS columns under global failure mode was found to be critically sensitive to three design rations including width to thickness, depth to thickness, and global slenderness ratios. However, local failure mode was principally affected by depth-to-thickness ratio and the initial axial load ratio.

ii. The axial shortening of the analyzed HSS columns was found to be directly proportional to the depth to thickness ratio and the initial axial load level.

iii. HSS columns having weights < 150 kg/m showed higher axial strength compared to W-shape columns. This may be attributed to the relatively small

thickness of W-shaped columns lighter than 150 kg/m, which in turn, leads to higher local and global slenderness rations.

iv. The results of the study indicated that the high ductility limitations of HSS columns adopted in the current American Institute of Steel Construction Manual (AISC) need to be reconsidered for being too conservative for the limit of width to thickness ratio but not for the depth to thickness ratio.

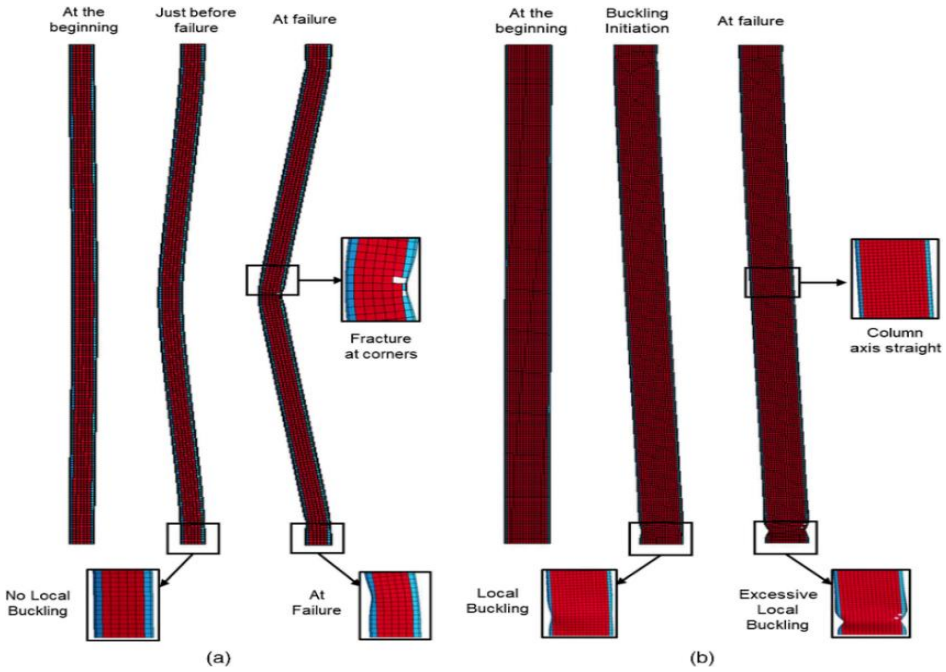

Fig (2-17): Main modes of HSS columns failure with combined loading; (a) global mode and (b) local mode. [34]

CHAPTER THREE

Methodology and Verification

3.1 General

The goal of this chapter is to explain the main steps that are followed to develop the nonlinear FE models that can analyze tree-like steel columns and then simulate them. First, there is the finite element verification, where one model will be created and analyzed first, and then compared with practical results obtained by Khamees (2021) [27]. Then a parametric study will be conducted to investigate other factors affecting the tree-like steel column. The models are drawn and simulated using FE ABAQUS/CAE 2017 software.

3.2 Structures Modeling and Analysis

To create ABAQUS models, three main steps will be followed. Pre-processing, simulation, and post-processing stages are all clearly defined below.

3.2.1 First stage: Pre-processing

It's the first stage in analyzing the tree-like steel column models. At this stage, the physical properties of the models will be defined. Starting from the drawing of parts through the properties, contact, meshing parts, element type, loading, boundary conditions, etc.

3.2.1.1 Parts and Assembly

Each model in this study consisted of five parts as follows:

1. 150 mm long, 80 mm wide, and 8 mm thick plates to serve fixing the steel at both the upper and lower ends.

2. A 400 mm long, 150 mm wide, and 20 mm thick rigid loading plate at the upper end that facilitates the loading process and serves as a diaphragm above the column.

3. Plane steel tree-like columns, where six different specimens are tested under axial and lateral loads.

All parts are drawn separately then assembled to gather as shown in Fig (3.1).

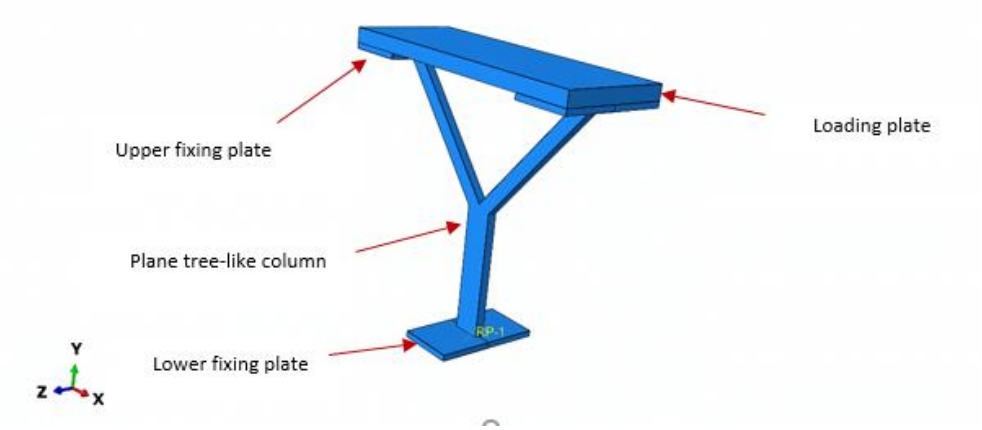

Fig (3.1): The Assembled Parts of Tree-Like Steel Column Model.

In this research six tree-like column specimens are used to study the behavior of the tree-like columns. All specimens have total height (HT) equals to 350 mm and total width (W) equals to 350 mm and branching height (HB)=175 mm. The dimensions for each column are presented in Table (3.1)**.** where the Specimen with rectangular cross section has the symbol TR-1-2 where (R) refers to the rectangular cross-sectional area, the number (1) means one branching level and the number (2) means two branches within the level. While the specimens with circular HSS have a name according to the symbol (TCn-BL-BN), where the letter (T) refers to the tree-like column, (C) refers to the circular HSS, (n) refers to the D/t ratio for circular cross sections, (BL) refers to the number of branching levels, and (BN) refers to the number of branches within the level.(A0)refers to the area of the trunk ,(A1) is the area of the first level branches and (A2) is the

area of the second level branches.(Ø1) is the angle between first level branches,(Ø2) is the angle between second level branches. The details of tree like column specimens are shown in Fig (3.2).

Table (3.1): Dimensions and Details of Specimens

Model's No.	Symbol	Details
1	**TR-1-2**	**For trunk** Rectangular cross-sectional area = 480mm^2 Cross section dimensions= 40mm×12mm **For branches** Rectangular cross-sectional area =240mm^2 cross section dimensions= 20mm×12mm
2	**TC8-1-2**	**For trunk** Circular HSS cross-sectional area = 480mm^2 Diameter = 35mm, thickness=4.4mm, d/t=8 **For branches** Circular HSS cross-sectional area =240mm^2 Diameter =25mm, thickness=3.1 mm, d/t=8
3	**TC14-0-0**	**For trunk** Circular HSS cross-sectional area = 480mm^2 Diameter = 47mm, thickness=3.3mm, d/t=14 **For branches** No branches (single column)

Continue table (3.1): Dimensions and Details of Specimens

4	**TC14-1-2**	**For trunk** Circular HSS cross-sectional area = 480mm^2 Diameter =47mm, thickness=3.3 mm, d/t=14 **For branches** Circular HSS cross-sectional area =240mm^2 Diameter =33mm, thickness=2.4mm, d/t=14
5	**TC14-2-4**	**For trunk** Circular HSS cross-sectional area = 480mm^2 Diameter =47mm, thickness=3.3 mm, D/t=14 **For first level branches** Circular HSS cross-sectional area =240mm^2 Diameter =33mm, thickness=2.4mm, D/t=14 angle between first level branches=83.4 branches **For second level branches** Circular HSS cross-sectional area =120 mm^2 Diameter =24mm, thickness=1.7 mm, D/t=14 angle between second level branches=42.1
6	**TC21-1-2**	**For trunk** Circular HSS cross-sectional area = 480mm^2 Diameter =57mm, thickness=2.7mm, d/t =21 **For branches** Circular HSS cross-sectional area =240mm^2 Diameter =41mm, thickness=1.9mm, d/t=21

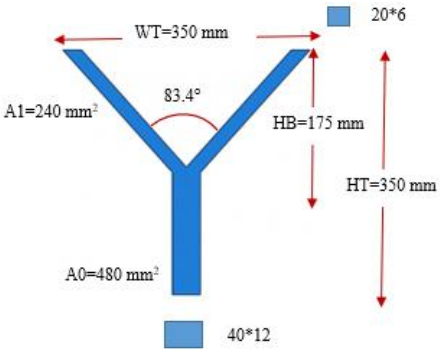

TR-1-2

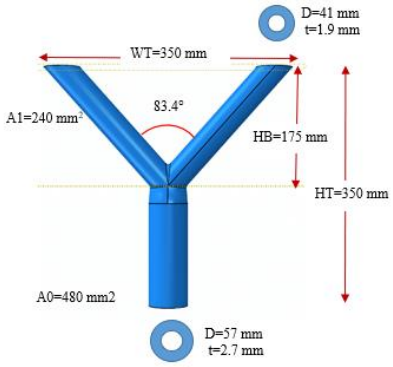

TC21-1-2

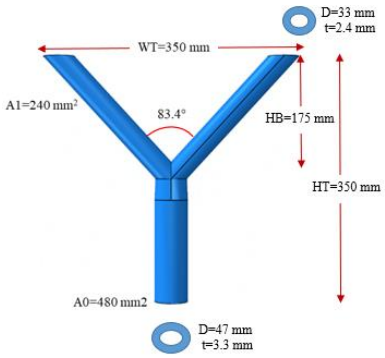

TC14-1-2

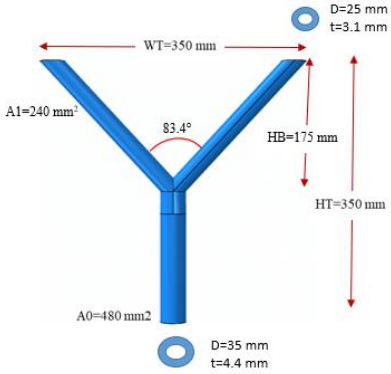

TC8-1-2

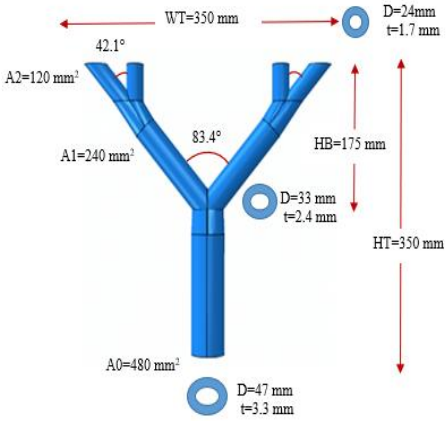

TC14-2-4

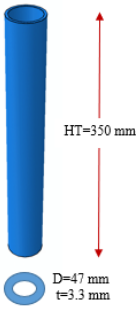

TC14-0-0

Fig (3.2): Details and Dimensions of Tree-Like Column Specimens

3.2.1.2 Properties of Material

Material modulus of elasticity, Poisson's ratio, and stress-strain relationship are among the most important properties that govern the response of structures analyzed under loads in 3D finite element analysis. Since all specimens are made of steel materials, Poisson's Ratio was set at 0.3 for all steel materials. Stress strain curves for the materials are shown in Fig (3.3). The steel modulus of elasticity was set at 203 GPa for the tree-like column specimens and 400 GPa for the loading plate to make it work as a rigid plate.

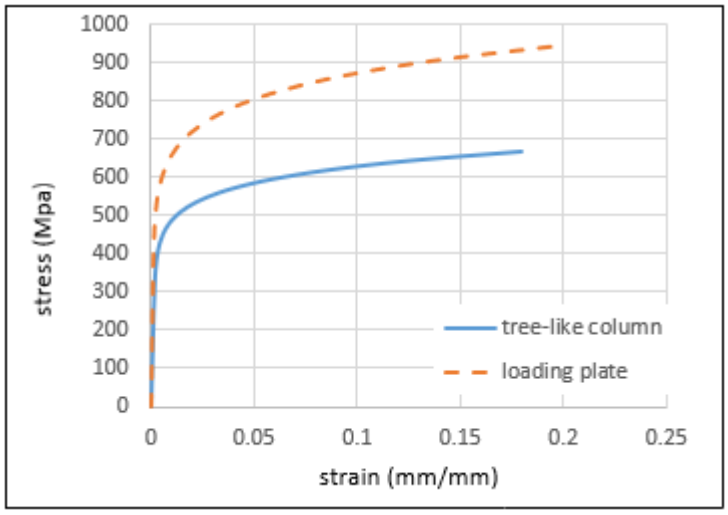

Fig (3.3): Stress Versus Strain Curves Used in the FE Models [26]

3.2.1.3 Interaction of Modeling

After assemblage of the parts, the attachment between all parts was a tie constraint. The lower fixing plate was restricted as a rigid body as shown in Figures (3.4), (3.5), and (3.6).

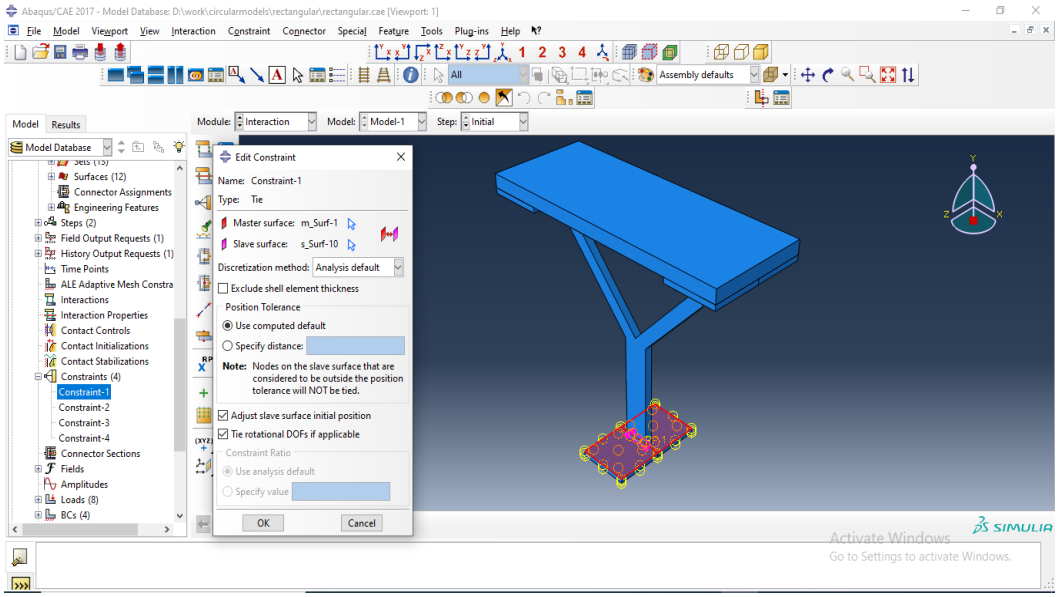

Fig (3.4): Interaction Between Lower Fixing Plate and Tree-Like Column Specimen

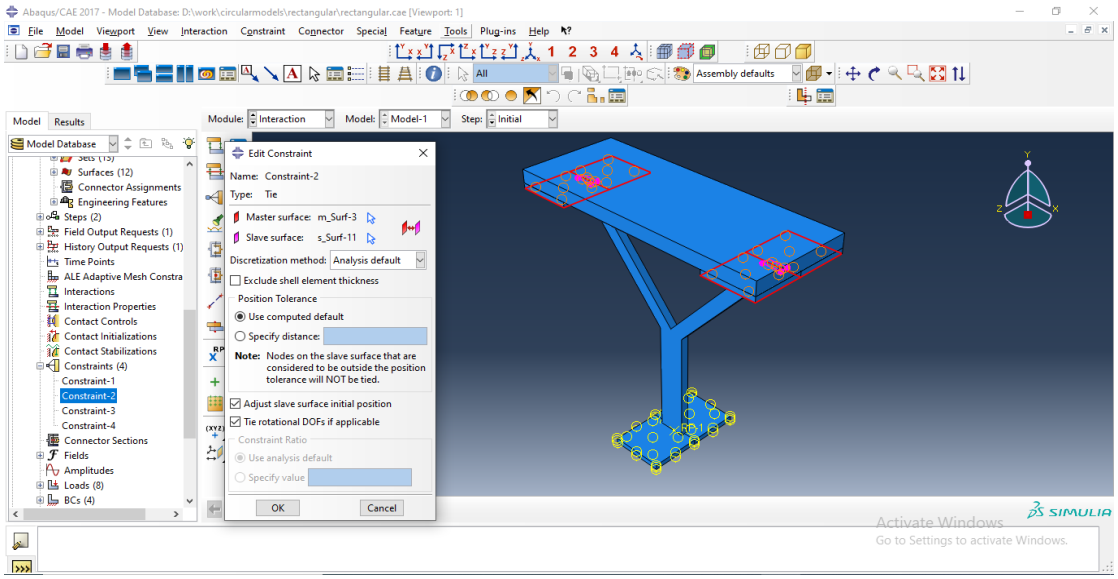

Fig (3.5): Interaction Between Tree-Like Column Specimen and the Upper Fixing Plates

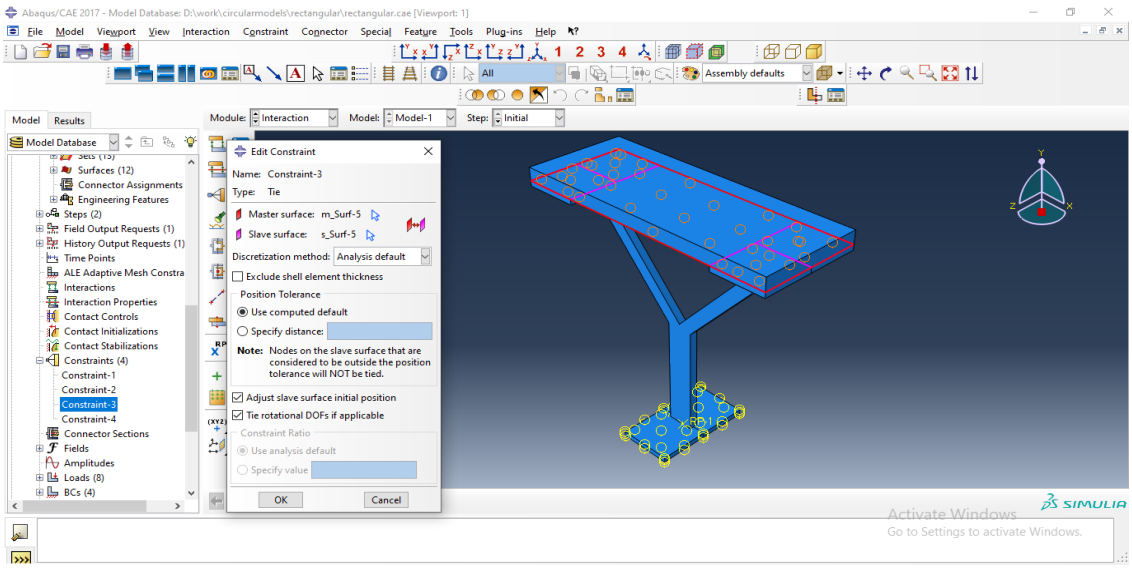

Fig (3.6): Interaction Between the Upper Fixing Plates and the Loading Plate.

3.2.1.4 Loading and Boundary Conditions

The finite element model is loaded at the same locations on the loading plate for all the tree-like column specimens. The axial load was applied to the loading plate in a manner of surface pressure, lateral loads acted as concentrated forces at set of nodes on the loading plate. The value of lateral load is applied as a ratio to the axial load, where the lateral to axial load ratio is taken as (0, 0.2, 0.4, 0.6, 0.8, and 1).

The boundary conditions of the models are modeled in three cases depending on the applied load as follows:

1. When axial load is only applied, the displacement is constrained in the x, y, and z directions at the lower fixing plate while it is allowed to move vertically in the y direction only at the upper end of the loading plate, as shown in Fig (3.7).
2. When axial load as well as lateral load are applied, the displacement is constrained in the x, y, and z directions at the lower fixing plate while it is

allowed to move vertically and laterally in the x and y directions at the upper end of the loading plate, as shown in Fig (3.8).

3. When lateral load is only applied, the displacement is constrained in the (x, y, and z) at the lower fixing plate while it is allowed to move laterally in the x direction only at the upper end of the loading plate, as shown in Fig (3.9).

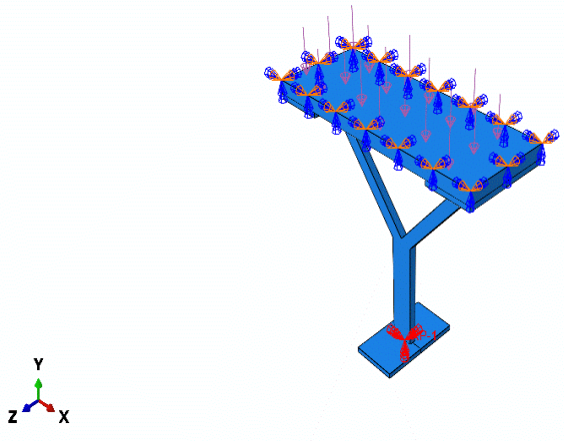

Fig (3.7): Applied load and Boundary Conditions When Axial Load Only is Applied

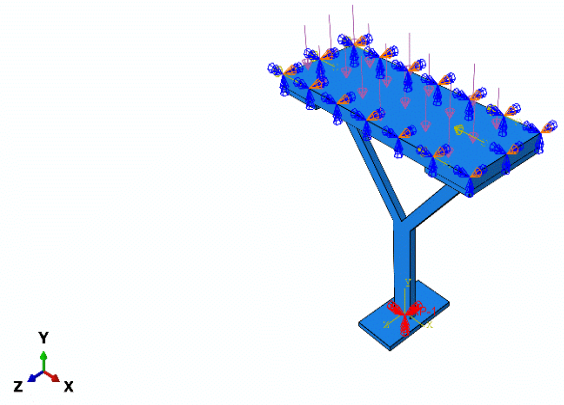

Fig (3.8): Applied Load and Boundary Conditions When Axial and Lateral Loads Are Applied

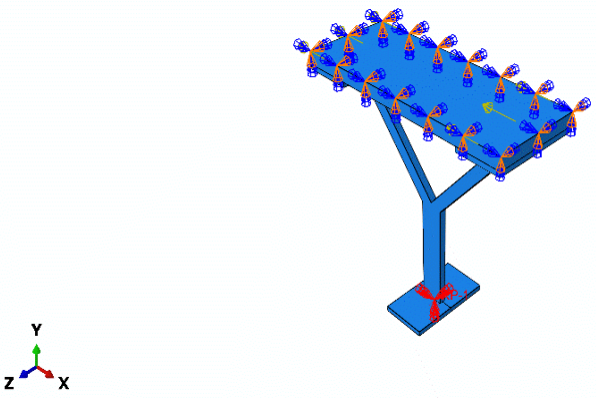

Fig (3.9): Applied Load and Boundary Conditions When Lateral Load Only is Applied

3.2.1.5 Meshing

Meshing is one of the more important steps in making a model because it has a significant effect on the accuracy of the results, the shape of failure, and the model's overall behavior. Two sections are necessary to be defined at meshing, which are element size and element type. Element size is important to achieve convergence of outcomes at the verification step. In this study, the number of elements was changed to obtain the same behavior for the models and tested specimens in terms of failure mode. The element size is set at 8 for all models. The mesh density for the specimens is shown in Fig (3.10). The selection of element type for any simulation is required to achieve the appropriate reliability. There are two categories for the ABAQUS/Standard solid element: the first (linear) interpolation portion and the second (quadratic). For two-dimensional analyses, the first type of element is used, and the second type is used for three-dimensional analysis. ABAQUS offers several options, such as linear, quadratic, brick, etc. Because of the intricate details of the models, this study adopts a 10-node quadratic tetrahedron element type with improved surface stress visualization. This type was recommended in literature [35].

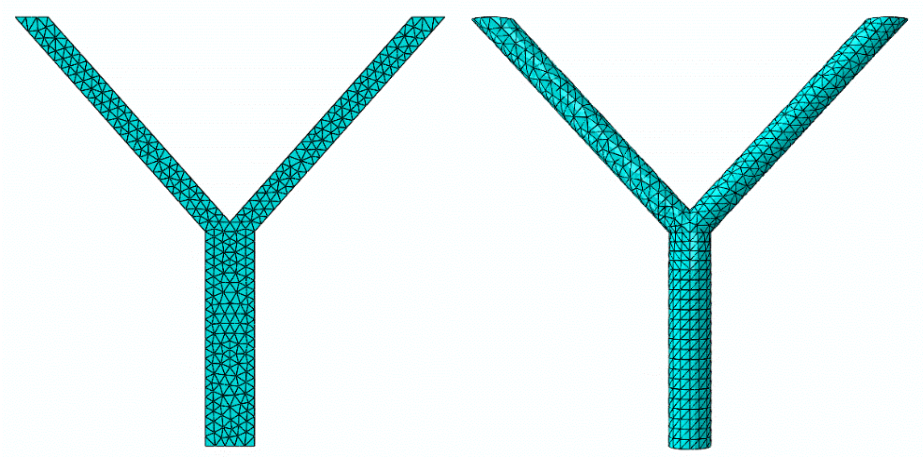

a **b**

Fig (3.10): Models Mesh Density, (a) Rectangular Model, (b) HSS Circular Model

3.2.2 Second stage: Simulation Process

The simulation is usually run in the background. The ABAQUS input file that has already been prepared solves the numerical difficulty mentioned in the model at this stage. To solve non-linear problems, ABAQUS employs the Newton-Raphson approach in simulation. In contrast to linear regression, the load applied to the process in a nonlinear situation is gradual. At the end of each load increase, ABAQUS divides the simulation step into multiple load increments and determines an average system consistency. Depending on the capacity for a particular load increase, ABAQUS may require numerous iterations to find an appropriate solution [36]. On the other hand, the approximate solution is the combined integration of all the load incremental replies. ABAQUS offers incremental and iterative approaches to solve non-linear problems. The analytical process, load increase, and iteration are the three phases of the simulation stage. Loading and analysis requests are typically part of the assessment phase. Static riks was the sort of analysis used in this study because it is more sensitive to local buckling. In the increase phase, the user specifies the first load increment, and

ABAQUS calculates the successive increments. Iteration continues until the residual force is calibrated by ABAQUS to the tolerance value specified. As a result, following each load increase, the system should follow the balancing criteria, and the appropriate output request values should be placed in the output database file.

3.2.3 Third Stage: Post-Processing

At this stage, the program gives what variables are to be measured after the end of the simulation, for example, pressures, stresses, reaction forces, displacements, failure modes, etc. In this research, axial and vertical failure loads and displacements must be established, as well as the failure mode, which is important to show the behavior of models under loading.

3.3 Verification

For load deflection performance, maximum strength capacity, and failure mode, the TR-1-2 finite element model was verified using the experimental results obtained by Khamees (2021) [27]. The model analyzed under gravitational static pressure. the load-deflection curve for the tree-like column that was obtained by the finite element analysis and experimental work is shown in Figure (3.11). The difference between the FE Simulation and experimental failure load is (-5.6%) and the correlation coefficient between load points for both experimental and FE results is 0.94, as shown in Figure (3.12). Both the results of the experiments and the corresponding FE simulation identified the same mode of failure as shown in Fig (3.13).

Table (3.2): Experimental Results [27] **Versus FE Results for TR-1-2 Model**

TR-1-2	Failure load (kN)	Vertical displacement (mm)
Experimental results By (Khamees)	53	1.215
FE results	50	1.280

After verifying the model, the model exposed to a variety of axial and lateral loads. Other specimens with pipe HSS were established and analyzed by using ABAQUS program

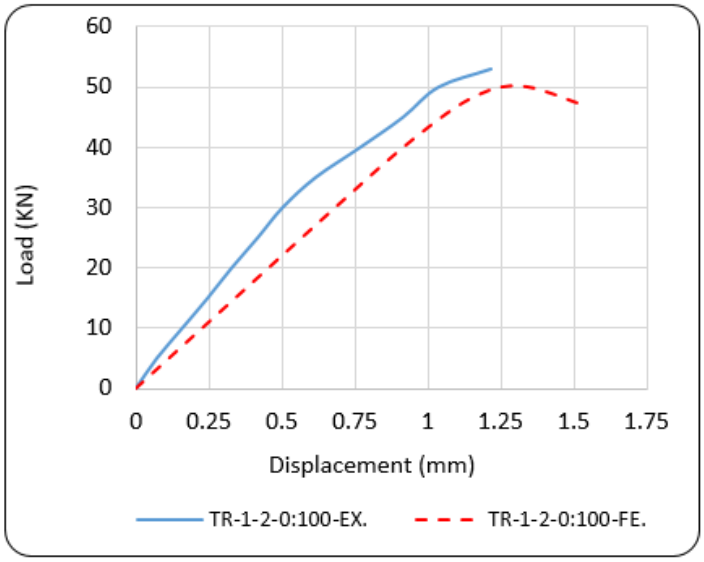

Figure (3.11): Load Deflection Curve of TR-1-2-0:100 for Experimental Specimen Versus Calibrated Finite Element Model [27]

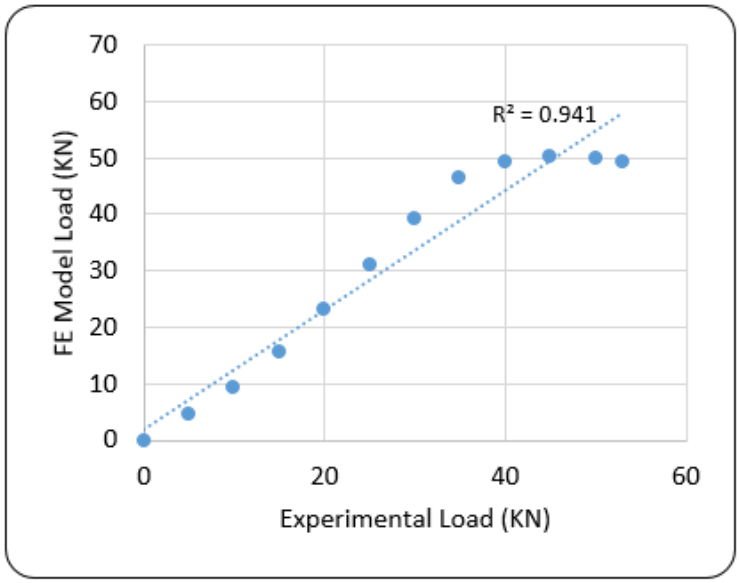

Fig (3.12): Correlation Between Experimental Load and Finite Element Load for TR-1-2-0:100

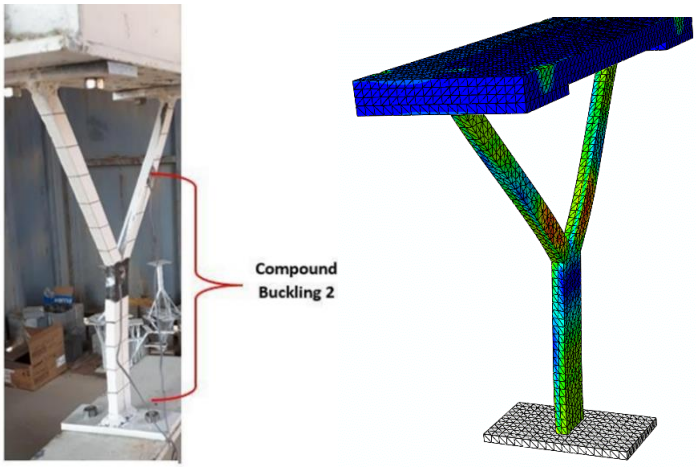

Fig (3.13): Mode of Failure for Experimental Specimen Versus Calibrated FE Mode [27]

CHAPTER FOUR

Results and Discussion

4.1 General

The results of the finite element analysis conducted by the ABAQUS program for all analyzed models are presented and discussed in this chapter. First, the models were exposed to an axial load only, then the lateral load to axial load ratio was increased from 0 to (20%, 40%, 60%, 80%, and 100%), respectively. The last case was loaded with lateral load only. The results included ultimate load, maximum deflection, and failure mode for all models.

4.2 Tree-Like Columns Groups

To understand the behavior of tree-like columns under the geometrical variables easily and clearly, the tree-column models will be classified into the following groups:

Group No. 1: This group consists of two models. The first model has a rectangular cross-sectional area and the second model has a hollow circular cross-sectional area. This column has a D/t ratio of 21, and the two models have one branching level and two branches within the level, as shown in Fig (4.1).

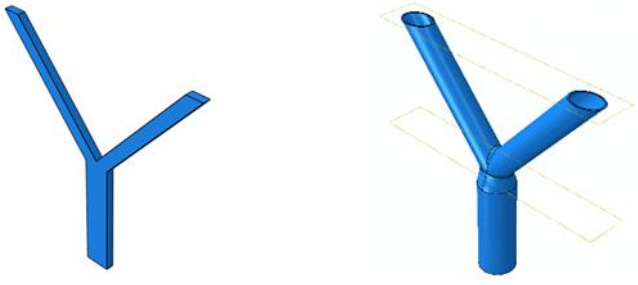

TR-1-2 TC21-1-2

Fig (4.1): Group No.1 (Influence of the Shape of Cross-Sectional Area)

Group No. 2: This group includes three tree-like column models with pipe HSS cross -sectional area and varying (D/t) ratios (21, 14 and 8), for studying the effect of (D/t) ratio on the response of the tree-like columns, all columns with one branching level and two branches within the level, as shown in Fig (4.2).

TC21-1-2 TC14-1-2 TC8-1-2

Fig (4.2): Group No.2 (Effect of the D/t Ratio).

Group No. 3: Three models with different number of branching levels (zero branching level or non-branched, one branching level column, and a column with two branching levels) are found in this group to study the influence of the number of branching levels (BL) on the behavior of the tree-like columns with pipe HSS cross sectional area and D/t ratio equal to 14 as shown in Fig (4.3).

TC14-0-0 TC14-1-2 TC14-2-4

Fig (4.3): Group No. 3 (Effect of Number of Branching Level).

4.3 Non -Branched Column

The hollow circular cross-sectional area of the non-branched column TC14-0-0 model was created using pipe HSS with a standard weight and D/t ratio of 14. All specimens with zero branching level and zero branches and have the same dimensions. The results for this column with different loading cases are presented in Table (4.1) and the load displacement curves for both axial and lateral response are shown in Figures (4.4) and (4.5) respectively.

Table (4.1): Results of a Circular non-Branched Column (TC14-0-0) with Different Loading Conditions

Specimen symbol	lateral /axial load ratio	Axial failure load (kN)	Axial displacement at failure(mm)	Lateral failure load (kN)	Lateral displacement at failure (mm)
TC14-0-0-0:100	0/100	85.877	1.875	0	0
TC14-0-0-20:100	20/100	44.605	2.572	8.921	3.368
TC14-0-0-40:100	40/100	26.665	3.988	10.665	5.413
TC14-0-0-60:100	60/100	18.895	6.479	11.505	7.634
TC14-0-0-80:100	80/100	15.135	6.718	12.108	9.319
TC14-0-0-100:100	100/100	12.504	6.976	12.501	9.786
TC14-0-0-100:0	100/0	0	0	39.055	14.238

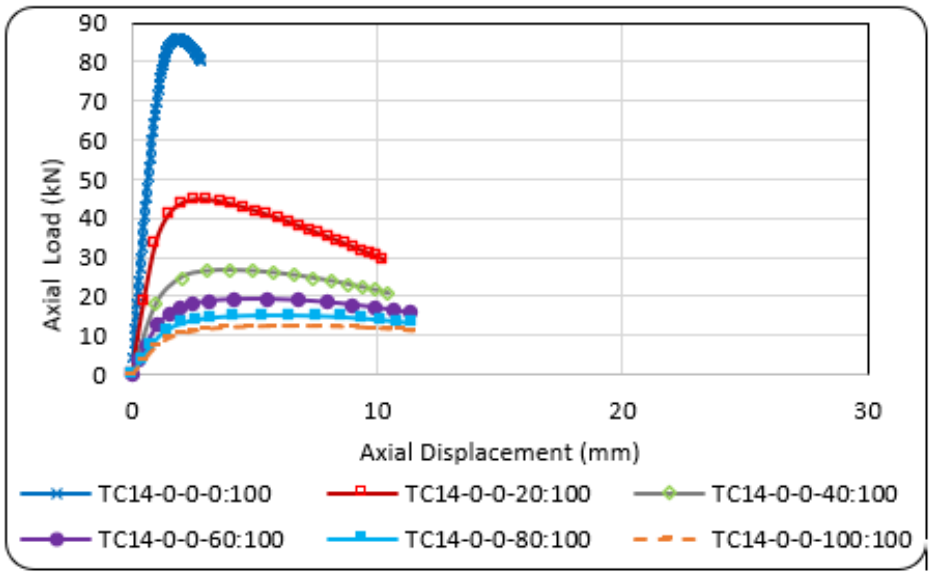

Fig (4.4): Axial Load-Displacement Response for TC14-0-0 Model at Different Loading Ratios

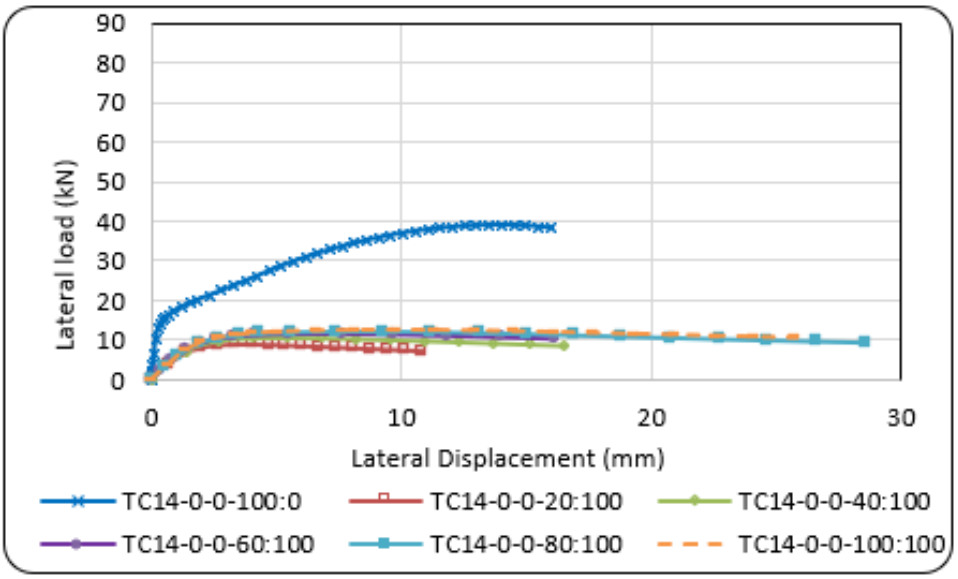

Fig (4.5): Lateral Load-Displacement Response for TC14-0-0 model at Different Loading Ratios

4.3.1 Axial Failure Load and Displacement

According to the axial load displacement response for TC14-0-0, the column appears to be more resistant when subjected to pure axial load. Presence of lateral loading reduces the axial failure load. This reduction in failure load depends on the lateral load that applied to the column. When the lateral to axial load ratio increases by about (20, 40, 60, 80, and 100) %, respectively, the axial failure load decreases by (48, 69, 78, 82, and 85) % as shown in Fig (4.6). This decrease in axial load is accompanied by an increase in axial displacement where the axial displacement increases by (37.2, 112.6, 245.5, 258.3 and 272) %, as shown in Fig (4.7).

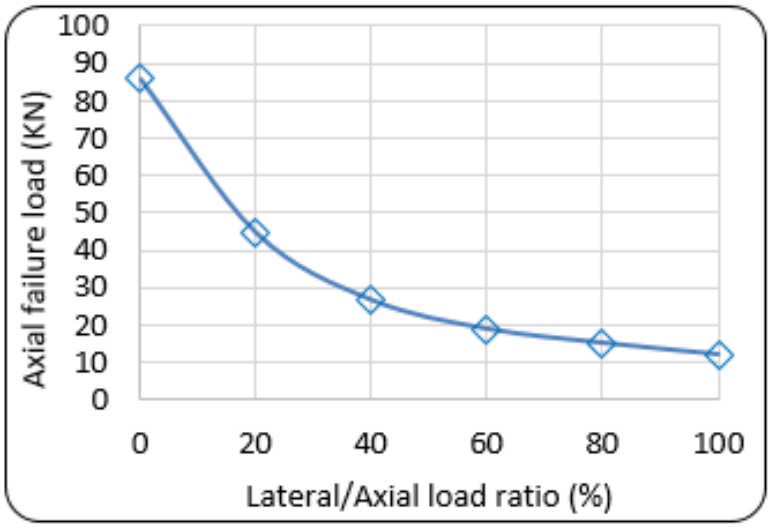

Fig (4.6): Axial Failure Load Versus Load Ratio for TC14-0-0 Model

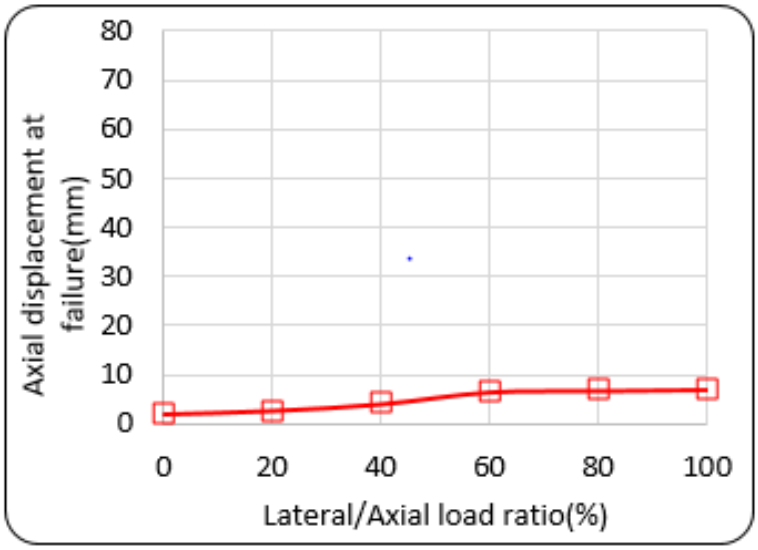

Fig (4.7): Axial Displacement at Failure Versus Load Ratio for TC14-0-0 Model

4.3.2 Lateral Failure Load and Displacement

For TC14-0-0, the lateral failure load was presented graphically for different ratios of lateral to axial load, as shown in Fig (4.8). It can be noticed that when the lateral to axial load ratio increases by about (40, 60, 80, and 100) %, respectively, the lateral failure load increases by (18.4, 28, 39, and 44.4) %. However, the maximum lateral failure load is 25.7 kN when no axial load is applied. Fig (4.9) shows the lateral displacement at failure for different loading ratios. It is obvious that the lateral displacement increases significantly by (60.7, 126.6, 176.7, 190.5) % as the loading ratio increases. When the column is subjected to lateral loading alone, the lateral displacement is high, while it is reduced by 31% if the column is exposed to combined loading. This reduction of lateral displacement may possibly be due to an increase in column axial weight that directly influences the lateral displacement.

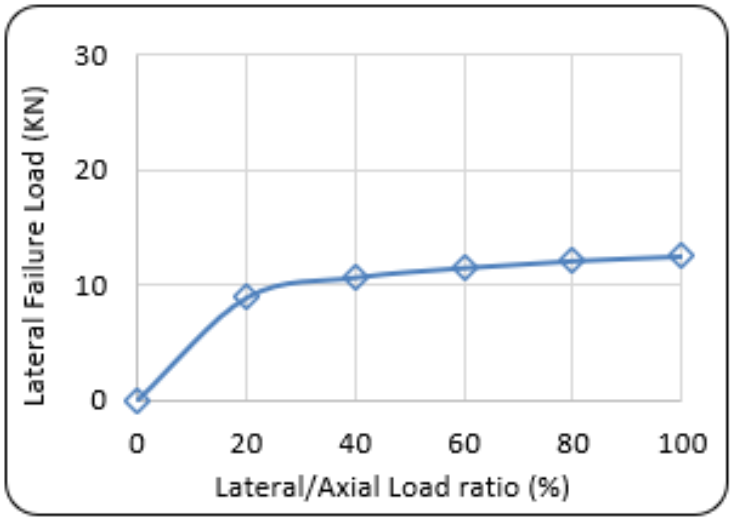

Fig (4.8): Lateral Failure Load Versus Load Ratio for TC14-0-0 Model

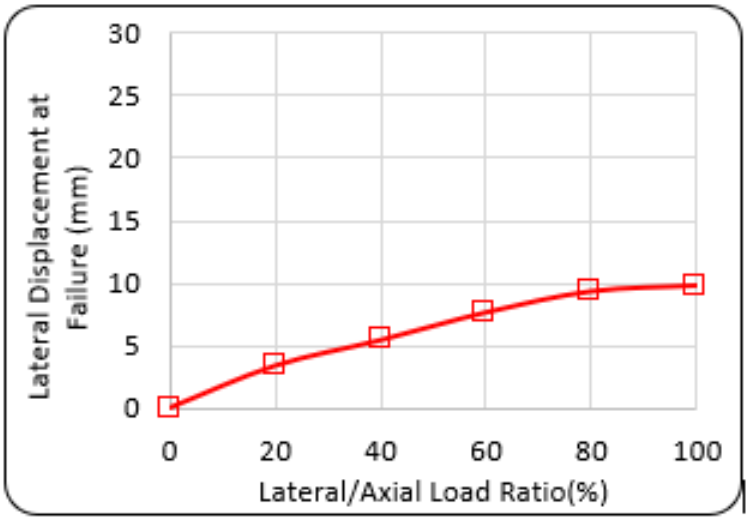

Fig (4.9): Lateral Displacement at Failure Versus Load Ratio for TC14-0-0 Model

4.3.3 Failure mode

The failure modes of the single column TC14-0-0 model for the three cases (axial loading, axial plus lateral loading, and lateral loading only) are shown in Fig (4.10). from the key of the von mises stresses we can notice that the material

yields near the column base the stresses are increased significantly with the increase of lateral to axial load ratio.

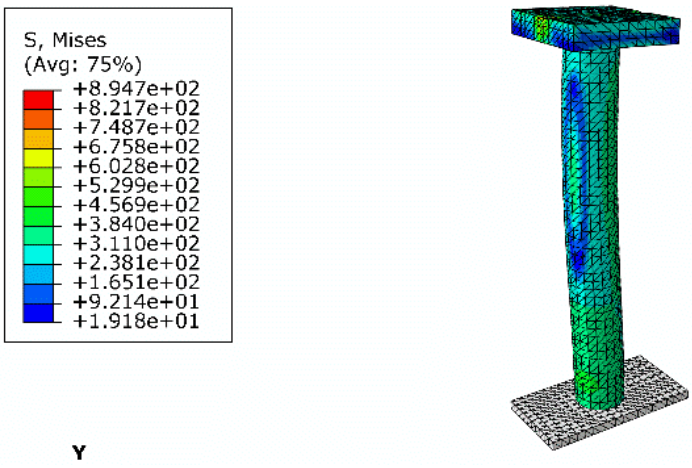

(a) TC14-0-0-0:100

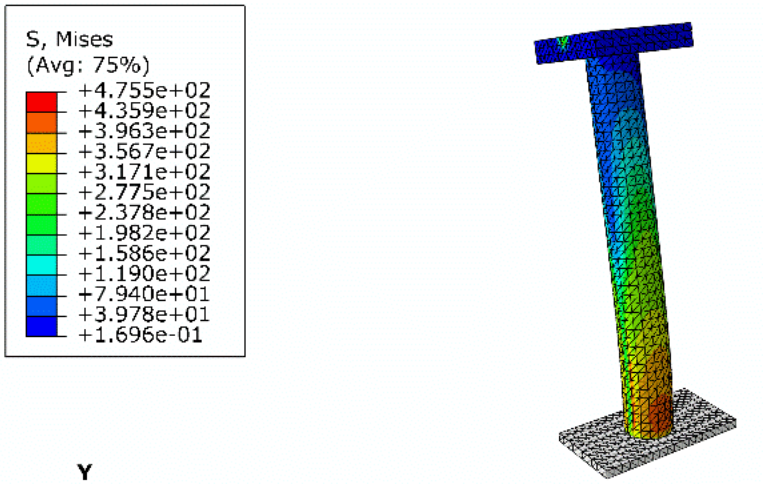

(b) TC14-0-0-20:100

Fig (4.10): Failure Modes for Single Column TC14-0-0

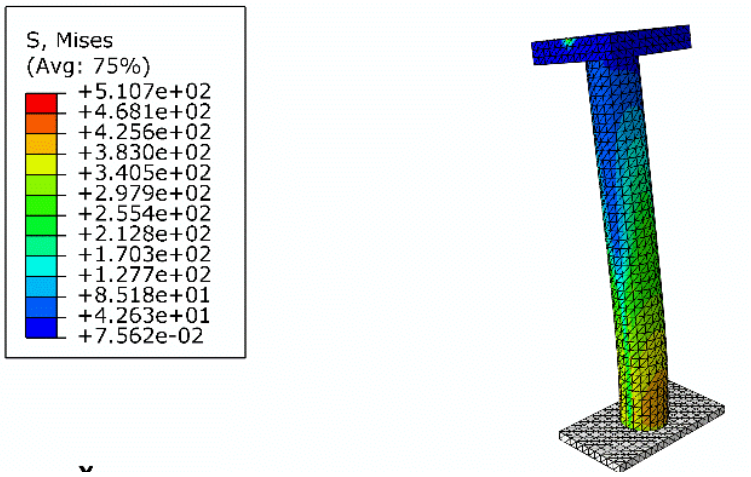

(c) TC14-0-0-40:100

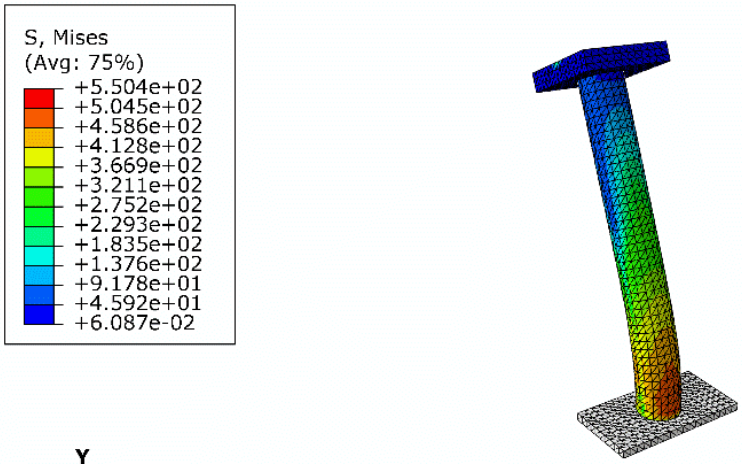

(d) TC14-0-0-60:100

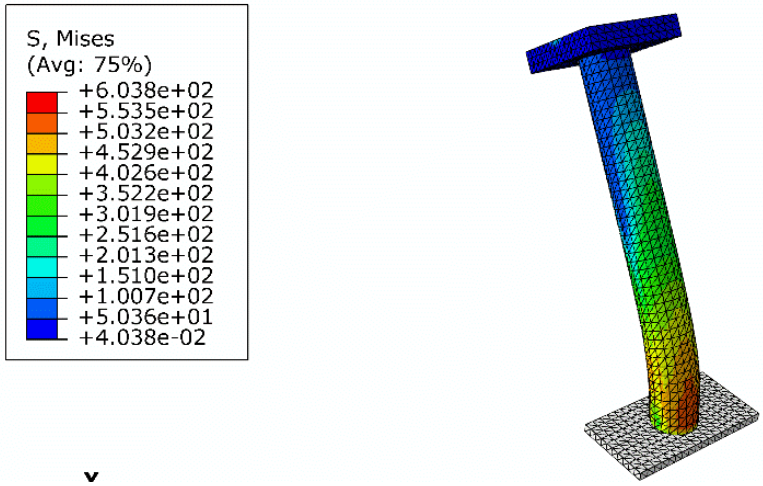

(e) TC14-0-0-80:100

Continue Fig (4.10): Failure Modes for TC14-0-0 Column.

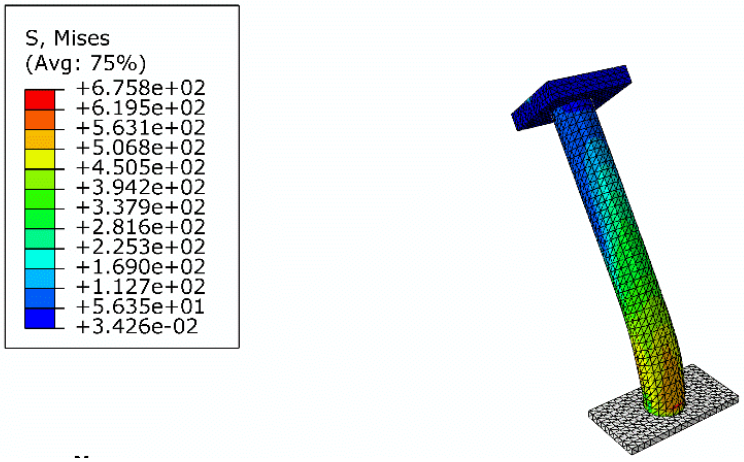

(f) TC14-0-0-100:100

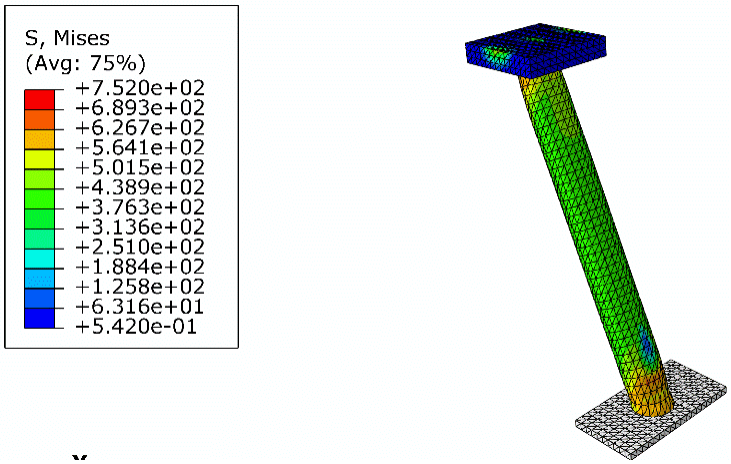

(g) TC14-0-0-100:0

Continue Fig (4.10): Failure Modes for TC14-0-0 Column.

4.4 columns with one branching level.

These columns are made up of a trunk and branches, each of which has one branching level and two branches within it. Four models will be shown in this section. All models have one branching level, but they differ in the shape of the cross-sectional area.

4.4.1 Tree like Column with Rectangular Cross Section

The tree-like column TR-1-2 model with a rectangular cross-sectional area was developed using 12 mm steel plate. The results for this column with the seven loading cases are calculated and presented in Table (4.2).

Table (42): Results of Rectangular Tree -like Column (TR-1-2) with Different Loading Conditions.

Specimen symbol	Lateral/axial load ratio	Axial failure load (kN)	Axial displacement at failure(mm)	Lateral failure load (kN)	Lateral displacement at failure (mm)
TR-1-2-0:100	0/100	50	1.28	0	0
TR-1-2-20:100	20/100	22.7	7.90	4.54	15.37
TR-1-2-40:100	40/100	13.2	11.58	5.26	23.04
TR-1-2-60:100	60/100	9.5	18.54	5.70	35.77
TR-1-2-80:100	80/100	7.5	28.67	6.03	52.54
TR-1-2-100:100	100/100	6.8	37.38	6.87	64.49
TR-1-2-100:0	100/0	0	0	34.15	87.96

The axial and lateral load deflection curves for this column are shown in fig (4.11) and (4.12). The curves became very close after applying 60% of the lateral/axial load ratio, which means that a small amount of horizontal load causes the model to fail with less axial load and higher displacement.

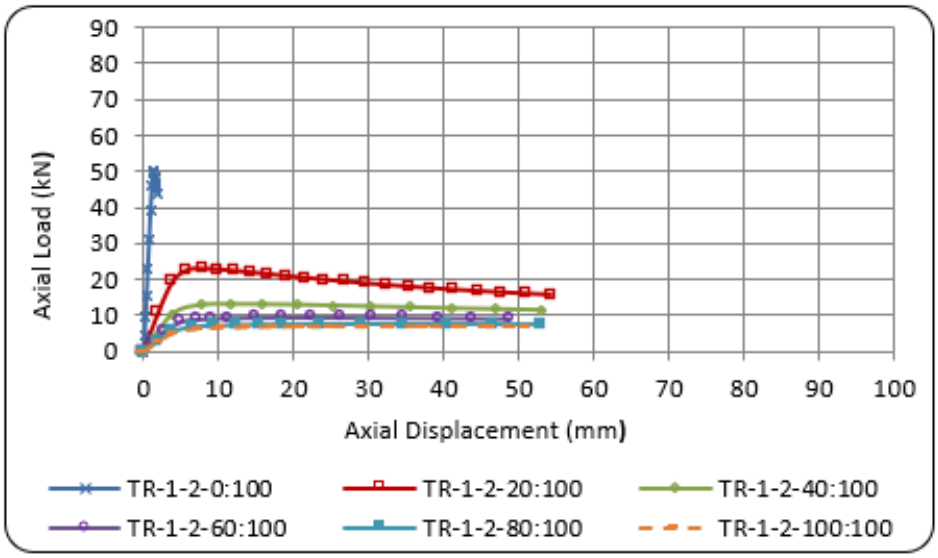

Fig (4.11): Axial Load-Displacement Response for TR-1-2 Model at Different Loading Ratios

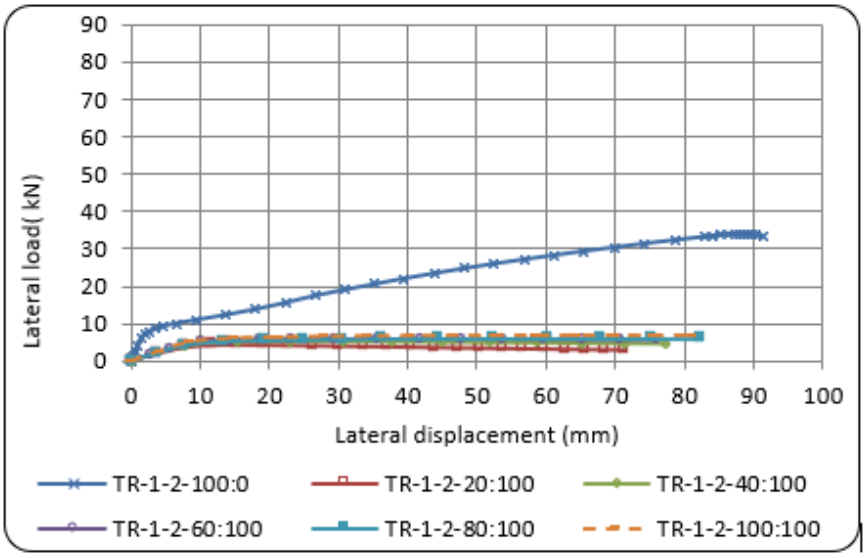

Fig (4.12): Lateral Load-Displacement Response for TR-1-2 Model at Different Loading Ratios.

4.4.1.1 Axial Failure Load and Displacement

For the TR-1-2 Model, the axial failure load reaches its maximum value, which is 50 kN, if the applied load is axial load only, when the lateral to axial load ratio increases by about (20, 40, 60, 80, and 100) %, respectively, the axial failure load decreases by (54.5, 73.6, 81, 85, and 86) % as illustrated in Fig (4.13). Fig (4.14)

represents the axial displacement at failure for different loading ratios. The axial displacement increases significantly by (517, 804, 1348, 2139 and 2820) %. As the loading ratio increases. The presence of axial loading with lateral load worked to decrease the lateral displacement of the column by 27%.

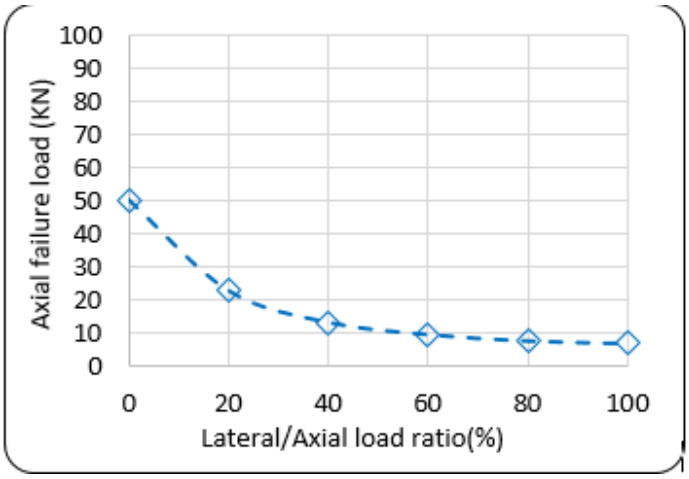

Fig (4.13): Axial Failure Load Versus Load Ratio for TR-1-2 Model

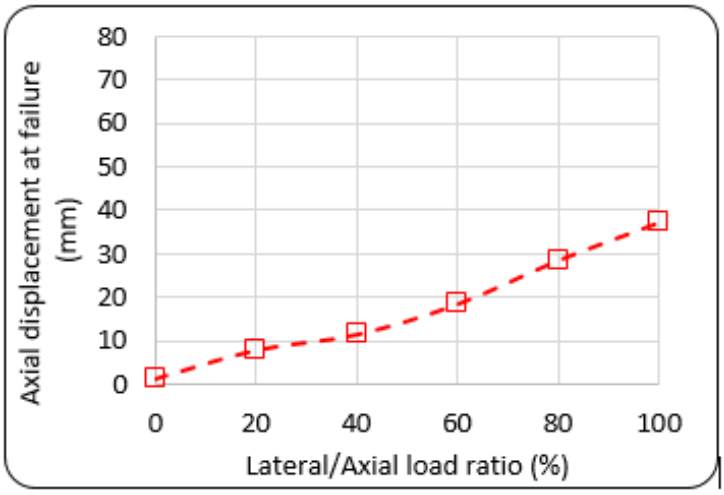

Fig (4.14): Axial Failure Displacement Versus Load Ratio for TR-1-2 Model

4.4.1.2Lateral Failure Load and Displacement

The lateral failure load versus lateral to axial load ratios for TR-1-2 are shown in fig (4.15). When the load ratio increases by about (40, 60, 80, and 100) %, respectively, the lateral failure load increases by (15.6, 25.5, 32.8, and 51) %. While when the applied load is lateral load only, the failure load is 34 kN The

lateral displacement at failure increased significantly by (50, 133, 242 and 320) %.as shown in fig (4.16).

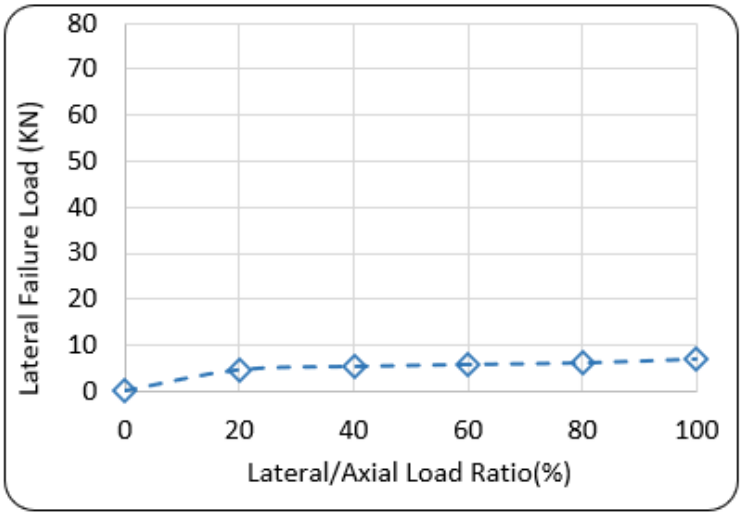

Fig (4.15): Lateral Failure Load Versus Load Ratio for TR-1-2 Model.

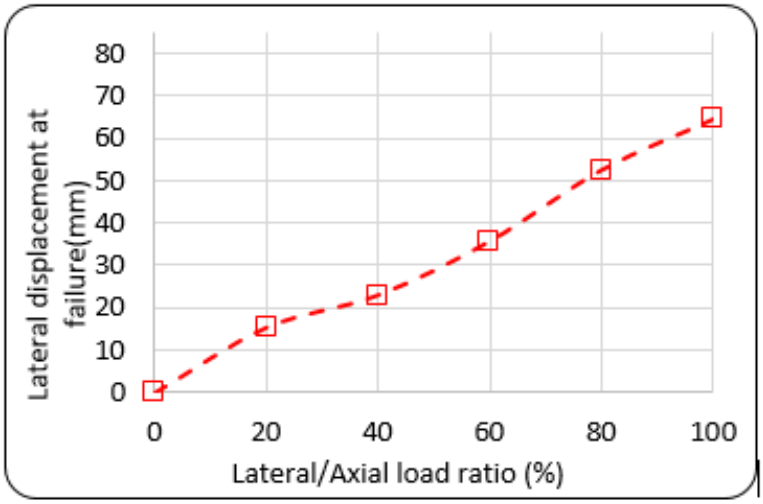

Fig (4.16): Lateral Failure Displacement Versus Load Ratio for TR-1-2 Model

4.4.1.3 Failure mode

The failure modes for the tree-like column TR-1-2 are shown in Fig (4.17). from the von mises stress key in (Mpa), it can be seen that when the lateral to axial load ratio is zero (axial load is the only load applied to the column) the maximum stress value is mainly at the lower end of the trunk, the stress in the branches is

obviously less than the stress at the trunks lower end. by increasing the lateral to axial load ratio, the stress at the joint area is gradually increases.

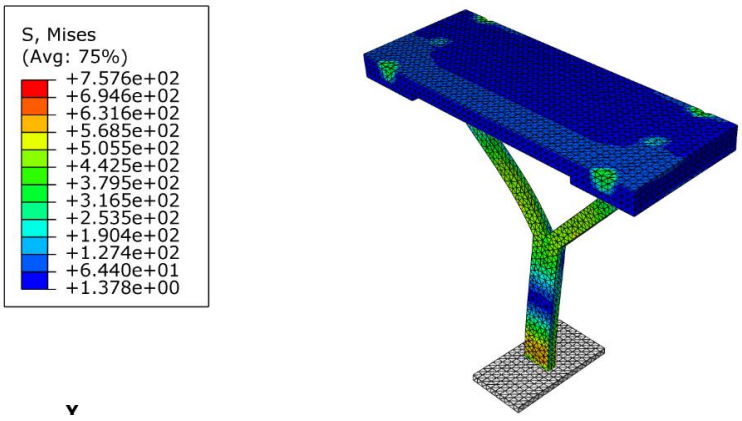

(a) TR-1-2-0:100

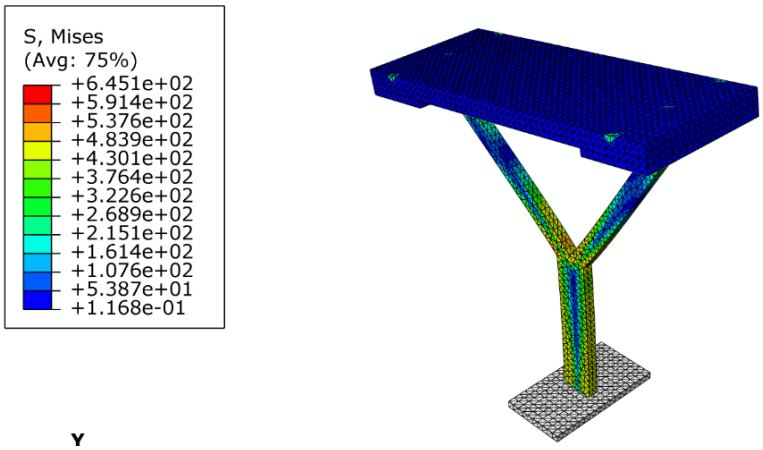

(b) TR-1-2-20:100

Fig (4.17): Failure Modes for TR-1-2 Column

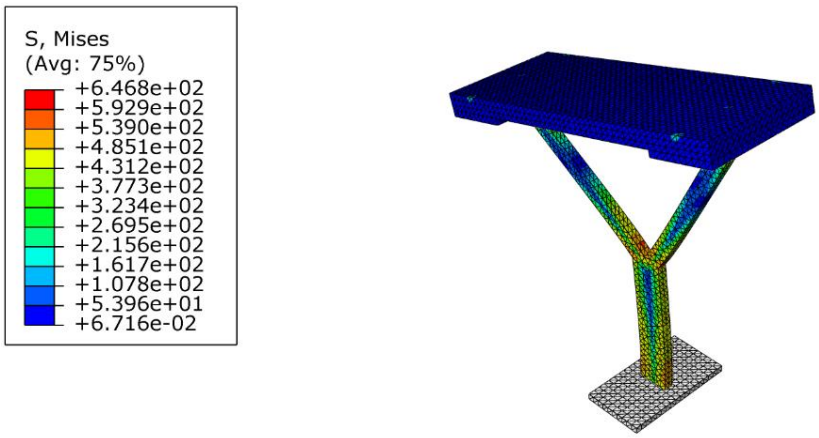

(c) TR-1-2-40:100

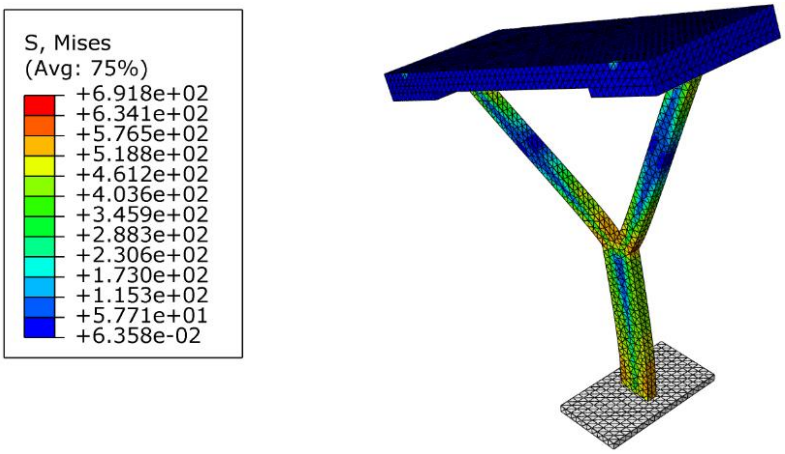

(d) TR-1-2-60:100

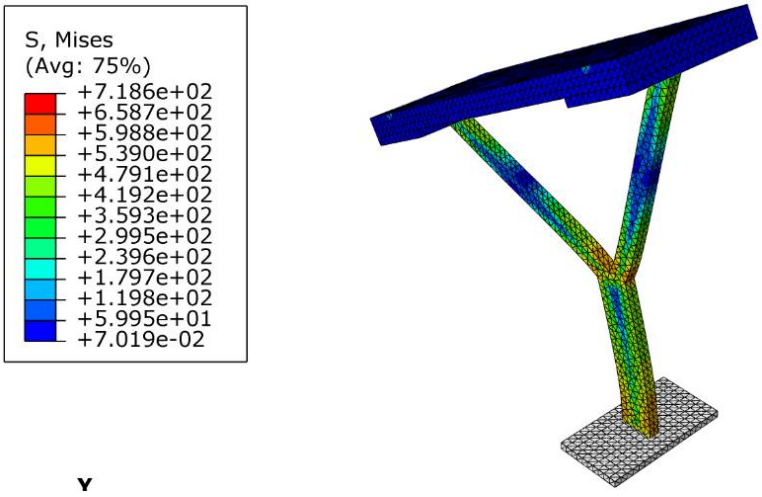

(e) TR-1-2-80:100

Fig (4.17): Failure Modes for TR-1-2 Column

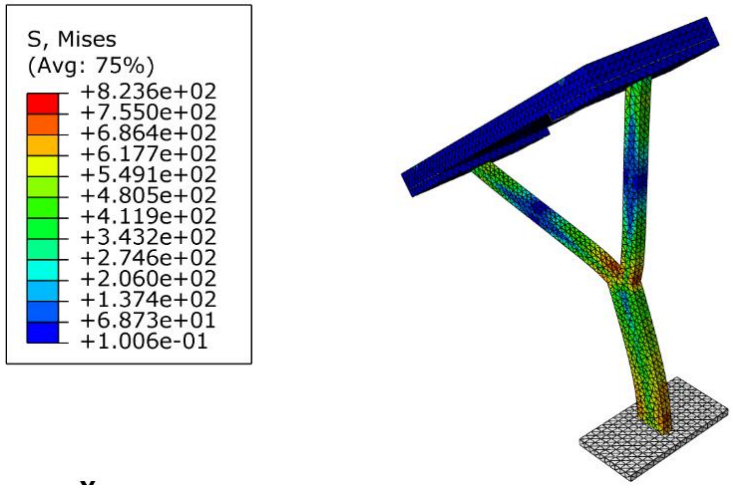

(f) TR-1-2-100:100

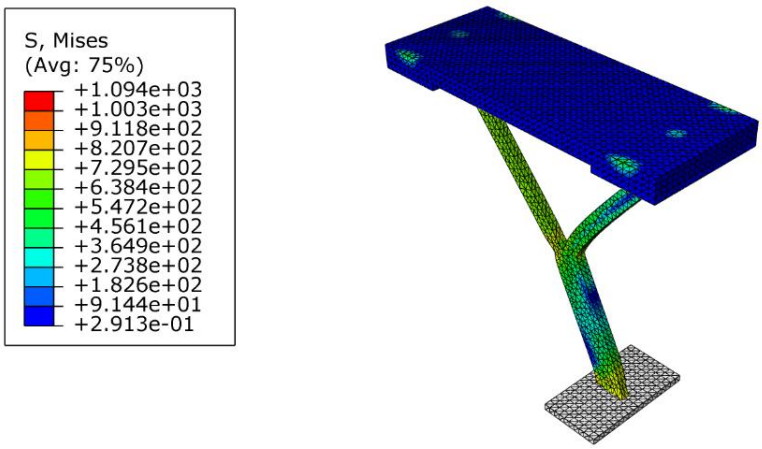

(g) TR-1-2-100:0

Continue Fig (4.17): Failure Modes for TR-1-2 Column

4.4.2 Tree like Column with circular HSS Cross Section

In this section there are three models with circular cross-sectional area and one branching level. the three models are differing in the outer diameter to thickness ratio (D/t), where this ratio is increased each time to study the behavior of tree-like column at each ratio.

4.4.2.1 Tree-like Column with circular HSS and D/t ratio equals to 21.

The tree-like column TC21-1-2 model has a circular cross-sectional area created with pipe HSS and one branching level, with a (D/t) ratio of 21. Results of the seven loading cases are calculated and presented in Table (4.3) while the axial and lateral load deflection curves for the TC21-1-2 column are shown in figures (4.18) and (4.19).

Table (4-3): Results of Circular Tree-Like Column (TC21-1-2) With Different Loading Conditions

Spacemen symbol	lateral/axial load ratio	Axial failure load (KN)	Axial displacement at failure (mm)	Lateral Failure Load (KN)	Lateral displacement at failure (mm)
TC21-1-2-0:100	0/100	45	6.173	0	0
TC21-1-2-20:100	20/100	20.309	6.974	3.99	13.931
TC21-1-2-40:100	40/100	11.509	10.665	4.603	23.798
TC21-1-2-60:100	60/100	8.270	13.442	4.962	30.738
TC21-1-2-80:100	80/100	6.550	19.921	5.240	49.394
TC21-1-2100:100	100/100	5.492	23.941	5.492	76.585
TC21-1-2-100:0	100/0	0	0	25.752	92.088

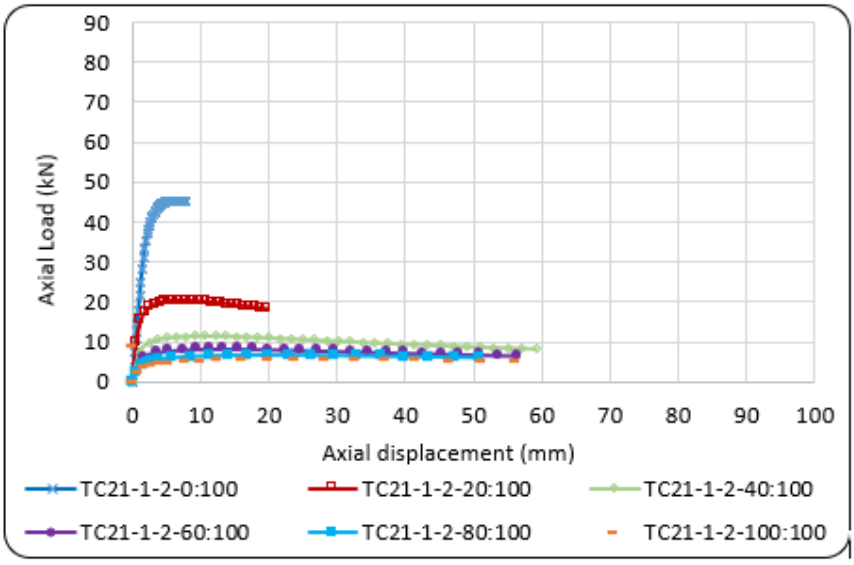

Fig (4.18): Axial Load-Displacement Response for TC21-1-2 Model at Different Loading Ratios

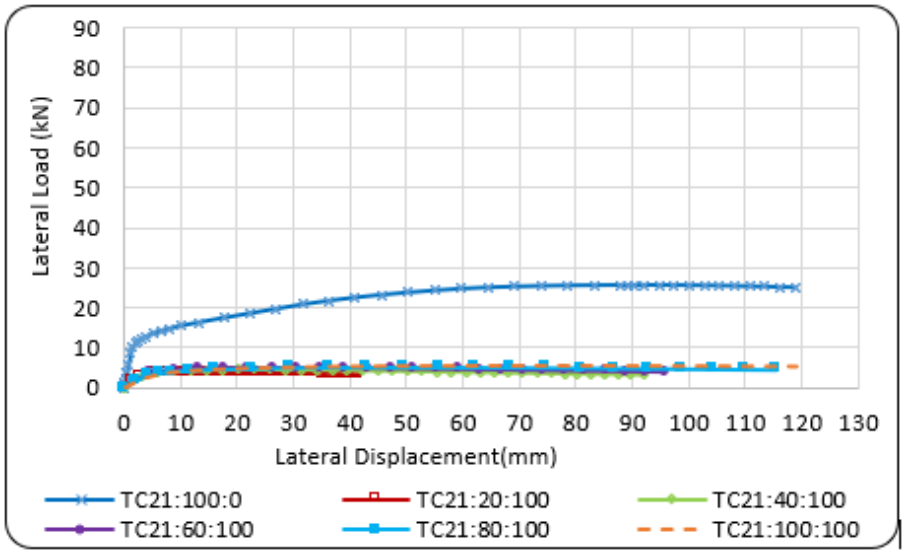

Fig (4.19): Lateral Load-Displacement Response for TC21-1-2 Model at Different Loading Ratios

4.4.2.1.1 Axial Failure Load and Displacement

When the lateral to axial load ratio is zero, the axial failure load is 45 kN, and this value decreases as the lateral to axial load ratio increases; increasing the ratio by about (20, 40, 60, 80, and 100) %, respectively, reduces the axial failure load by (55.6, 74.4, 81.6, 85.4, and 87.8) %, as given in Figure (4.20). Figure (4.21)

demonstrates that the axial displacement at failure is increased significantly by (13, 73, 118, 223 and 288) % with the decrease of failure load.

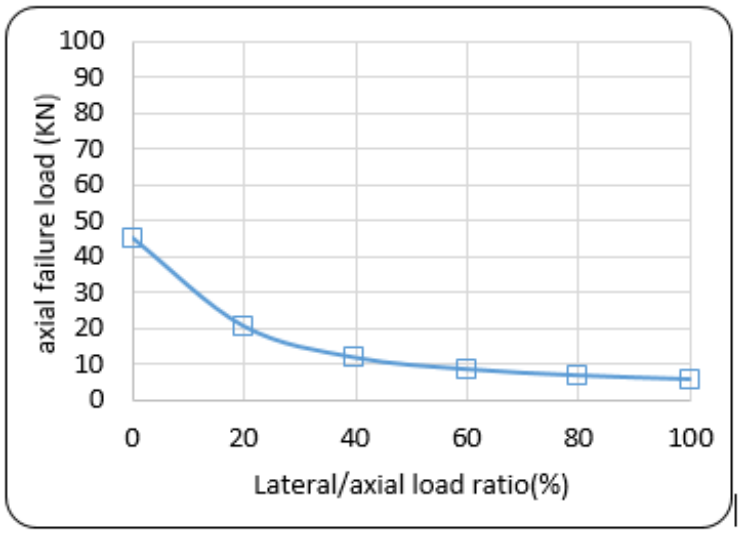

Fig (4.20): Axial Failure Load Versus Load Ratio for TC21-1-2 Model

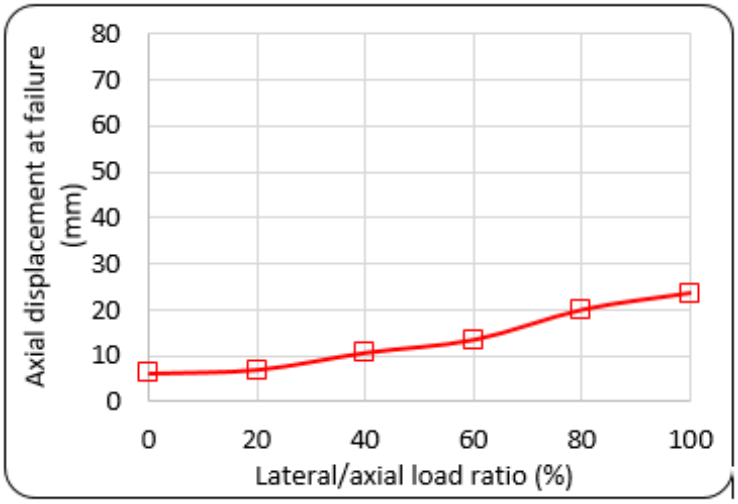

Figure (4.21): Axial Failure Displacement Versus Load Ratio for TC21-1-2 Model

4.4.2.1.2 Lateral Failure Load and Displacement

The relation between lateral failure loads and the ratio of lateral load to axial load is shown in figure (4.22). The results demonstrate that the lateral failure load increases with increasing lateral load ratio, where by increasing the ratio by about (40, 60, 80, and 100) %, respectively, the lateral failure load increases by (15.3,

24.2, 31.2, and 37.5) %. However, the maximum lateral failure load is 25.7 kN when no axial load is applied. Also, the increase in lateral failure load is accompanied by an increase in lateral displacement at failure where the lateral displacement increases significantly by (71, 120, 245 and 449) % as given in Fig. (4.23).

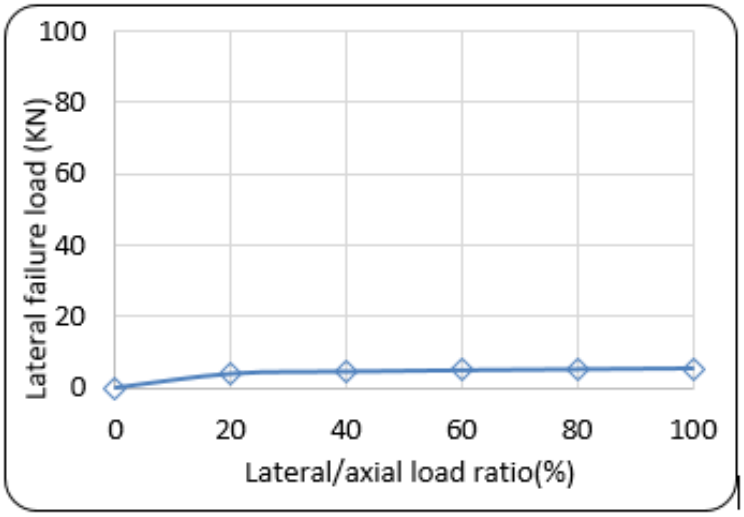

Fig (4.22): Lateral Failure Load Versus Load Ratio for TC21-1-2 Model

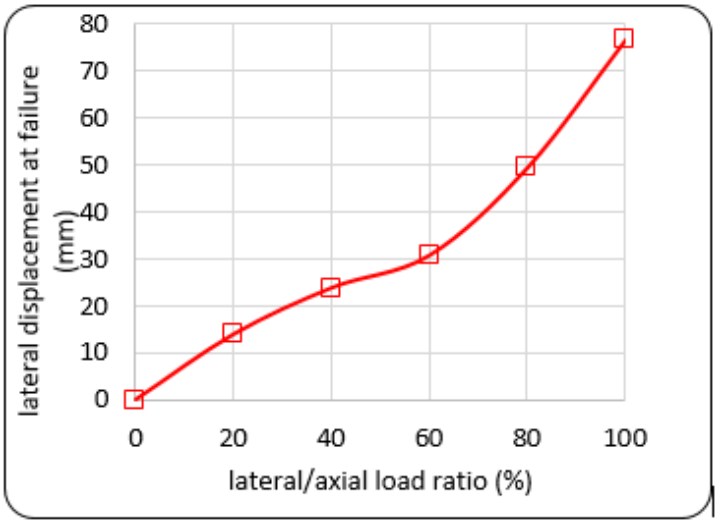

Fig (4.23): Lateral Failure Displacement Versus Load Ratio for TC21-1-2 Model

4.4.2.1.3 Failure mode

From the von mises stress key in (Mpa)when the applied load is axial load only, and because the joint is the more critical part of the tree-like column, the

maximum stress value is mainly at the joint core area. The stresses at joint increases significantly by increasing the lateral to axial load ratio, the Fig (4.24) shows the failure mode for the TC21-2 column under different load cases.

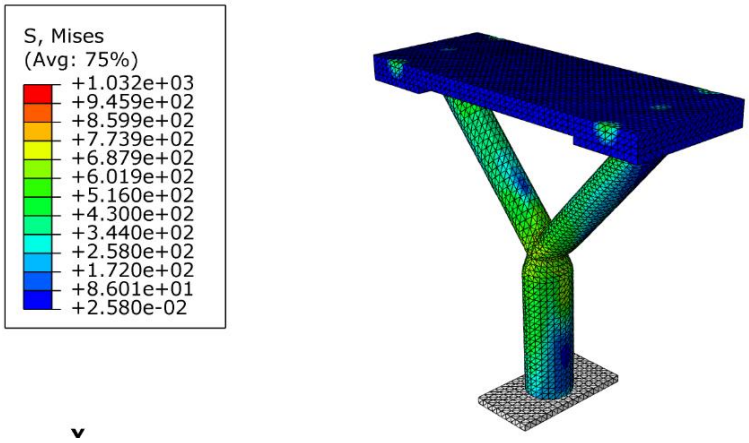

(a) Tc21-1-2-0:100

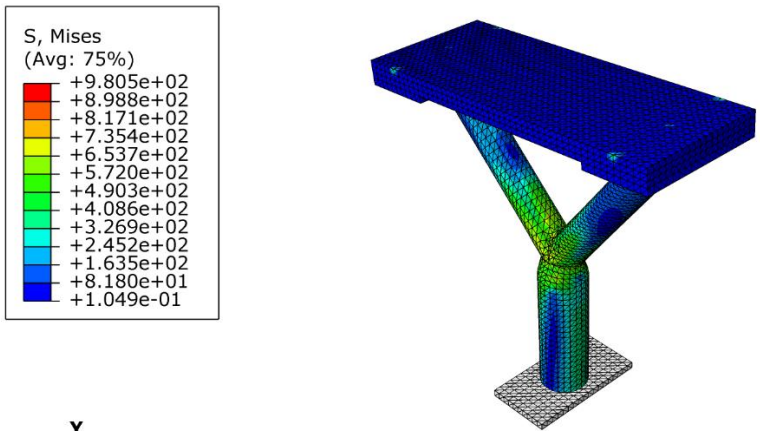

(b) Tc21-1-2-20:100

Fig (4-24): Failure Modes for TC21-1-2 Column

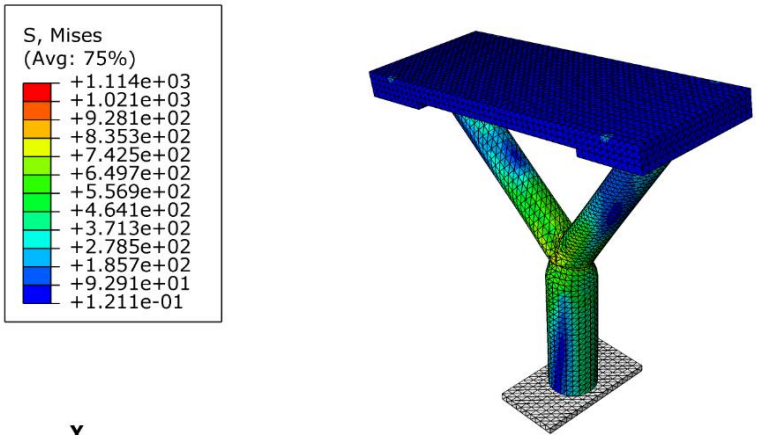

(c)Tc21-1-2-40:100

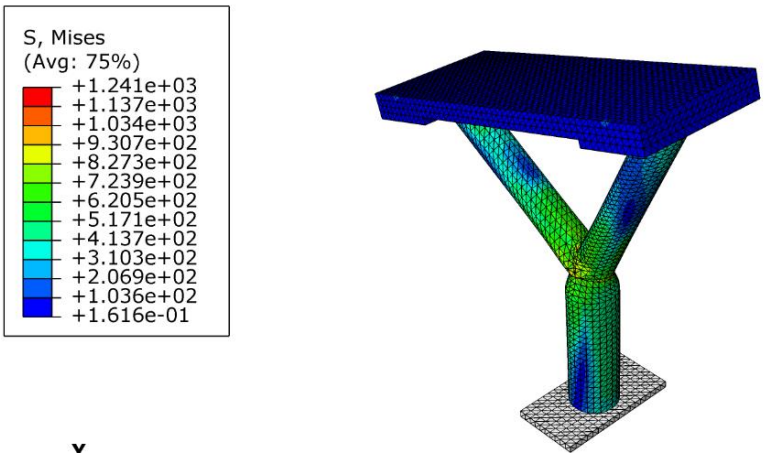

(d) Tc21-1-2-60:100

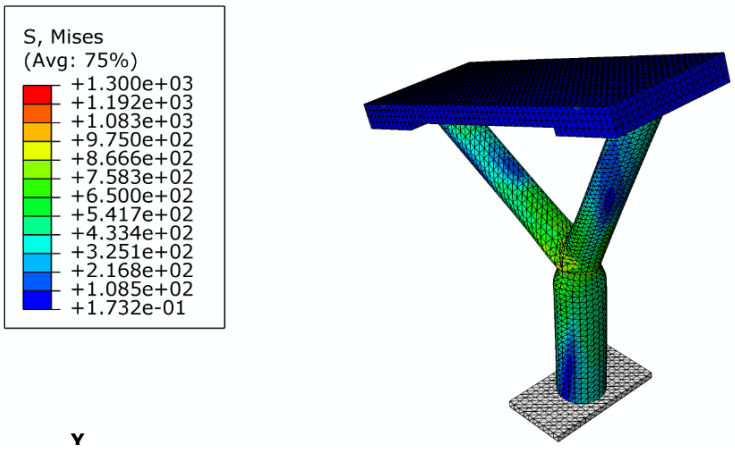

(e) Tc21-1-2-80:100

Continue Fig (4-24): Failure Modes for Tc21-1-2 Column

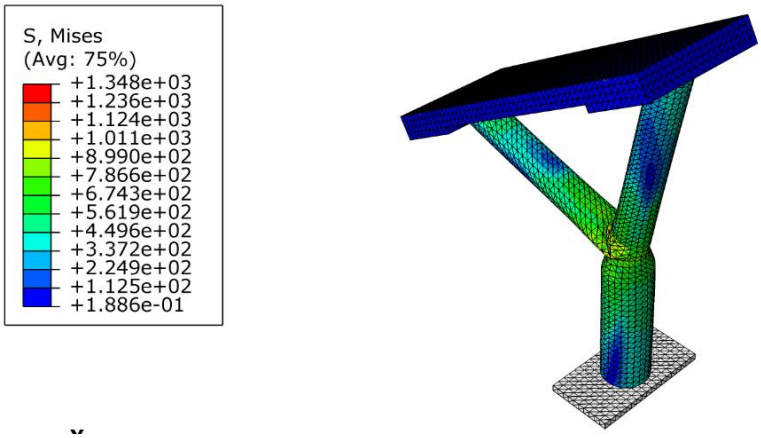

(f) Tc21-1-2-100:100

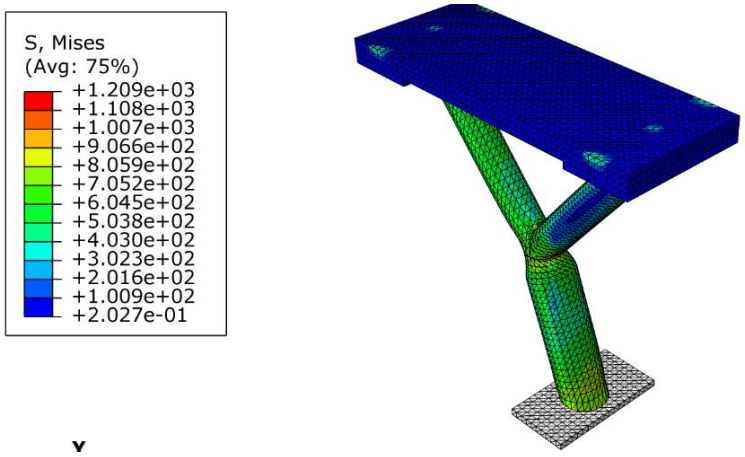

(g) Tc21-1-2-100:0

Continue Fig (4-24): Failure Modes for Tc21-1-2 Column

4.4.2.2 Tree like Column with circular Cross Section and D/t ratio equals to 14.

The TC14-1-2 tree-like column model was developed by using pipe HSS with a (D/t) ratio of 14. The results of the varying lateral loading ratios are calculated and presented in Table (4.4). While the axial and lateral load curves of deflection are given in Figs. (4.25) and (4.26).

Table (4.4): Results of Circular Tree like Column (TC14-1-2) with Different Loading Conditions

Spacemen symbol	Lateral/axial load ratio	Axial failure load (kN)	Axial displacement at failure (mm)	Lateral failure load (kN)	Lateral displacement at failure (mm)
TC14-1-2-0:100	0/100	50	3.865	0	0
TC14-1-1-20:100	20/100	22.974	5.1458	4.594	12.394
TC14-1-2-40:100	40/100	13.788	8.309	5.515	18.497
TC14-1-2-60:100	60/100	9.868	11.326	5.921	22.635
TC14-1-2-80:100	80/100	7.709	13.359	6.167	29.532
TC14-1-2-100:100	100/100	6.339	13.852	6.339	33.364
TC14-1-2-100:0	100/0	0	0	27	47.343

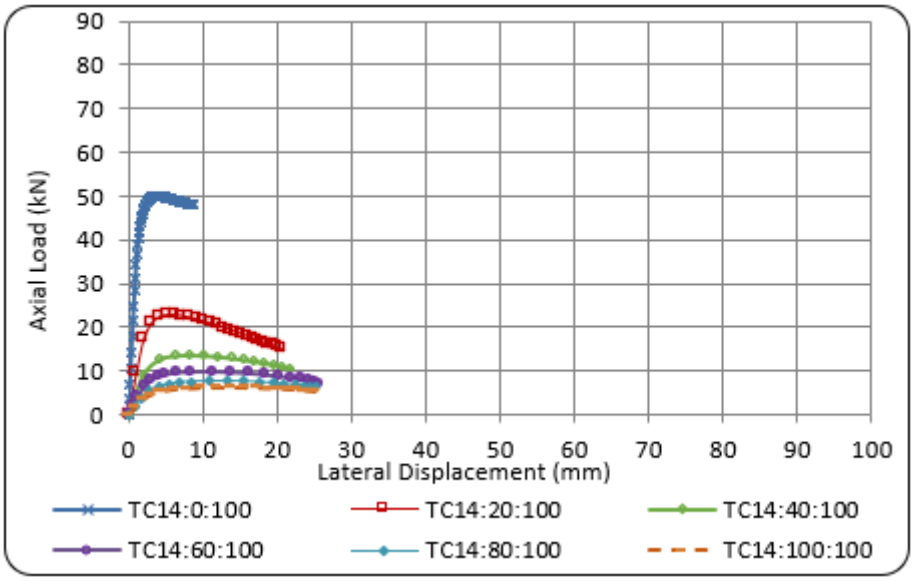

Fig (4-25): Axial Load-Displacement Response for TC14-1-2 Model at Different Loading Ratios

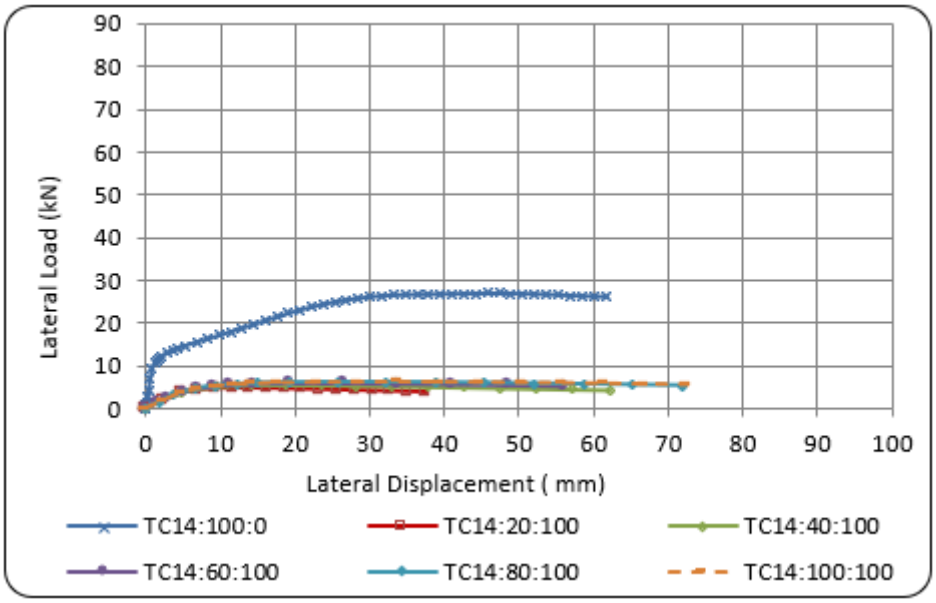

Fig (4.26): Lateral Load-Displacement Response for TC14-1-2 Model at Different Loading Ratios

4.4.2.2.1 Axial Failure Load and Displacement

The results showed that the application of lateral load can reduce the axial failure load of the column. This reduction in axial failure load depends on the ratio of lateral load that is applied to the column. By increasing the lateral to axial load ratio by about (20, 40, 60, 80, and 100) %, respectively, the axial failure load decreases by (54, 72.4, 80.3, 84.6, and 87.3) % as shown in fig (4.27). While the axial displacement increased by (33, 115, 193, 245 and 258) % as shown in fig (4.28).

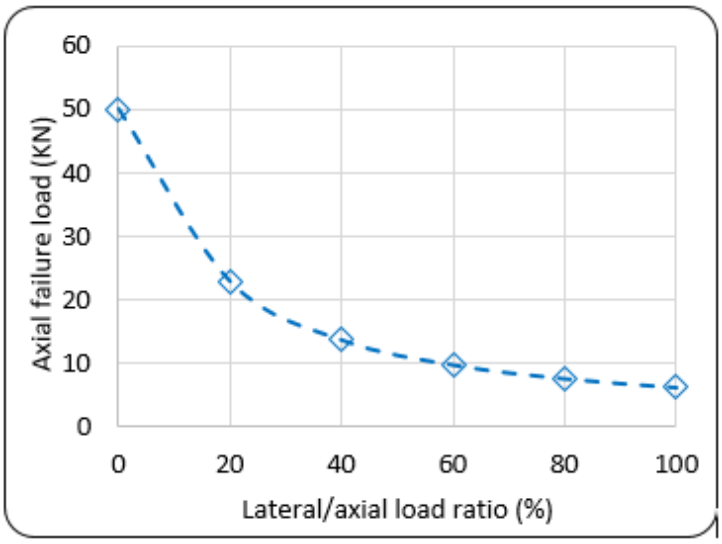

Fig (4.27): Axial Failure Load Versus Load Ratio for TC14-1-2 Model

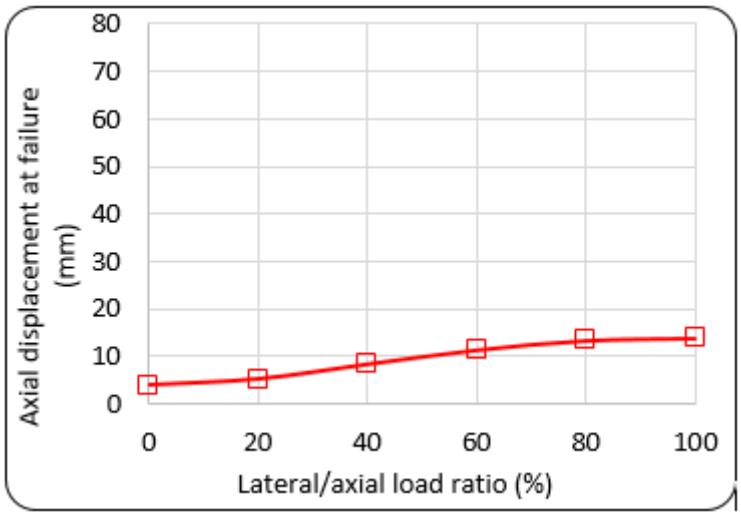

Fig (4.28): Axial Failure Displacement Versus Load Ratio for TC14-1-2 Model

4.4.2.2.2 Lateral Failure Load and Displacement

The maximum lateral load and displacement will increase with the lateral-to-axial load ratio's increase. As shown in figure (4.29), increasing the ratio by about (40, 60, 80, and 100) % increase the lateral failure load by (20, 28.9, 34.2, and 38). However, the maximum lateral failure load is 25.7 kN when no axial load is applied. The lateral displacement at failure is significantly increased by (49, 82, 138 and 196%) as presented in Figure (4.30), also the application of axial load

can reduce the lateral displacement of the tree-like column under combined loading because of the extra weight from the axial load.

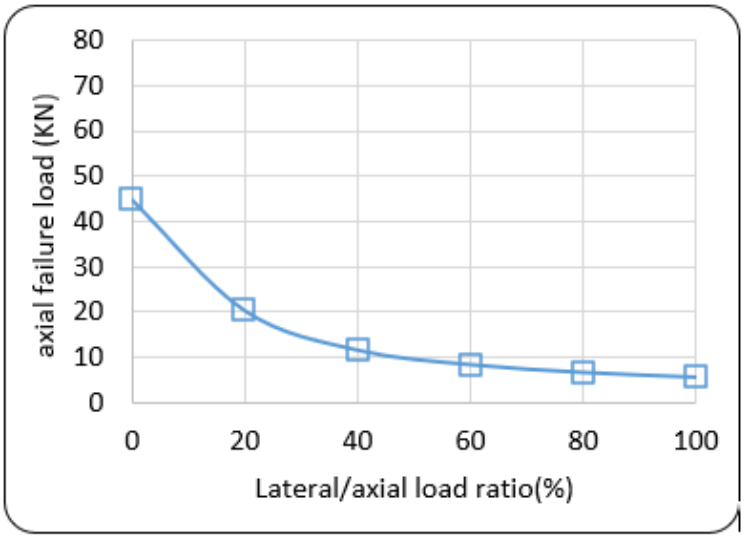

Figure (4.29): Lateral Failure Load Versus Load Ratio for TC14-1-2 Model

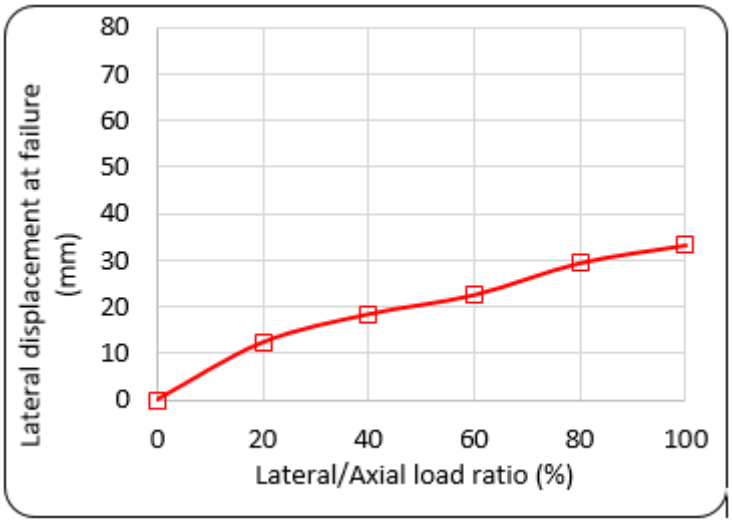

Figure (4.30): Lateral Failure Displacement Versus Load Ratio for TC14-1-2 Model

4.4.2.2.3 Failure mode

The failure modes for the TC14-1-2 model are shown in Fig (4.31). since the joint area is the critical part of the tree-like column. The stresses are large at this area as compared with other parts. when a combined load is applied to the tree-like column. The mises stresses increased significantly at the joint.

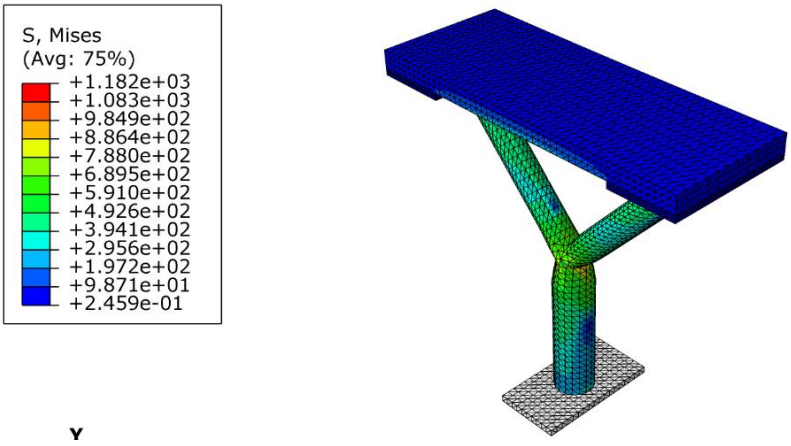

(a)TC14-1-2-0:100

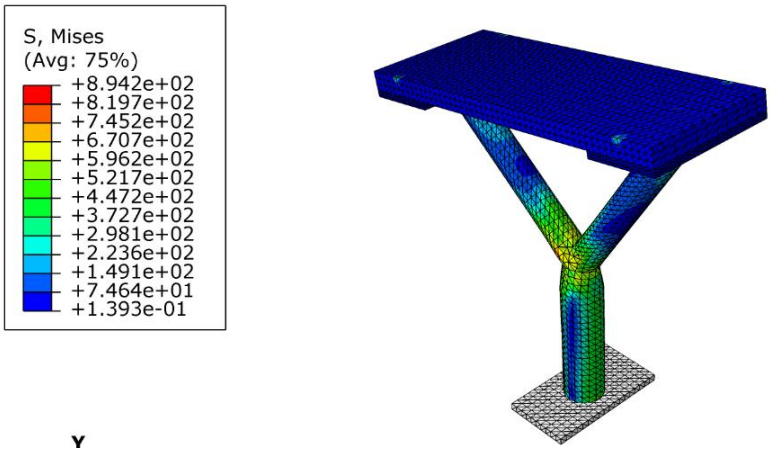

(b) TC14-1-2-20:100

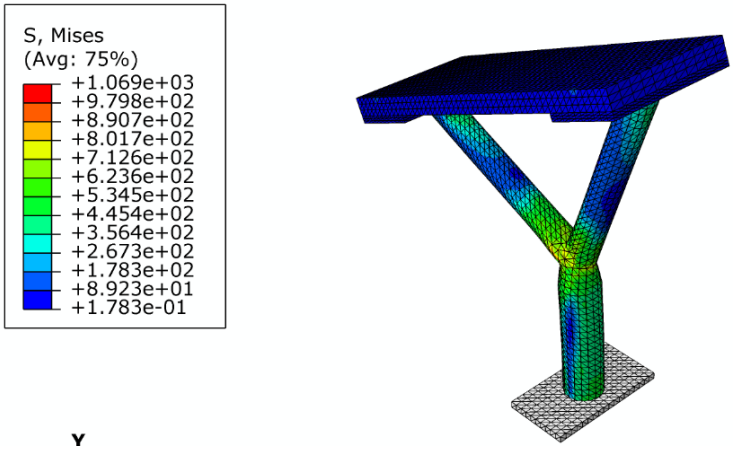

(c) TC14-1-2-40:100

Fig (4.31): Failure Modes for TC14-1-2 Column

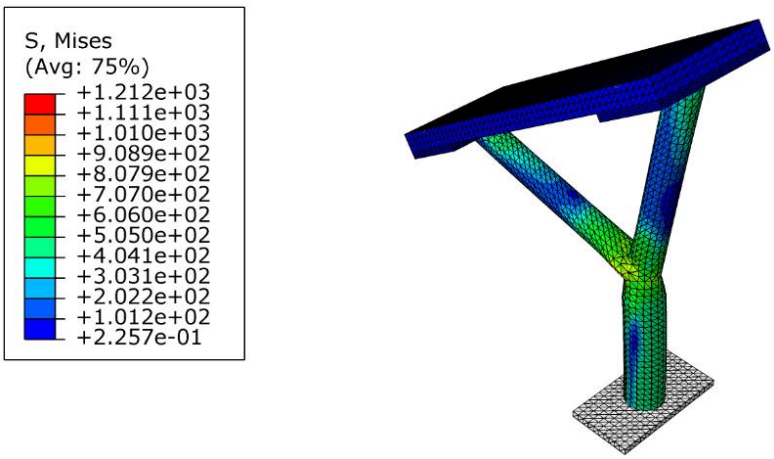

(d) TC14-1-2-60:100

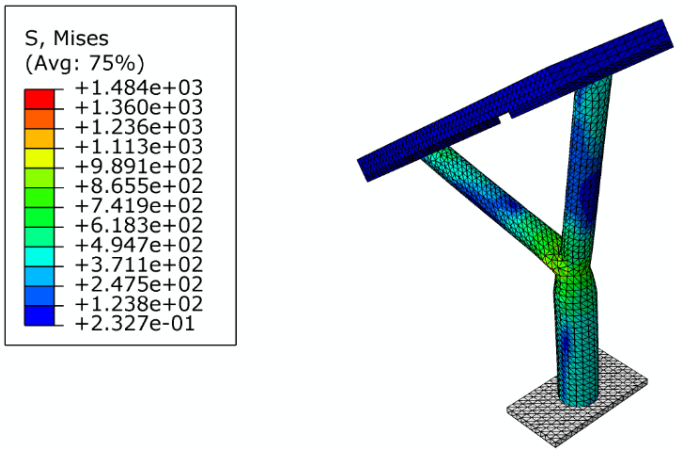

(e) TC14-1-2-80:100

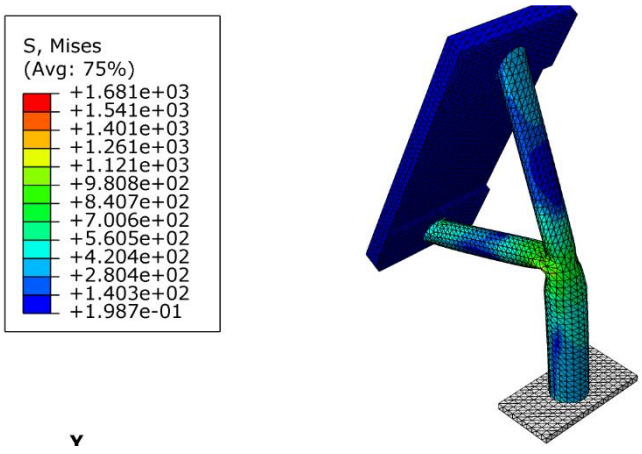

(f) TC14-1-2-100:100

Continue Fig (4.31): Failure Modes for TC14-1-2 Column

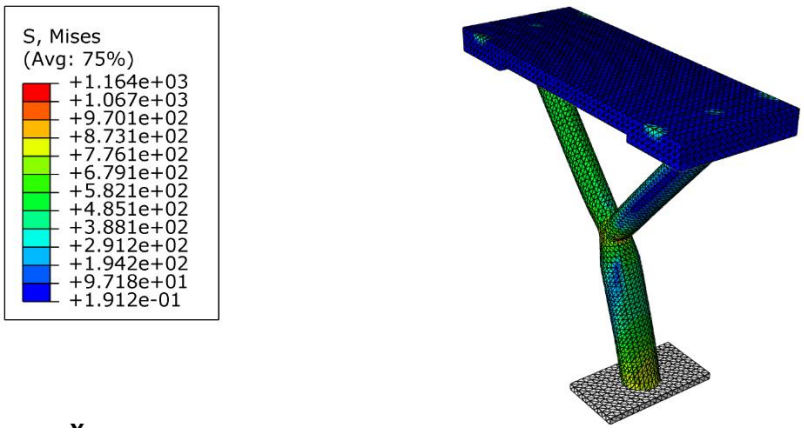

(g) Tc21-1-2-100:0

Continue Fig (4.31): Failure Modes for TC14-1-2 Column

4.4.2.3 Tree like Column with circular Cross Section and D/t ratio equals to 8.

The results of TC8-1-2 for the different lateral loading ratios are calculated and presented in Table (4.5). The model was developed by using pipe HSS with a (D/t) ratio of 8. Axial and lateral load deflection curves for the column are shown in Figs. (4.32) and (4.33).

Table (4.5): Results of Circular Tree- Like column (TC8-1-2) with Different Loading Conditions

Spacemen symbol	Lateral/axial load ratio	Axial failure load (kN)	Axial displacement at failure(mm)	Lateral failure load (kN)	Lateral displacement at failure (mm)
TC8-1-2-0:100	0/100	56	2.632	0	0
TC8-1-2-20:100	20/100	26.238	6.860	5.247	12.413
TC8-1-2-40:100	40/100	15.530	7.557	6.212	15.306
TC8-1-2-60:100	60/100	11.168	10.307	6.701	17.362
TC8-1-2-80:100	80/100	8.784	12.085	7.027	20.337
TC8-1-2-100:100	100/100	7.280	13.798	7.580	23.061
TC8-1-2-100:0	100/0	0	0	29.2	34.278

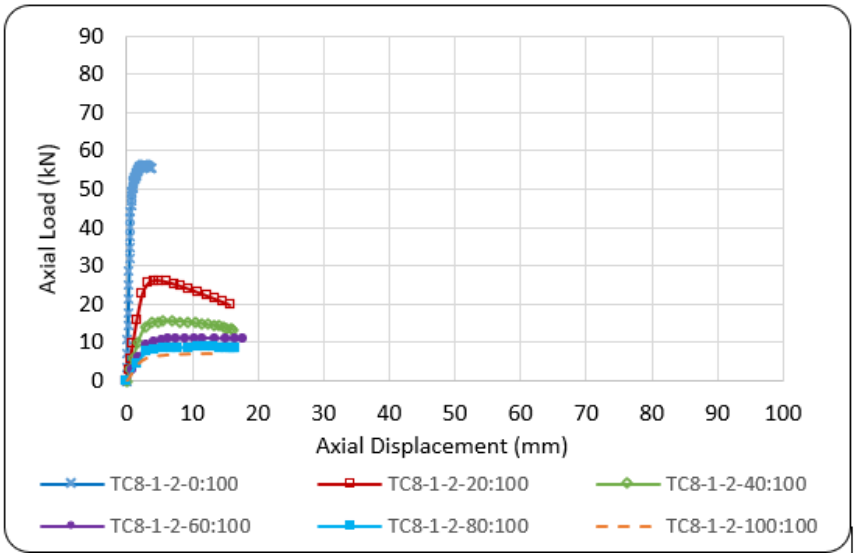

Fig (4.32): Axial Failure Load Versus Load Ratio for TC8-1-2 Model

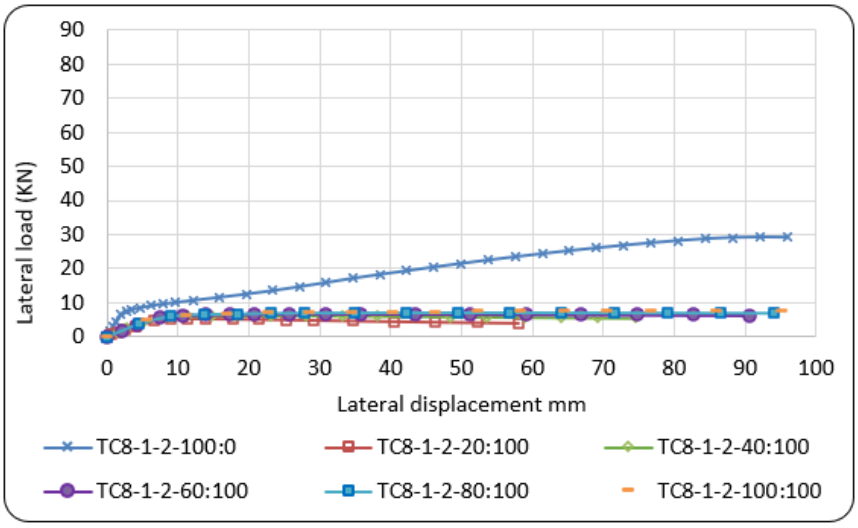

Fig (4.33): Lateral Failure Load Versus Load Ratio for TC8-1-2 Model

4.4.2.3.1 Axial Failure Load and Displacement

If the applied load is an axial load, the axial failure load reaches its maximum value of 56 kN only when the lateral to axial load ratio increases by approximately (20, 40, 60, 80, and 100) %, respectively. Fig (4.34) shows that the axial failure load decreases by (53, 72.3, 80.1, 84.3, and 87.6) %. Due to the combination of axial and lateral loads, the axial displacement increased significantly by (160, 187, 291, 355 and 424) %, as shown in Fig (4.35).

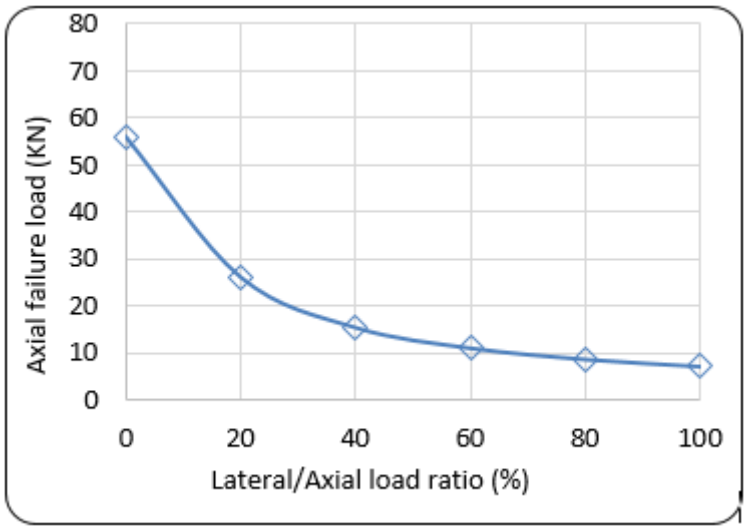

Fig (4.34): Axial Failure Load Versus Load Ratio for TC8-1-2 Model

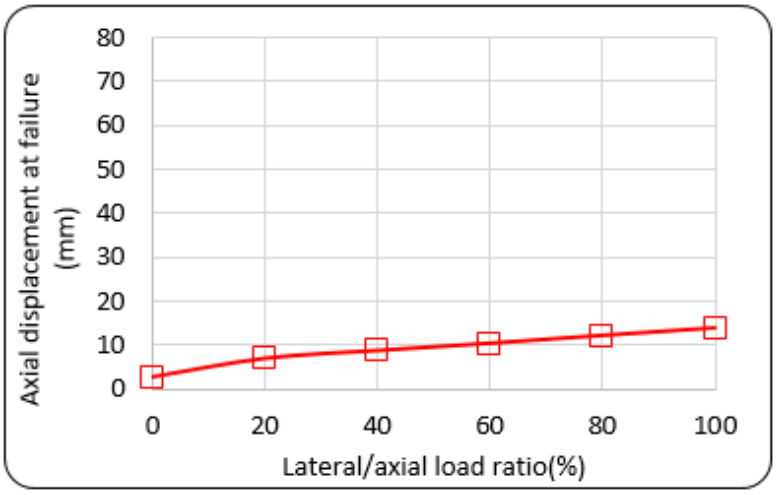

Fig (4.35): Axial Failure Displacement Versus Load Ratio for TC8-1-2 Model

4.4.2.3.2Lateral Failure Load and Displacement

The lateral failure load increased slightly by increasing the ratio of lateral to axial load as shown in Fig (4.36). It can be noticed that when the lateral to axial load ratio increases by about (40, 60, 80, and 100) %, respectively, the lateral failure load increases by (18.4, 27.7, 34, and 44.7) %. While the maximum lateral failure load is 29.2 KN when no axial load is applied. The lateral displacement increased significantly by (23.6, 39.9, 63.8 and 85.7) % with the increase of the applied

lateral load as shown in Fig (4.37). The presence of an axial load decreased the lateral displacement because of the increasing in axial weight of the column.

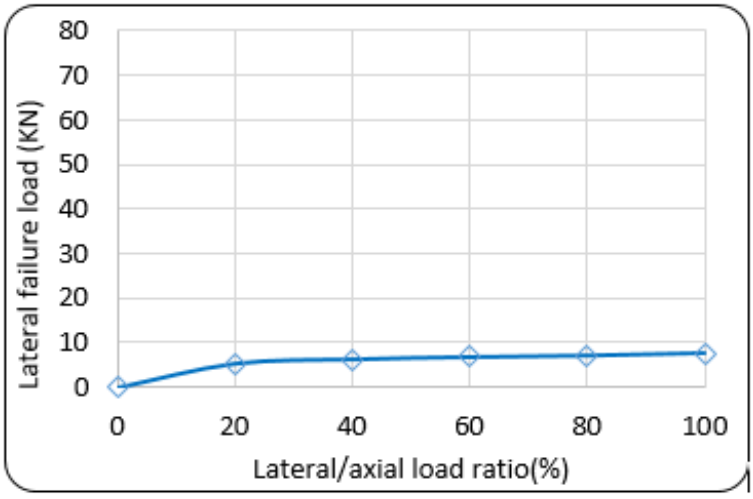

Fig (4.36): Lateral Failure Load Versus Load Ratio for TC8-1-2 Model

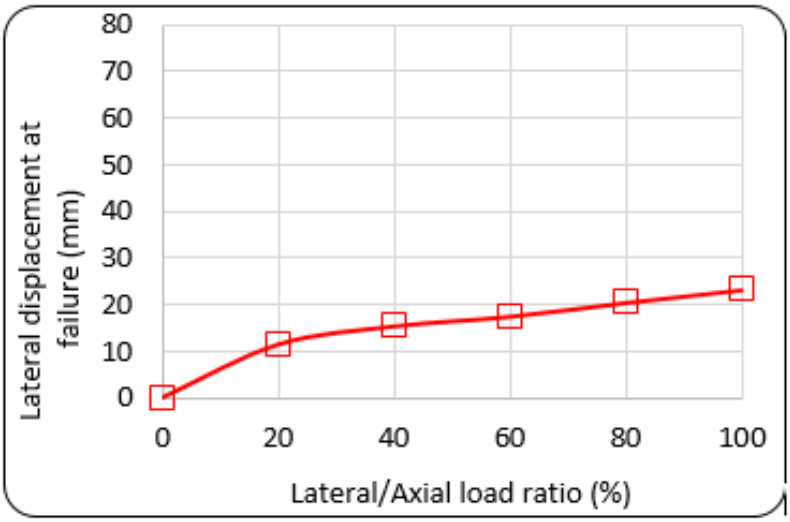

Fig (4.37): Failure Displacement Versus Load Ratio for TC8-1-2 Model

4.4.2.3.3 Failure mode

The failure mode of TC8-1-2 for the three cases (axial loading, axial plus lateral loading, and lateral loading only) are shown in Fig (4.38). from the mises stresses we can notice that when axial load only is applied the material yields at the branches and joint. The trunk yielding is appeared at combined loading cases as well as joint yielding. the mises stress are increased significantly with the increase of lateral to axial load ratio.

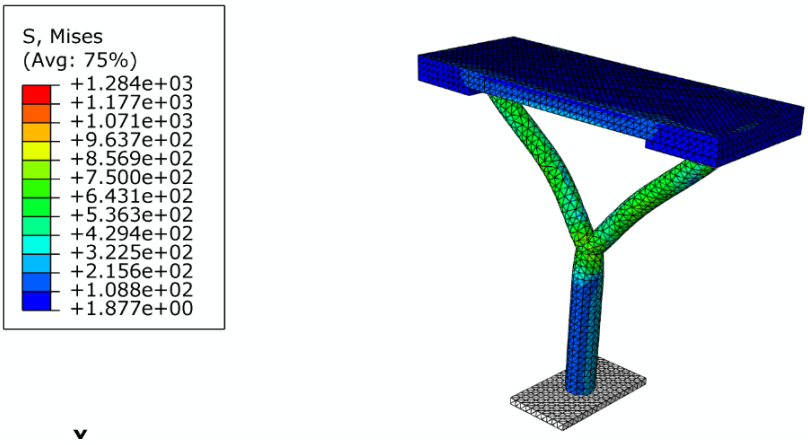

(a)TC8-1-2-0:100

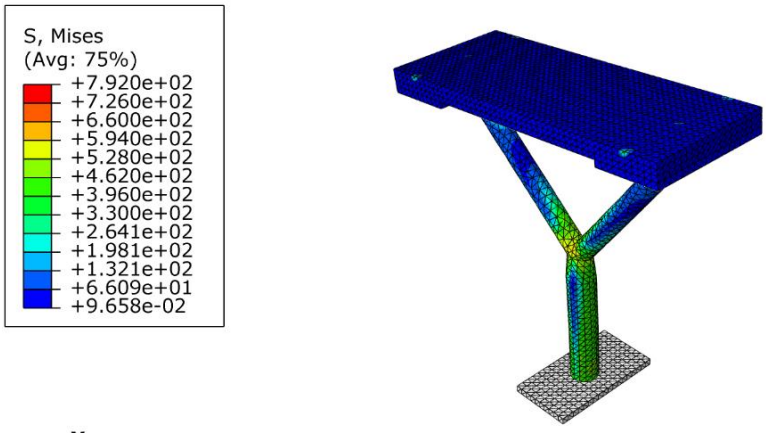

(b) TC8-1-2-20:100

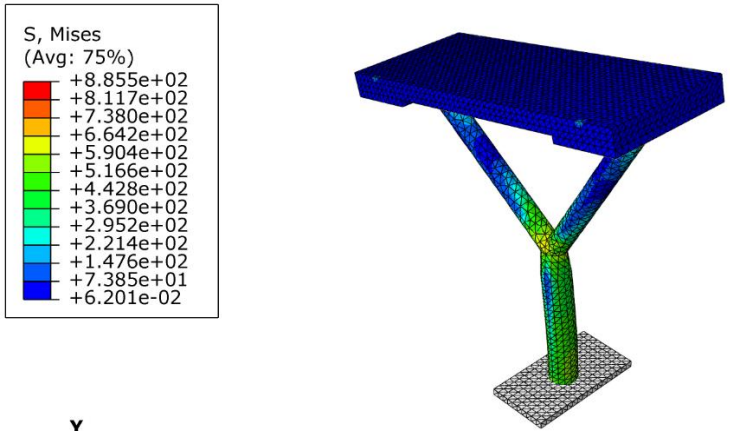

(c)TC8-1-2-40:100

Fig (4.38): Failure Modes for TC8-1-2 Column

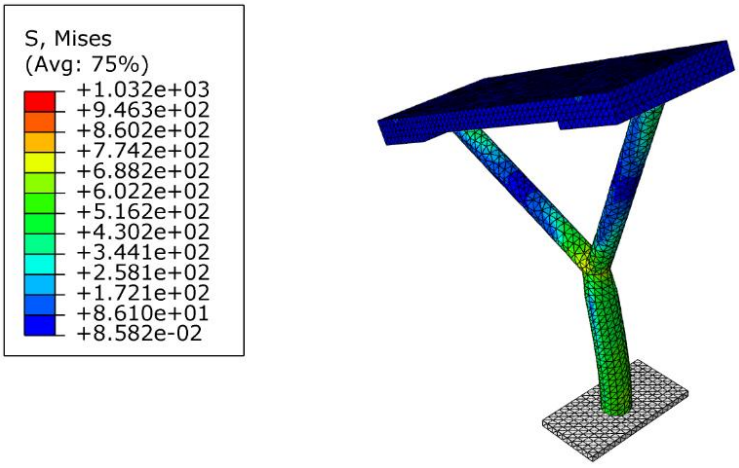

(d) TC8-1-2-60:100

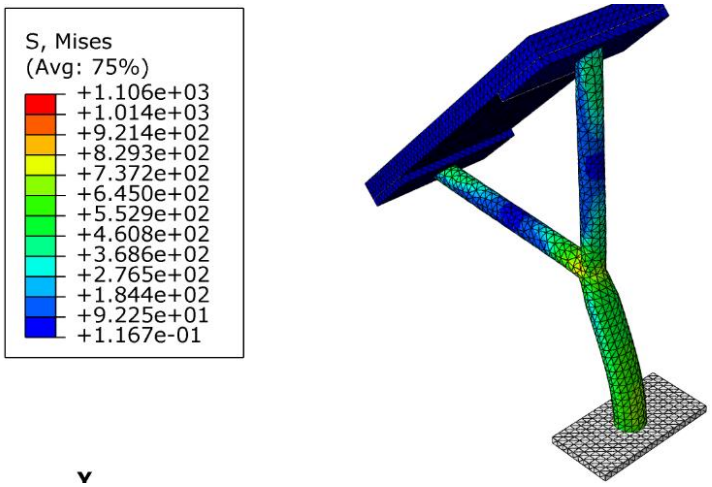

(e)TC8-1-2-80:100

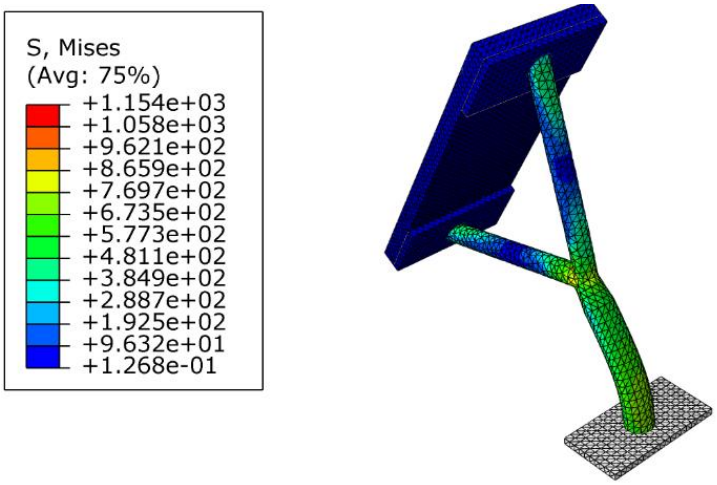

(f)TC8-1-2-80:100

Continue Fig (4.38): Failure Modes for TC8-1-2 Column

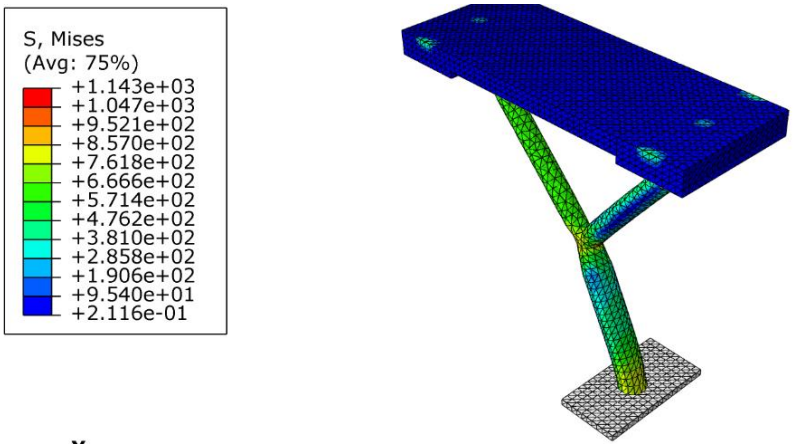

(f)TC8-1-2-100:0

Continue Fig (4.38): Failure Modes for TC8-1-2 Column

4.5 column with two branching levels.

The TC14-2-4 column has a circular cross-sectional area created with pipe HSS and a D/t ratio of 14. The column is made up of a trunk and two branching levels, each level with two branches. The results for the seven loading cases are calculated and presented in Table (4.6). The axial and lateral load deflection curves for the column shown in figures (4.39) and (4.40).

Table (4.6): Results of Circular Tree-Like Column (TC14-2-4) with Different Loading Conditions

Spacemen symbol	Lateral /axial load ratio	Axial failure load (kN)	Axial displacement at failure(mm)	Lateral failure load (kN)	Lateral displacement at failure(mm)
TC14-2-4-0:100	0/100	55	6.191	0	0
TC14-2-4-20:100	20/100	24.325	11.120	4.864	19.090
TC14-2-4-40:100	40/100	14.306	17.189	5.722	25.201
TC14-2-4-60:100	60/100	10.281	21.432	6.168	37.843
TC14-2-4-80:100	80/100	8.087	29.019	6.425	51.980
TC14-2-4-100:100	100/100	6.706	33.425	6.706	58.536
TC14-2-4-100:0	100/0	0	0	31	82.098

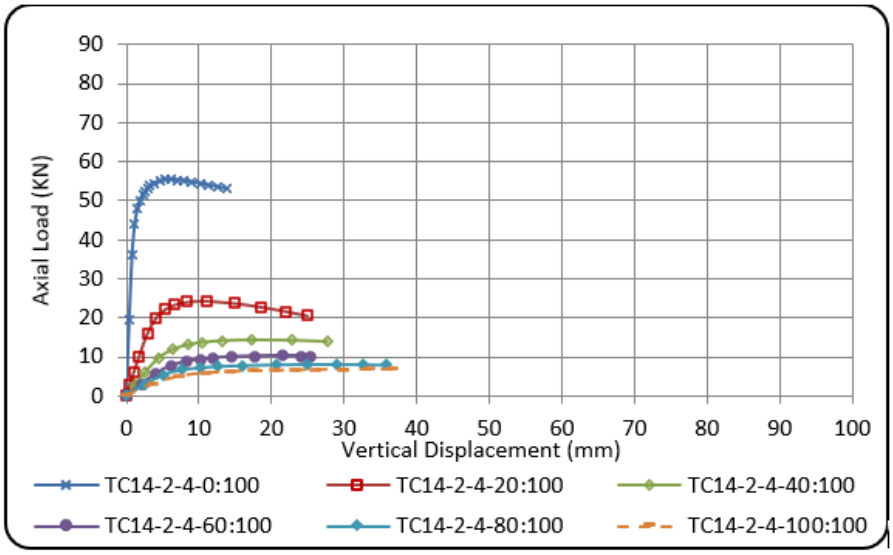

Fig (4.39): Axial Load-Displacement Response for TC14-2-4 Model at Different Loading Ratios

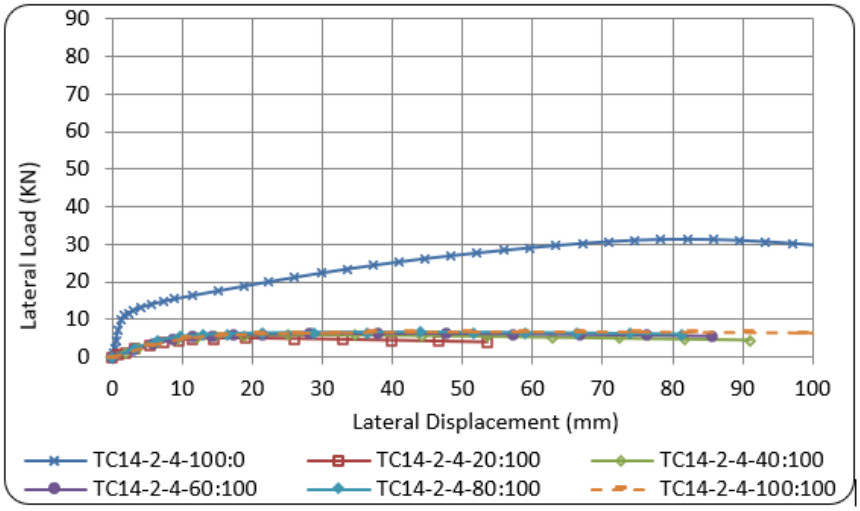

Fig (4.40): Lateral Load-Displacement Response for TC14-2-4 Model at Different Loading Ratios

4.5.1Axial Failure Load and Displacement

The axial failure load for TC14-2-4 under the action of axial load only is 55.3 KN. This value decreases significantly by increasing the value of the applied lateral load, where if the axial to lateral load ratio increases by about (20, 40, 60, 80, and 100) %, respectively, the axial failure load decreases by (56, 74, 81.4, 85.4, and 87.8) %, as shown in fig (4.41). Where after applying 60% of the lateral load, the decrease in the axial failure load tends to be the same. The

axial displacement at failure increased significantly by (79.6, 177, 246, 368.7, 439.8) %.

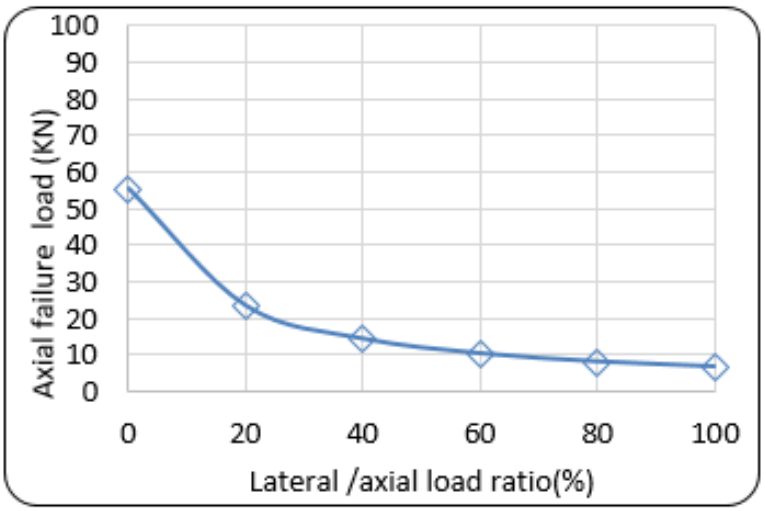

Fig (4.41): Axial Failure Load Versus Load Ratio for TC14-2-4 Model

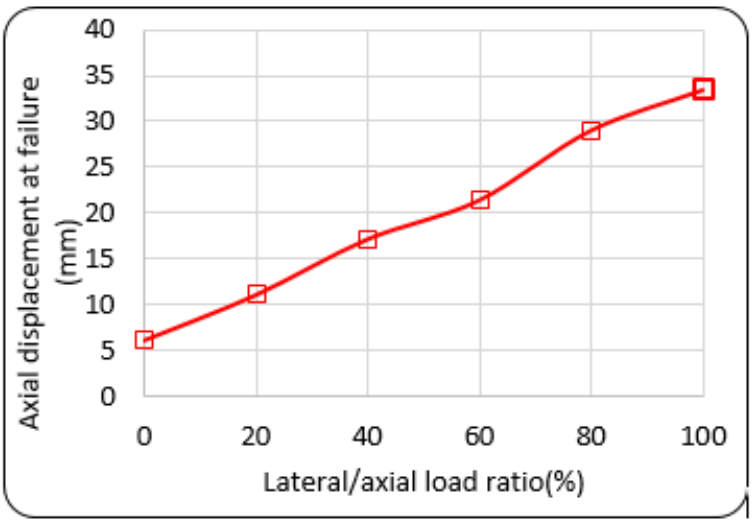

Fig (4.42): Axial Failure Displacement Versus Load Ratio for TC14-2-4 Model

4.5.2 Lateral Failure Load and Displacement

The results revealed that increasing the ratio of the lateral load to axial load induces a decrease in the axial failure load of the column for different ratios of lateral to axial load as shown in Figure (4.43). It can be noticed that when the lateral to axial load ratio increases by about (40, 60, 80, and 100) %, respectively, the lateral failure load increases by (18.6, 27, 32, and 37.8) %,

While the maximum lateral failure load is 31.2 kN when no axial load is applied. Figure (4.44) shows the lateral displacement at failure for different loading ratios. It is obvious that the lateral displacement increases significantly by (32, 98.23, 172.3, 206) % as the loading ratio increases. The presence of axial load works to decrease the lateral displacement of the column; if the applied load is lateral load only, the lateral displacement is 82.098 (mm). While applying axial load at the same time with lateral load leads to a decrease in the lateral displacement of about 29% because of the increase in the column axial weight.

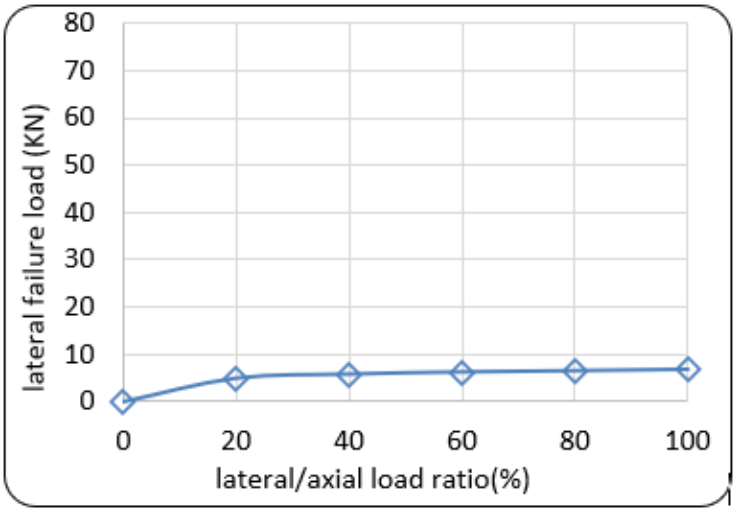

Fig (4.43): Lateral Failure Load Versus Load Ratio for TC14-2-4 Model

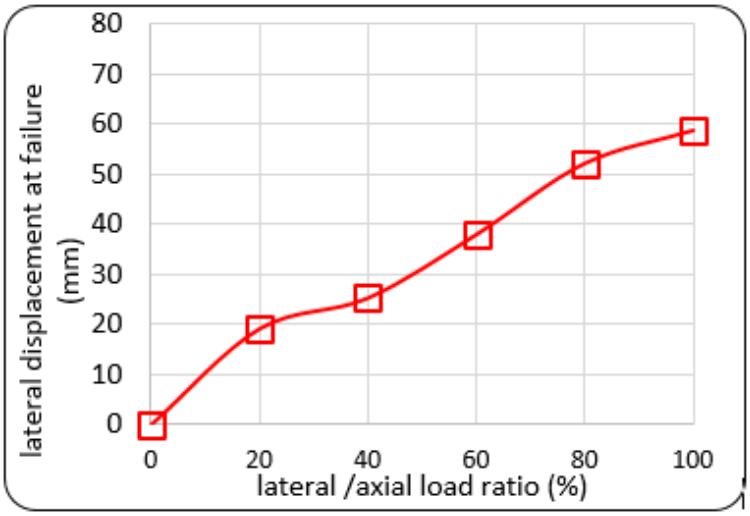

Fig (4.44): Lateral Failure Displacement Versus Load Ratio for TC14-2-4 Model

4.5.3 Failure mode

the failure mode for the TC14-1-2 Model for all loading cases are shown in Fig (4.45). the stresses are higher at the joint between main branches and trunk. the stresses are increased with the increase of the lateral to axial load ratio.

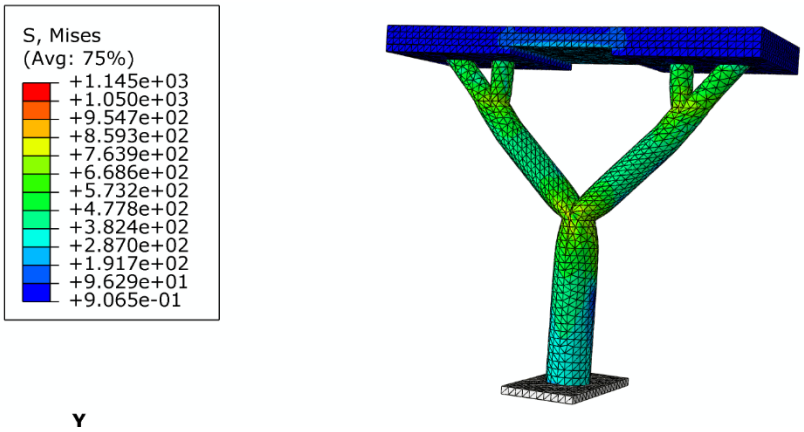

(a)TC14-2-4-0:100

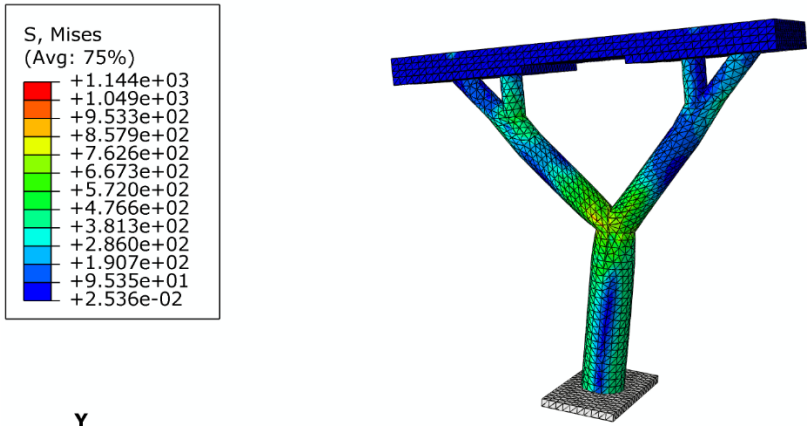

(b) TC14-2-4-20:100

Fig (4.45): Failure Modes for T14-2-4 Column

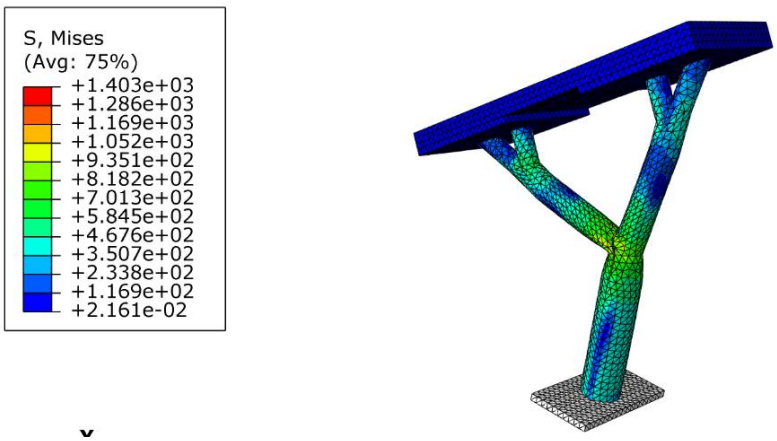

(c)TC14-2-4-40:100

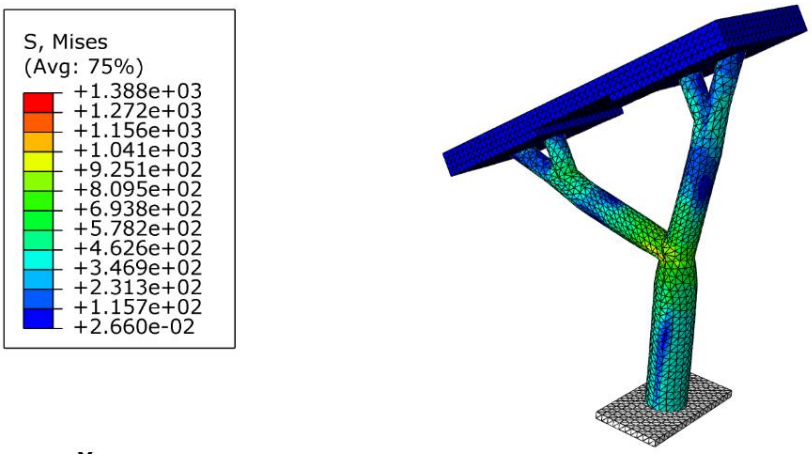

(d) TC14-2-4-60:100

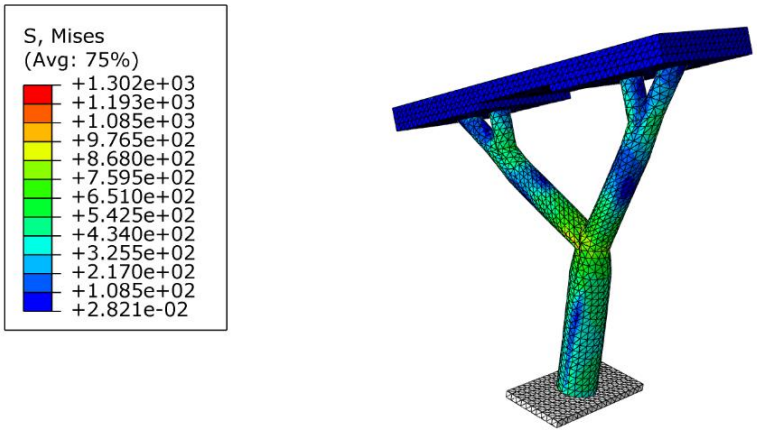

(e)TC14-2-4-80:100

Continue Fig (4.45): Failure Modes for T14-2-4 Column

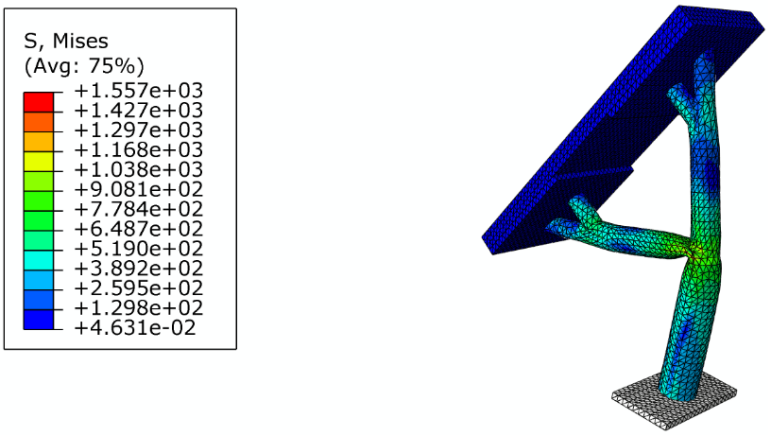

(f) TC14-2-4-100:100

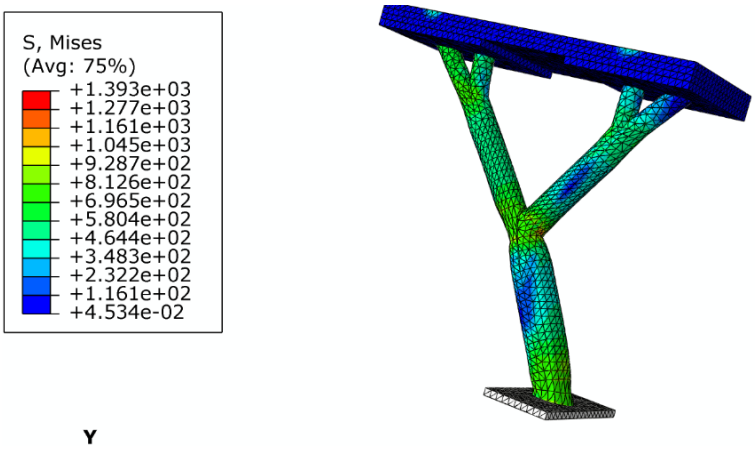

(g)TC14-2-4-100:0

Continue Fig (4.45): Failure Modes for T14-2-4 Column

4.6 effect of the shape of the cross-sectional area on the behavior of the tree-like columns.

This study was conducted on two models that are defined in group No1 (Fig 4.1). The first model has a rectangular cross-sectional area and the other one has a pipe HSS cross-sectional area and a D/T ratio of 21. The results show that the model with a rectangular cross section is more resistant to axial and lateral load than the circular model, as shown in figures (4.46) and (4.47), where by changing the cross section from rectangular to circular, the failure

load is decreased by -10% for the case of axial loading only and by -24.6% for the case of lateral loading only. While displacement increased by +328% for the case of axial loading and by +5.7% for the case of lateral loading. Reduction in failure load may be because of the ratio of the outer diameter to thickness is large where by increasing D/t ratio the stiffness is decreased.

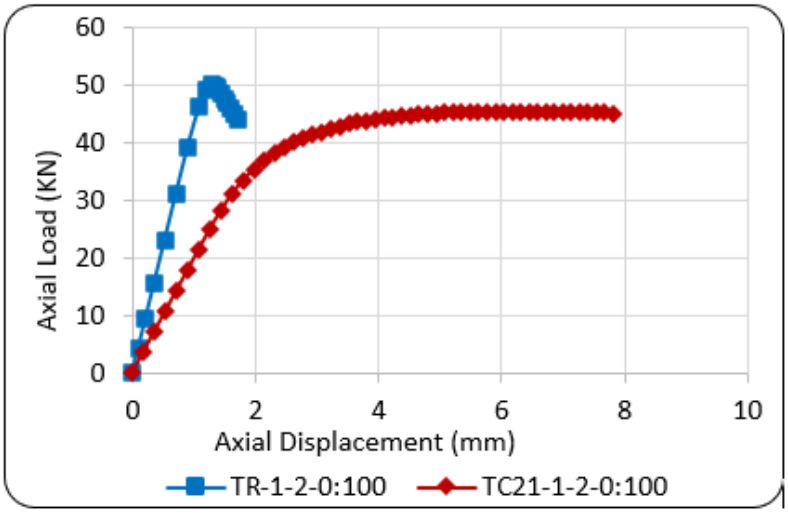

Fig (4.46): Axial Load Deflection Curves for TR-1-2-0:100 and TC21-1-2-0:100 Columns

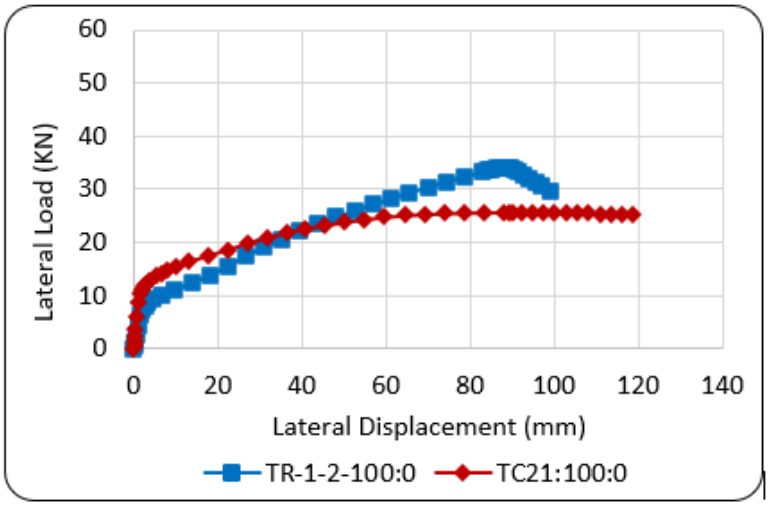

Fig (4.47): Lateral load Deflection Curves for TR-1-2-100:0 and TC21-1-2-100:0 Columns

4.7 effect of the ratio of the outer diameter to thickness (D/t) on the behavior of tree-like columns

To investigate the effect of the (D/t) ratio on the response of tree-like columns for both axial and lateral loading cases, three models of pipe HSS sections were used, and the (D/t) ratios were (21, 14 and 8), as defined in group No2 (Fig 4.2). the (D/t) ratio has a significant influence on the axial and lateral failure loads and displacements where for the case of axial loading only decreasing the D/t ratio from 21 to (14 and 8) respectively, increases the axial failure load by (+11.1 and +24.4) % while the axial displacement decreases significantly by (-37.4 and -57.4) % respectively. As shown in fig (4.48) and (4.49), Also for the case of lateral loading only decreasing the D/t ratio from 21 to (14 and 8) respectively, increase the lateral failure load by (+4.8 and +13.4) % while the lateral displacement at failure decreases significantly by (-19.2 and -62.7) %, respectively as shown in figures (4.50) and (4.51). This increase in failure load and decrease in displacement may be due to the enhanced stiffness of the column. Also, columns with a small diameter to thickness ratio have more curvature than those with a high D/t ratio. This curvature works as a brace to resist loads.

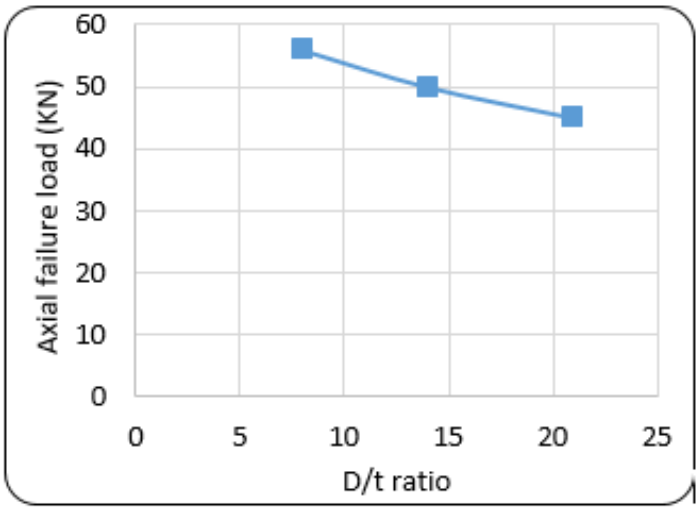

Figure (4.48): Axial Failure Load Versus the D/t Ratio

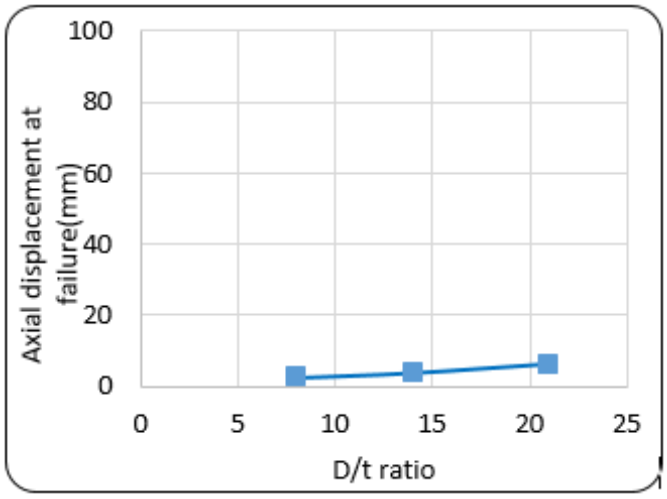

Figure (4.49): Axial Displacement at Failure Versus D/t Ratio

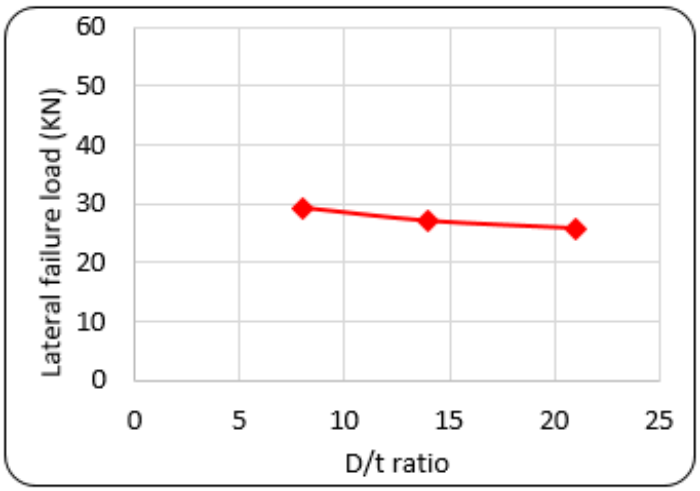

Figure (4.50): Lateral Failure Load (KN) Versus the D/t Ratio

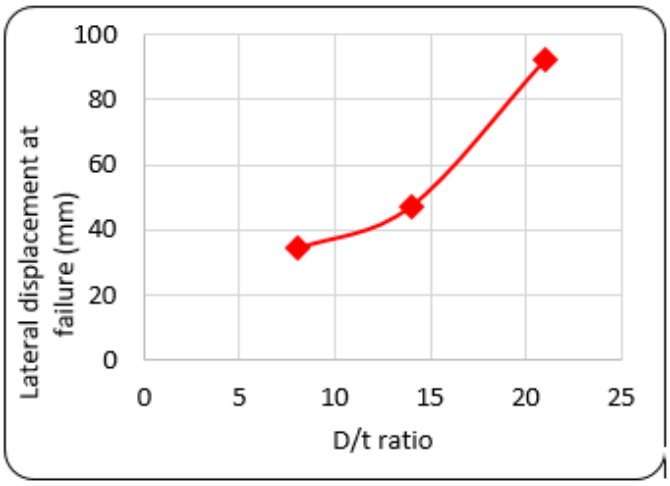

Figure (4.51): Lateral Displacement at Failure Versus D/t Ratio

4.8 effect of the number of branching levels on the response of the tree-like columns

In order to understand the effect of branching level number on the behavior of the tree like column, three models with different numbers of branching levels (zero, one, and two) as defined in group No1 (Fig 4.3). The results showed that when the tree-like columns under axial load only increasing the number of branching levels from zero to 1 decrease the axial failure load by -41.7% and increase the axial displacement by +106%, while increasing the number of branching levels from 1 to 2 increase the axial failure load and displacement by +10% and +60% respectively as shown in figs (4.53) and (4.54).

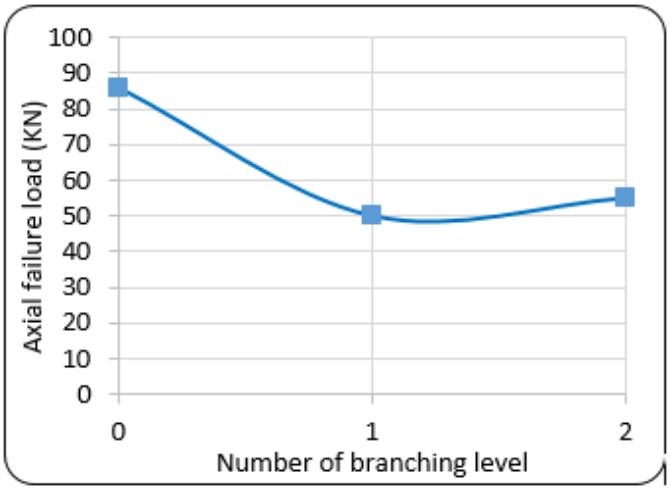

Fig (4.52): Axial Failure Load Versus Number of Branching Levels

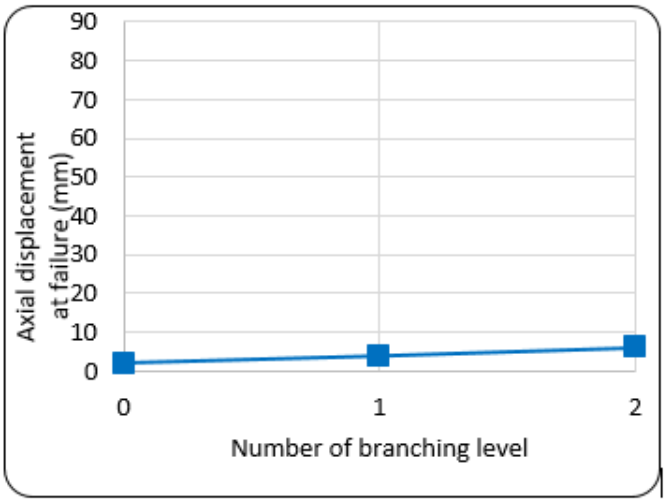

Fig (4.53): Axial Displacement at failure versus number of branching levels

For the case of lateral loading only and as shown in figures (4.55) and (4.56) it's found that increasing the number of branching levels from zero to 1 decrease the lateral failure load by -30.7% and increase the lateral displacement by +230%, while increasing the number of branching levels from 1 to 2 increase the lateral failure load and displacement by +14% and +73% respectively. This increase may be due to the increase in branch length, which makes the tree-like column more flexible

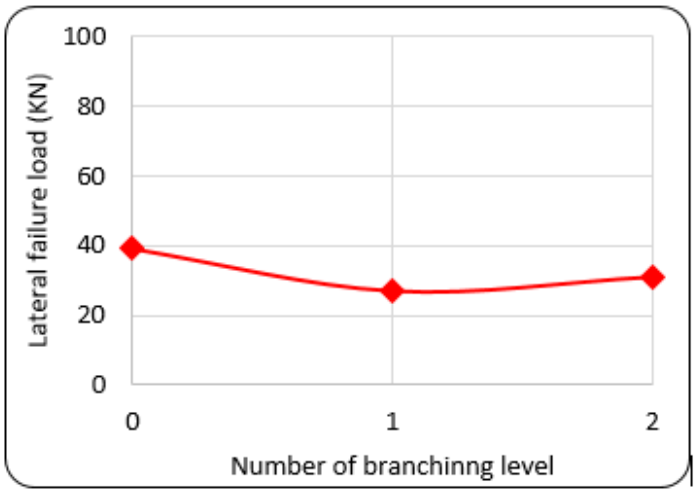

Fig (4.54): Lateral Failure Load Versus Number of Branching Levels

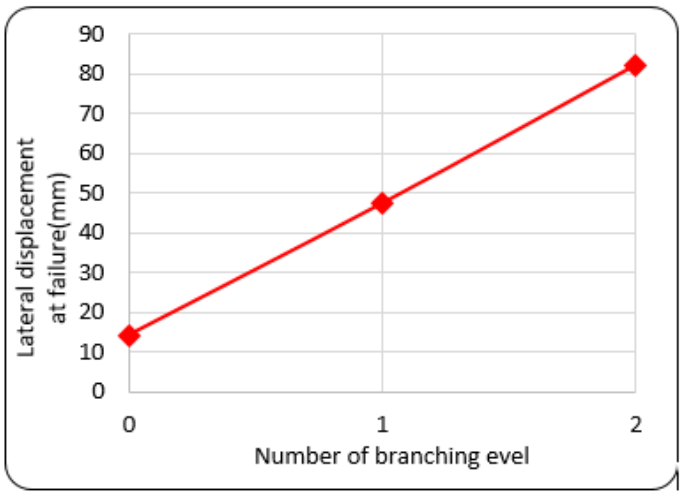

Fig (4.55): lateral Displacement at Failure Versus Number of Branching Levels

CHAPTER FIVE

Conclusions and further work recommendation

5.1 conclusions

Depending on the obtained results from the finite element simulation by the ABACUS program for the tree-like steel column models subjected to axial and lateral loads, within the range of this research, the following conclusions can be mentioned:

1. At combined loading cases the results demonstrated that the axial failure load is decreased by the increase of lateral load to axial load ratio were increasing the lateral load ratio from zero to (20, 40, 60, 80 and 100) %, respectively reduce the axial failure load between ((48-56), (69-74.4), (78-81.6) (82-85.4) and (85-88)) % respectively, while the axial displacement increases significantly between ((13-160), (73-187), (118-291), (223-355), (258-424)) %.
2. Increasing the lateral to axial load ratio from 20 to (40, 60, 80, and 100) %, respectively increases the lateral failure load between ((15-20), (24-28), (31-39), (37-44)) respectively, also the lateral displacement increased significantly between ((23-71), (39-120), (63-245), (85-450)) %.
3. Decreasing the (D/t) ratio from 21 to (14 and 8) respectively increases the axial failure load by (11.1 and 24.4) respectively while the axial displacement decreases significantly by (37.4 and 57.4) % respectively.
4. Increasing the number of branching level (BL) from **zero** to **1**, decreases axial and lateral failure loads by 41.7% and 30.7% respectively, while the axial and lateral displacements increase by 106% and 230% respectively. That means the tree-like columns are not recommended to use except for urgent architectural necessity.

5. Increasing the number of branching level (BL) from **1** to **2** increase the axial and lateral failure loads by 10% and 14% respectively, while the axial and lateral displacements are increase by 60% and 73% respectively.
6. the presence of axial load in combination with lateral load works to reduce the lateral displacement between (17 - 48.6) %.
7. The joint area is the critical part of tree-like column and stresses are higher at that part.

5.2 Recommendations for Future Work

In all researches that are related to tree-like columns, the behavior of those columns is studied under the influence of axial loads only there are no researches conducted under the influence of lateral loads. For future works, the following recommendations are proposed:

1. Investigating experimentally the behavior of tree-like steel columns under combined loading cases.
2. Investigating numerically tree-like columns with multi-trunk cases (two, three, et).
3. Investigating experimentally, the unsymmetrical case of a tree-like column.
4. Studying the effect of the shape parameters like the branch height and branch width on the behavior of tree-like columns subjected to combined loads.
5. Investigating experimentally the branching joint of the tree-like columns under combined loads.

References:

[1] M. Lacy, “Review of Alternate Realities: Mathematical Models of Nature and Man,” AI Mag., vol. 11, no. 2, p. 78, 1990.

[2] E. E. Bernard and M. R. Kare, Biological prototypes and synthetic systems, vol. 1. Plenum Press New York, 1962.

[3] J. M. Benyus, Biomimicry: Innovation inspired by nature. Morrow New York, 1997.

[4] G. YELER, “Influences of the living world on architectural structures: an analytical insight,” Uludağ Univ. J. Fac. Eng., vol. 20, no. 1, pp. 23–38, 2015.

[5] C. Dyrbye and S. O. Hansen, Wind loads on structures. 1997.

[6] L. Rosa, G. Tomasini, A. Zasso, and A. M. Aly, “Wind-induced dynamics and loads in a prismatic slender building: A modal approach based on unsteady pressure measurements,” J. Wind Eng. Ind. Aerodyn., vol. 107, pp. 118–130, 2012.

[7] A. S. A. S. committee on building code requirements for minimum design loads in buildings. A58, American Standard Building Code Requirements for Minimum Design Loads in Buildings and Other Structures, vol. 13. US Government Printing Office, 1945.

[8] I. M. Rian and M. Sassone, “Tree-inspired dendriforms and fractal-like branching structures in architecture: A brief historical overview,” Front. Archit. Res., vol. 3, no. 3, pp. 298–323, 2014.

[9] J. Barrallo and S. Sánchez-Beitia, “The geometry of organic architecture: the works of Eduardo Torroja, Felix Candela and Miguel Fisac,” in Proceedings of Bridges 2011: Mathematics, Music, Art, Architecture, Culture, 2011, pp. 65–72.

[10] Internet, “www.pinterest.com.”.

[11] P. Perugini and S. Andreani, “Pier Luigi Nervi’s columns: flow of lines and forces,” J. Int. Assoc. Shell Spat. Struct., vol. 54, no. 2–3, pp. 137–148, 2013.

[12] P. Von Buelow, “Following a thread: a tree column for a tree house,” 2006.

[13] P. Von Buelow, “A Geometric Comparison of Branching Structures in Tension and in Compression versus Minimal Paths,” 2007.

[14] L. Linsen, B. J. Karis, E. G. McPherson, and B. Hamann, “Tree growth visualization,” 2005.

[15] J. Martínez-Calzón and P. J. S. Cruz, “Treatment of the form in structural engineering,” in Proceedings of the First International Conference on Structures and Architecture, 2010, pp. 7–10.

[16] W. Nerdinger, Frei Otto. Complete Works: Lightweight Construction - Natural Design, 2nd printi. Birkhäuser, 2005.

[17] M. et al. Neureuther, Computational generation of tree structures in Ramifications, natural constructions- Lightweight architecture and nature. Stuttgart: University of Stuttgart, 1992.

[18] J. Hunt, W. Haase, and W. Sobek, “A design tool for spatial tree structures,” J. Int. Assoc. Shell Spat. Struct., vol. 50, no. 1, pp. 3–10, 2009.

[19] J. H. Houston, “Developing Dendrifrom Facades Using Flow Nets as a Design Aid,” 2011.

[20] W. M. Y. Feng, “DESIGN ON THE DENDRITIC STRUCTURE WITH STEEL TUBES,” Steel Constr., 2006.

[21] P. Von Buelow, “Following a thread: a tree column for a tree house,”

2006.

[22] C. J. et Al., “Research and application of tree columns in the long-span spatial structure,” steel Constr., vol. 25, no. 121, pp. 16–21, 2010.

[23] C. C. J. B. C. Guoyong, “The sensitivity-based morphogenesis method for framed structures,” China Civ. Eng. J., 2013.

[24] J. Sánchez-Sánchez, F. Escrig Pallarés, and M. T. Rodríguez-León, “Reciprocal tree-like fractal structures,” Nexus Netw. J., vol. 16, no. 1, pp. 135–150, 2014

[25] Z. Zhao, B. Liang, and H. Liu, “Topology establishment, form finding, and mechanical optimization of branching structures,” J. Brazilian Soc. Mech. Sci. Eng., vol. 40, no. 11, pp. 1–11, 2018.

[26] A. A. Khamees and K. K. Shadhan, “Experimental study on structural behaviour of branching steel columns,” IOP Publishing, 2020.

[27] A. A. Khamees and K. K. Shadhan, “Experimental Investigation of Dendriform Structure Under Static Loading,” J. Appl. Sci. Eng., vol. 24, no. 1, pp. 57–64, 2021.

[28] J. C. De Oliveira, S. Willibald, J. A. Packer, C. Christopoulos, and T. Verhey, “Cast steel nodes in tubular construction-Canadian experience,” in TUBULAR STRUCTURES-INTERNATIONAL SYMPOSIUM-, 2006, vol. 11, p. 523.

[29] W. Weihua and Du Wenfeng, “loaded analysis of spatial cast-steel joint with four branches in a tree-like structure,” J. Henan university (natural Sci., vol. 44, no. 4, pp. 738–742, 2014

[30] Z. H. Zhu, W. F. Du, Z. F. Sun, and L. M. Zhu, “The bionic optimization and analysis and calculation of the cast-steel joint with three branches,” in

Applied Mechanics and Materials, 2014, vol. 548, pp. 1618–1622.

[31] W. Du, Y. Sun, and M. Yang, “Bearing capacity of the cast-steel joint with branches under eccentric load,” J. Constr. Steel Res., vol. 135, pp. 285–291, 2017.

[32] A. A. Nassr, A. G. Razaqpur, M. J. Tait, M. Campidelli, and S. Foo, “Dynamic response of steel columns subjected to blast loading,” J. Struct. Eng., vol. 140, no. 7, p. 4014036, 2014.

[33] T. Yu, Y. M. Hu, and J. G. Teng, “Cyclic lateral response of FRP-confined circular concrete-filled steel tubular columns,” J. Constr. Steel Res., vol. 124, pp. 12–22, 2016.

[34] O. A. Sediek, T.-Y. Wu, J. McCormick, and S. El-Tawil, “Collapse behavior of hollow structural section columns under combined axial and lateral loading,” J. Struct. Eng., vol. 146, no. 6, p. 4020094, 2020.

[35] Raphael Jean Boulbes, Troubleshooting Finite-Element Modeling with Abaqus: With Application in Structural Engineering Analysis, 1st ed. Springer, 2020.

[36] SIMULA CO., Abaqus/CAE User’s Manual. SIMULIA Worldwide Headquarters, 2017.

الخلاصة

هناك القليل من الدراسات حول السلوك الإنشائي للأعمدة الفولاذية ذات الفروع والتي تسمى الأعمدة الشبيهة بالأشجار. تم استخدام هذه الأنواع من الأعمدة في العديد من الهياكل حول العالم خاصة تلك الهياكل ذات المساحة الكبيرة. كان الغرض من هذه الدراسة هو فحص حمل الفشل ، ازاحات الفشل العمودية والجانبية ، ونمط الفشل للأعمدة الفولاذية الشبيهة بالشجرة والمعرضة لمزيج من التحميل المحوري والجانبي. تم تحديد نسبة الحمل الجانبي إلى الحمل المحوري ، وشكل مساحة المقطع العرضي (A) ،ونسبة القطر الخارجي إلى السماكة (D / t) وعدد مستويات التفرع (BL) كمتغيرات للتصميم.تم انشاء نموذج لاخطي ثلاثي الابعاد باستخدام برنامج(ABAQUS / CAE 2017) , تكون مساحة المقطع العرضي للجذع (A0) تساوي 480 ملم ^{2} ، مساحة فروع المستوي التفرعي الاول تساوي نصف مساحة المقطع العرضي للجذع (A1 = A0 / 2) ، إجمالي الارتفاع والعرض للعينة يساوي 350 ملم. تم التحقق من النموذج باستخدام النتائج التجريبية التي تم الحصول عليها من باحث آخر من حيث استجابة الحمل والإزاحة.بعدها تم انشاء خمسة نماذج اخرى للتحقيق في متغيرات التصميم. تعرض كل نموذج لسبع حالات من التحميل (تحميل محوري فقط ، تحميل محوري بالاضافة الى تحميل جانبي بنسبة (20 , 40, 60 , 80 , 100)%من التحميل المحوري ، وتحميل جانبي فقط). أظهرت النتائج أن زيادة نسبة الحمل الجانبي إلى المحوري بنسبة (20 ، 40 ، 60 ، 80 , 100)% على التوالي تقلل من حمل الفشل المحوري بين ((48-56) , (69-74.4) , (78-81.6), (82-85.4) و(85-87.8))% على التوالي. بينما يتم زيادة ازاحات الفشل العمودية والجانبية بشكل كبير.أيضًا تغيير مساحة المقطع العرضي من المستطيل إلى الأنبوبي بنسبة D / t تساوي 21 ، يؤدي الى تقليل حمل الفشل بنسبة 10% في حالة التحميل المحوري فقط وبنسبة 24.6% في حالة التحميل الجانبي فقط. كذلك فان تقليل نسبة D / t من 21 إلى (14 و 8) على التوالي يؤدي إلى زيادة حمل الفشل المحوري بنسبة (11.1 و 24.4)% ، بينما يزيد حمل الفشل الجانبي بنسبة (4.8 و 13.4)%. ان وجود الحمل المحوري مع الحمل الجانبي يعمل على تقليل الإزاحة الجانبية بين (17 و 48.6)% لنماذج الأعمدة الشبيهة بالشجرة. علاوة على ذلك ، فإن زيادة عدد مستوى التفريع من 1 إلى 2 يزيد من أحمال الفشل المحوري بنسبة 10% . منطقة المفصل هي الجزء الحرج من العمود الشبيه بالشجرة وتكون الاجهادات أعلى في هذا الجزء.

جمهورية العراق
وزارة التعليم العالي والبحث العلمي
جامعة بابل
كلية الهندسة
قسم الهندسة المدنية

تحليل العناصر المحددة للأعمدة الفولاذية الشبيهة بالأشجار تحت تاثيراحمال عمودية وجانبية

رسالة

مقدمة الى كلية الهندسة / جامعة بابل كجزء من متطلبات الحصول على درجة الماجستير في الهندسة / الهندسة المدنية / الانشاءات

من قبل

رباب جلوب دخن ناصر

اشراف

أ . م . د. خالد كريم شدهان

1444 A.H 2022 A.D